Computational Analysis of a Combined Heat and Power Steam Turbine for a Small Modular Reactor

Master's thesis in Innovative Sustainable Energy Engineering

Sylvi Räisänen

DEPARTMENT OF SPACE, EARTH AND ENVIRONMENT

CHALMERS UNIVERSITY OF TECHNOLOGY

Gothenburg, Sweden 2024

www.chalmers.se

Computational Analysis of a Combined Heat and Power Steam Turbine for a Small Modular Reactor

Sylvi Räisänen

Master's Thesis 2024

Examiner: Prof. Teodora Retegan Vollmer, Chalmers

Supervisors: Prof. Risto Lahdelma, Aalto University;

MSc. Mikko Lehto, Fortum Power and Heat Oy

Department of Space, Earth and Environment

Chalmers University of Technology

SE-412 96 Göteborg

Sweden

Telephone + 358 50 352 5919

Computational Analysis of a Combined Heat and Power Steam Turbine for a Small Modular Reactor

Sylvi Räisänen
Department of Space, Earth and Environment
Chalmers University of Technology

Abstract

The Finnish district heating system has historically relied on combined heat and power production. A shift in the energy sector, induced by climate change and the energy crisis, is challenging the viability of conventional combined heat and power plants. The ability of renewable fuels to sustainably replace the retired fossil fuels raises concerns. On the other hand, electric alternatives, such as heat pumps and electric boilers, contribute to the growing imbalance of electricity supply and demand. The district heating system is seen to lack a reliable method of sustainable heat production.

Small modular reactors (SMRs) could answer this demand by producing combined heat and power (CHP). Additional heat production could increase the profitability of an SMR project, and CHP SMRs may offer advantages in terms of operational flexibility. However, the heat production efficiency of CHP SMRs remains uncertain without practical experience. To clarify the issue, this thesis presents the computation of the coefficient of performance (COP) for several CHP SMR secondary cycles. The secondary cycle models are constructed based on a small pressurized water reactor concept with an extraction-condensing steam turbine, and they are simulated using Solvo software. To illustrate the practical implications of the COP, the annual operation of one CHP SMR cycle is simulated according to heat demand corresponding to the Finnish city of Tampere.

The simulation results indicate the COP of a CHP SMR to range between 3 and 7. In theory, the COP can be increased by enhancing steam expansion work and by minimizing entropy generation. In practice, this implies utilizing low-pressure heating, preheating feedwater, and lowering cooling water temperature. When sized according to local peak power and operated based on heat demand, the simulation suggests that a CHP SMR could supply the majority of annual district heating demand in Tampere. The load following capabilities of the turbine are found to be sufficient, and it is shown that coupling a heat storage with a CHP SMR reduces required peak production capacity. Overall, the findings of this thesis highlight the importance of the steam cycle in the performance of a nuclear power plant.

Keywords: combined heat and power, small modular reactors, district heating, steam turbine, nuclear power, coefficient of performance

Table of Contents

Preface

Abbreviations

1 Introduction 1

1.1 Objectives and Methodology 3

1.2 Thesis Structure 4

2 Introduction to Nuclear Power 5

2.1 Nuclear Power Plants 6

2.1.1 Small Modular Reactors 7

3 District Heating 11

3.1 District Heating Demand 11

3.2 District Heating Distribution 14

3.3 District Heating Production 16

3.3.1 Combined Heat and Power Production 17

3.3.2 Separate Heat Production 19

3.3.3 Heat Storages 21

3.3.4 Nuclear District Heating 22

4 Fundamentals of Steam Power 23

4.1 Rankine Cycle 24

4.1.1 Secondary Cycle of a Pressurized Water Reactor 28

4.2 Combined Heat and Power Production 29

4.2.1 Coefficient of Performance of Heating 31

5 Dimensioning the SMR0 Secondary Cycle 33

5.1 Initial Data and Process Parameters 34

5.2 Steam Generator 35

5.3 Steam Turbine and Generator 35

5.4 Superheaters and Feedwater Preheaters 36

5.5 Moisture Separator and Pumps 38

5.6 Condenser and Cooling Solution 38

6 SMR0 Solvo Model 40

6.1 Solvo® Simulation Software 40

6.2 Model Components 41

6.2.1 Steam Turbine and Generator 42
6.2.2 Reheaters and Feedwater Preheaters 43
6.2.3 Moisture Separator and Pumps 43
6.2.4 Condenser and Cooling Solution 44
6.3 Simulation Results 45
7 Combined Heat and Power Steam Cycle Models 46
7.1 Calculation of the Coefficient of Performance of Heating 46
7.2 District Heating Components 46
7.3 SMR1 47
7.4 SMR2 51
7.5 SMR3 56
7.5.1 Modifications to the Condensing Configuration 56
7.5.2 Combined Heat and Power Configuration 58
7.5.3 Effect of Heat Sink Temperature 59
7.5.4 Effect of Optimization for Heat Production 60
7.6 Summary of Models 62
8 Operational Analysis 63
8.1 Supporting Heat Production Capacity 67
8.2 Load Following Capabilities 70
9 Discussion and Conclusions 72
9.1 Summary of Results 72
9.2 Discussion and Prospects for Future Research 73
9.3 Limitations and Sources of Error 76
9.4 Conclusion 77
Bibliography 78
List of Appendices 84

Preface

This master's thesis was produced for the Fortum New Nuclear business unit as a contribution to the ANItA competence center with the support of EDF and NUWARD. I am deeply grateful to EDF and NUWARD for giving me the opportunity to delve into such an interesting subject.

In my work, I have received considerable backing from my colleagues who have kindly shared their time and knowledge for the sake of this thesis. Most notably, I would like to thank my advisor Mikko Lehto. His assistance and insight have been truly invaluable during the entire project, and the outcome of this thesis would not have been the same without his expertise.

Moreover, I have had the pleasure of working with and studying in two universities. I would like to thank Professor Risto Lahdelma from Aalto University for the active supervision, valuable feedback, and interesting conversations. I am grateful also to Professor Teodora Retegan Vollmer from Chalmers University for generously supporting my work and introducing me to the world of radiochemistry.

Needless to say, a big thank you goes to all my Fortum team members for encouraging me and keeping me entertained during this long process. I am particularly grateful to Konsta Värri for his moral support, and to Nici Bergroth and Antti Rantakaulio, whose turbine enthusiasm served as great inspiration for my work.

I would not be writing this without the endless patience of my family. I'd like to thank my parents for their unconditional support in everything I do, and my partner Juha-Matti for standing beside me during this project and throughout my academic and professional journey.

Espoo, 26.7.2024
Sylvi Räisänen

Abbreviations

BWR	Boiling Water Reactor
CHP	Combined Heat and Power
COP	Coefficient of Performance
DH	District Heating
HP	High-Pressure
IAEA	International Atomic Energy Agency
LNPP	Large Nuclear Power Plant
LP	Low-Pressure
PWR	Pressurized Water Reactor
SMR	Small Modular Reactor
TTD	Terminal Temperature Difference

1 Introduction

Since the first district heating networks built in the 1950's, combined heat and power generation has acted as the foundation of district heating in Finland. The production method is accountable for supplying over half of all Finnish district heating cost-effectively and reliably. Now, reflecting a global transformation of the energy sector, conventional combined heat and power plants are subject to phase-out. Without replacing capacity, Finland could lack stable baseload power and experience turbulence in energy prices and availability.

Joining the efforts of many other nations, Finland, too, has committed to completely abandoning fossil-fired energy production by the 2030's [1, p. 151] – an objective to both reduce emissions and advance energy security. The Finnish district heating industry is contributing to the mission with the target of decreasing greenhouse gas emissions to 10-20 % of current levels by the year 2035 [2]. Renewable biofuels have been adopted to replace fossil fuels, and the use of coal specifically has been banned [3]. Meanwhile, heat production through electric boilers in 2023 was 14-fold compared to 2022, and the utilization of heat pumps grew by 50 % during the time period of 2017-2022. A shift towards sustainability is thus visible: in 2023, the total share of renewable energy, heat recovery, and electric boilers amounted to 69 % of all district heating production. [4]

Nevertheless, the issue of sustainable heating is not quite resolved. Competing technologies and phasing out fossil fuels have resulted in the closure of large conventional combined heat and power (CHP) plants. A decade previously, the technology supplied three-fourths of all district heating – now, the share is slightly above 50 %. CHP plants bear significance in the stability of both heat and electricity markets by fixing heat prices and balancing fluctuations in electricity demand. The replacing heating solutions currently available may not be able to provide the same security sustainably. Electric boilers and heat pumps rely on electricity, the demand of which tends to peak at the same time as the demand for heat. On the other hand, the renewable fuels used for heat production emit greenhouse gas emissions comparable to fossil fuels.

To answer the demand for stable yet sustainable energy, a familiar technology is gaining momentum. The energy sector is currently witnessing the rising popularity of nuclear power. Unlike fossil fuels, nuclear power plants do not emit carbon dioxide during operation, making their significance in combatting climate change evident. The Nuclear Energy Agency mentions nuclear power as a key pathway to meet the net zero targets by 2050 and to limit global warming to less than 1,5 °C [5]. Geopolitical uncertainty of the 2020s has further highlighted the role of nuclear as a means of promoting energy security. The pro-nuclear trend is present in Finland as

well, as the most recent government program states the need for more nuclear power and expresses the willingness of policymakers to support the cause [1, p. 153].

The growing popularity of nuclear power is accelerated by the development of new nuclear technology, namely small modular reactors (SMRs). Current designs imply that SMRs may defy conventional CHP generation by providing both electricity and district heating with the ability to alternate between the two outputs. This operational concept differs from conventional backpressure CHP units, which have traditionally been constructed for heat production while electric power production is limited due to steam turbine design. Unlike large conventional CHP plants, the heat outputs of SMRs are planned to be small relative to their reactor thermal power, expanding the siting possibilities of the plants. The operational flexibility of SMRs thus presents an opportunity for the district heating industry. Investigating this opportunity is interesting as additional revenue from heat production could increase the overall profitability of an SMR project.

Historically, nuclear CHP has been proven to be a technically feasible solution. Successful demonstrations of the technology have been witnessed in, for example, Sweden, China, and Switzerland. However, these projects have relied on familiar large nuclear power plant technology. In addition, extracted amounts of heat have been small relative to the large demand in Nordic countries. Due to the early design phase of SMRs, there is no Nordic experience of CHP production with these reactors. It has thus not been proven how CHP SMRs would operate in practice, how they would integrate into the Nordic district heating scene, and what the efficiency of heat production would be. The efficiency of heat production largely defines the profitability and applicability of a CHP SMR into an energy mix.

Establishing the absolute efficiency of a CHP SMR is challenging and, for the sole purpose of evaluating heat production, perhaps even unmeaningful. Thermal efficiency considers factors beyond heat production capability, and an accurate calculation would have to consider plant internal consumption and the loads of all components included in the reactor and turbine islands. Therefore, an intuitive approach is to study the effect of heat production on electricity output. A ratio defining the produced heat to consumed electric power can be referred to as the coefficient of performance (COP). In the context of combined heat and power production, the COP describes the ratio of the obtained district heating power to the lost electric power. The COP serves as a performance indicator for CHP plants and enables comparison with heat pumps from an energy system perspective.

1.1 Objectives and Methodology

This thesis discusses combined heat and power generation for district heating with a small modular reactor. The topic is investigated from a technical perspective primarily by performing steam turbine calculations. The aim is to determine

1. the technical configuration of a CHP SMR steam cycle,
2. the corresponding coefficient of performance (COP) of heat production, and
3. the implications of the COP on the operation of a CHP SMR.

The first two aims will be achieved by first reviewing the literature on the principles of CHP production and then by modeling SMR steam cycles. The simulations are performed using Solvo software. In the simulation procedure, first a baseline model of a condensing SMR steam cycle referred to as SMR0 is constructed. Then, three CHP steam cycle configurations based on SMR0 are formed. The construction of the models is iterative, and each model aims to achieve gains in the COP and the district heating output. The baseline model of SMR0 is based on a small modular pressurized water dual-reactor concept (NUWARD, private communication, Febr. 2024[1]).

The third aim will be achieved by reviewing the implementation of a CHP SMR into a Finnish district heating network. The SMRs are matched with Finnish cities based on estimates of local peak power demands. The last CHP SMR configuration, SMR3, is evaluated individually by simulating its annual operation according to heat demand corresponding to the city of Tampere, Finland. Tampere is selected as the location of the analysis as half of the city's peak power demand corresponds to the rated heat capacity of SMR3. Trends in district heating demand are formed using Helsinki data from the years 2015-2022. This data is used due to its availability and public accessibility.

This thesis focuses on the secondary side of a pressurized water reactor. Primary side features are disregarded, and the reactor thermal power remains unchanged across all steam cycle models. In the context of combined heat and power production, the produced heat is considered to be applied towards district heating. Other cogeneration applications are overlooked. Annual operation is analyzed based on heat demand, and the electricity market is not considered. Conventional combined heat and power plants are defined as power plants where thermal energy is supplied through the combustion of a fuel, such as coal or biomass.
This thesis is produced as an in-kind contribution to ANItA (Academic-industrial Nuclear technology Initiative to Achieve a sustainable energy future). ANItA is a national center of excellence where academic and industrial stakeholders aim to research the potential of light-water small modular reactors in the Swedish energy system. The Competence Center is hosted by Uppsala University, and ANItA

[1] This model does not take into consideration any potential design evolutions of NUWARD SMR after February 2024.

partners include Chalmers Technical University, the Royal Institute of Technology, Vattenfall, Uniper, Fortum, Westinghouse Electric Sweden, and Studsvik Nuclear. [6]

1.2 Thesis Structure

This thesis is divided into three parts: literature review, experimental modeling, and analysis. The first part is comprised of Chapters 2, 3, and 4, which provide a description of the pivotal topics of this thesis. The chapters present the theoretical background of nuclear power, steam cycles, and district heating.

Chapters 5, 6, and 7 constitute the experimental section of the thesis and outline the modeling work. First, Chapter 5 reviews the dimensioning of the baseline SMR model in this thesis, SMR0. Chapter 6 addresses the simulation software utilized for the modeling procedures. Chapter 7 introduces the three CHP SMR steam cycle configurations, SMR1-3, formed by modifying the baseline model of SMR0. This chapter presents the calculation of the COP for each CHP steam cycle.

The modeling work is finalized by analyzing the yearly operation of a CHP SMR. Chapter 8 presents the operation of SMR3 according to estimated heat demand in the Tampere district heating network. The operation of the SMR is reviewed without and with supporting heat production capacity. Finally, Chapter 9 concludes the thesis by discussing the outcomes of the work. This chapter analyses the limitations of the work and establishes future topics of research.

2 Introduction to Nuclear Power

Nuclear energy was first used to produce electric power in December 1951 by the Experimental Breeder Reactor-I (EBR-I) in the United States. This became a starting point for the development of commercial nuclear reactors, the first of which began operation in the late 1950's [7, p. 1]. As of 2024, nuclear energy accounts for 10 % of global electricity production. Plants exist in 32 countries and provide a total power capacity of 413 GW [8]. The United States, France, and China are leaders in nuclear generation, with electric capacities of 97 GW, 61 GW, and 53 GW respectively. In the Nordic region, Finland and Sweden are the only countries with operating nuclear power plants. [9]

Sustainability has for long been a driver for new nuclear projects, and an evolving energy scene has further elevated the popularity of nuclear power particularly during the 2020s. Amid the rise of intermittent renewable energy and fluctuation in market conditions, the role of nuclear power as a stable energy source is emphasized. Military conflict, COVID-19, and geopolitical circumstances have reestablished the dynamics of the energy market. A trend in nuclear investments has emerged, focusing on increasing capacity and modernizing existing plants. Worldwide, close to 60 new reactors are under construction, with a majority of projects taking place in China [9]. The shift towards pro-nuclear has been rather rapid, and attitudes have changed in the course of only some years: in the IAEA's 2023 outlook for nuclear power estimates, the agency foresees roughly 25 % more nuclear capacity installed by 2050 than it did in 2020 [10].

Finland has five nuclear reactors at two sites with a total electric capacity of 4 394 MW. The first nuclear power unit, Loviisa 1, began operation in 1977, and the second Loviisa reactor followed in 1980. Both Loviisa 1 and 2 are pressurized water reactors of the VVER-440 type, with electric outputs of 507 MW [11]. On the west coast of Finland, boiling water reactors Olkiluoto 1 and 2 were deployed in 1978 and 1980 respectively [12]. Both units generate net electric outputs of 890 MW. The construction of a third reactor unit, Olkiluoto 3, was finalized in 2023. The reactor is an EPR-type unit with a comparatively high output of 1600 MW_e. The impact of Olkiluoto 3 on the Finnish energy generation portfolio has been profound – the share of nuclear electricity production rose from 35 % to 42 % merely within the timeframe of 2022 to 2023 [13]. Finland is dedicated to increasing nuclear capacity, and the Finnish government is determined facilitate the deployment of new nuclear [1]. Currently, the support for nuclear power in Finland is reported to be at a record high [14].

2.1 Nuclear Power Plants

Nuclear power plants generate electricity on the basis of a controlled nuclear fission reaction. During fission, the nucleus of an atom absorbs an extra neutron, causing it to split into fission products. This reaction releases heat, which can be captured in the nuclear reactor core and further converted into useful power. To fuel the fission reaction, a great majority of nuclear reactors utilize the isotope U-235 of uranium. While the uranium is emission-free, it is a nonrenewable resource. [15, p. 89] Nuclear power plants emit mainly warm water or water vapor, and the greenhouse gas emissions from nuclear power production are mostly generated by construction and fueling activities.

Nuclear reactors include a moderator substance to control the rate of the fission reaction and a coolant substance to remove heat. In most reactors, light water acts as both the moderator and the coolant. Such reactors are referred to as light-water reactors (LWRs), and they constitute the majority of existing commercial reactors. LWRs are further classified into boiling water reactors (BWRs) and pressurized water reactors (PWRs). The principal difference between the two reactor types is the method in which steam is generated. In a BWR, water is boiled to produce steam directly inside the coolant circuit in contact with the reactor. Contrarily, PWRs feature a separate coolant flow in a secondary cycle to which a steam generator transfers heat from the reactor core. Because the water in a PWR is not allowed to boil, the pressure in the primary circuit is substantially higher than in a BWR – approximately 150 bar versus 70 bar in BWRs. The schematics of a PWR and a BWR are shown in Figures 1 and 2. [15, pp. 293-294]

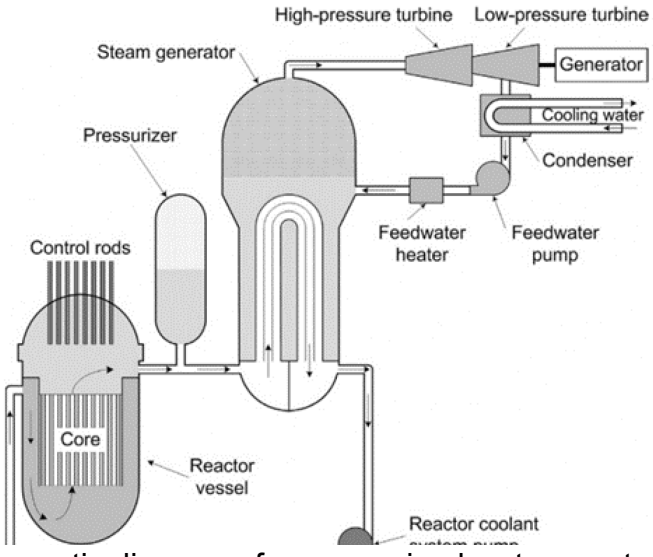

Figure 1: A schematic diagram of a pressurized water reactor. [15, p. 301]

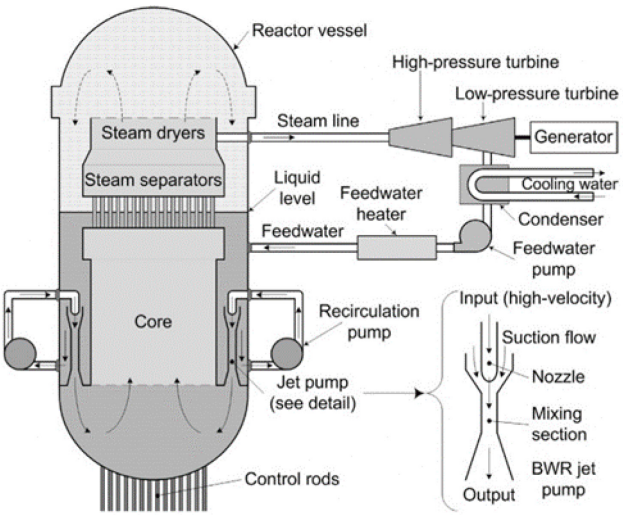

Figure 2: A schematic diagram of a boiling water reactor. [15, p. 302]

The marginal costs of operating a nuclear power plant are relatively low in contrast to the high capital investment of building the plant. Therefore particularly in Sweden and Finland, nuclear power plants are ordinarily operated for baseload electricity production purposes. Altering electrical output necessitates adjusting reactor thermal power, which must be executed in a carefully controlled manner. Adjusting electric power output is more common in countries such as France, where the majority of nuclear power plants have been converted for flexible operation [16, p. 2]. In all countries, a minimum level of adjustability is ensured to comply with electricity grid requirements imposed by the local grid code. Depending on the code, this usually implies the ability to alter electric output by ±1-5 % of rated capacity per minute. For reference, the IAEA mentions the ramp rate of a nuclear power plant with a rated capacity of 900-1 300 MW_e to be 30 MW/min [16, p. 17].

2.1.1 Small Modular Reactors

A common definition for a small modular reactor is that of the International Atomic Energy Agency (IAEA), according to which SMRs are reactors with an electric power output of less than 300 MW per module [17]. Today, SMR concepts are seen to prioritize improved design features and construction methods rather than aiming for a minimal output. Hence, the boundary of 300 MW is being pushed higher as several SMRs feature outputs closer to 400-500 MW.

The concept of purposefully constructing smaller reactors emerged soon after large nuclear plants saw significant growth in the 1960s. The very first commercial projects indicated that the financial burden and construction schedules of nuclear power plants were demanding. Thus already in 1985, the IAEA discussed “small and medium power reactors” or “SMPRs” in a report where it states that new smaller

reactors could aid in managing financial risk and construction times [18]. The industry has since seen numerous different designs of small reactors, most of which have remained conceptual. Support for modular versions of small reactors intensified in the 2010s, as development projects began attracting greater attention and financial backing. The momentum of SMR projects has since amplified as the popularity of nuclear power has grown towards the 2020s.

The incentive behind SMRs stems from potentially smaller risks. Conventional large nuclear power plants (LNPPs) are traditionally designed to reach a high electric capacity to reduce the overall cost of electricity [15, p. 307]. SMRs, on the other hand, are smaller in size, suggesting lower costs and shorter construction times. The reduced capital investment of SMRs is largely attributed to their manufacturing principle. Modular technology allows SMRs to be fabricated in-factory and assembled on site. In-factory manufacturing improves quality control and facilitates design standardization, the lack of which has previously led to prolonged and expensive construction projects [19]. Instead of economies of scale, SMR designs aim to benefit from economies of series enabled by standardized factory production.

Figure 3 displays global SMR project sites as of 2024. A great majority of SMR development projects are based in North America and Europe, with some also in Asia and Russia [20, p. 35]. One of the first deployments of SMRs in Western countries is expected in Canada, where Ontario Power Generation is deploying a total of four BWRX-300 units at the Darlington site. Commercial operation is to begin in 2029. Complying with climate targets, many other SMR projects also aim for deployment by the 2030's and large-scale implementation by the 2050's. According to a forecast by the Nuclear Energy Agency, SMRs could reach an installed capacity of 375 MW_e by 2050 [5, p. 27].

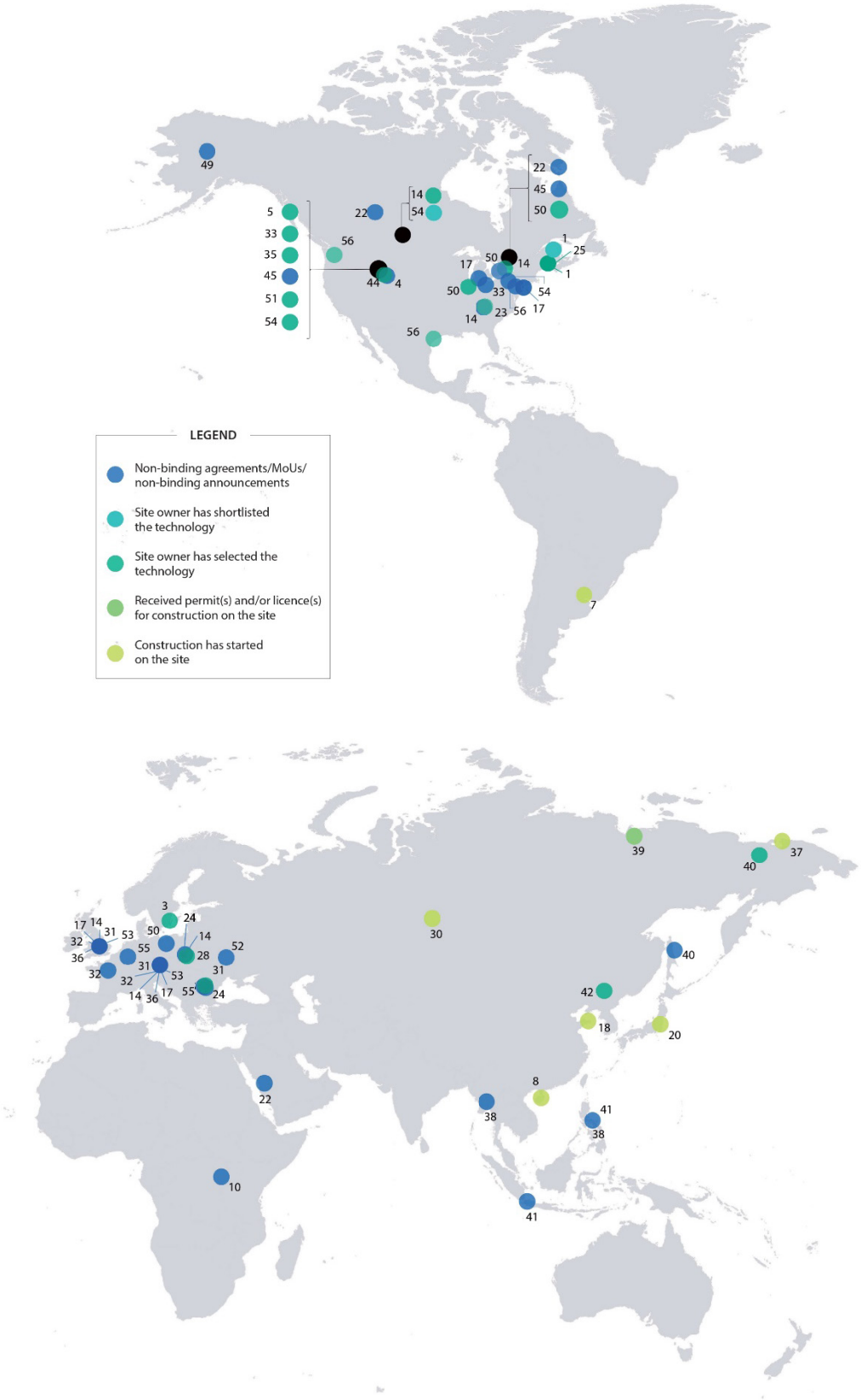

Figure 3: Global SMR sites and projects. [20, pp. 36-37]

The novel designs of SMRs promote flexibility in several areas. Whereas LNPPs face strict prerequisites in terms of siting, SMRs are designed to be placed more freely and closer to consumers. A modular design offers the potential for scaling according to local need. The applications of SMRs are planned to extend outside of traditional baseload power production, with some potential roles in desalination, hydrogen production, and district heating [20, p. 20]. As of 2024, the Nuclear Energy Agency (NEA) has identified 98 different SMR designs [20, p. 11]. Designs vary considerably in power and temperature outputs as well as technology types and operational characteristics. In addition to land-based operation, SMR concepts include marine and mobile versions.

Due to years of experience in LNPPs, it follows that land-based SMR designs utilizing light water technology are furthest in developmental status. Light water SMRs incorporate scaled-down technology from large conventional light-water nuclear power plants. Smaller cores and smaller amounts of nuclear material allow for less safety systems, which are often designed to function passively. The majority of light water SMR vendors intend to use low-enriched uranium fuel in the currently commercially available form [20, p. 33]. Individual SMR designs may feature innovative solutions, such as an integrated primary circuit, where the components of the circuit are enclosed within the reactor pressure vessel.

3 District Heating

District heating (DH) is a centralized heating system used to supply heat for industrial, commercial, and residential purposes. The system involves heating water at a power plant and supplying the hot water to customers through underground pipes. Once the water has reached an end-user, it releases heat in the customer-side heat exchanger and returns to the power plant through separate return pipes. The same water is reheated and cooled in a continuous cycle.

District heating is a cost-effective heating option for densely populated regions, notably in cold climates. In such areas, the same infrastructure can be used to serve a number of consumers, maximizing efficiency and minimizing costs. The market share of DH is particularly high in the Baltics as well as the Nordics, with the exception of Norway [21]. In Finland and Sweden, district heating accounts for approximately half of residential heating demand, and in Denmark the share exceeds 60 % [22]. Outside of Europe, district heating is a prominent system in Russia as well as China and exists to a certain extent also in the United States [23].

In Finland, district heating has been a prevalent heating method for almost a century. The feasibility of a wide heating network was investigated already during the 1930's, although combined heat and power production had been used to heat buildings at a small scale since the beginning of the 1900's [24, p. 3]. This eventually led to building the first district heating network for the Olympic village in Helsinki, 1940. [24, p. 3] District heating of the Helsinki area officially began in December of 1952 and extended to the city of Espoo the following year [25, pp. 15-16]. Today, district heating is the most popular heating method in Finland. The Finnish district heating system involves over 16 000 km of piping infrastructure and distributes heat to over 50 % of all residents in the country. [26]

The advantages of district heating essentially amount to stability, reliability, and flexibility. The primary production method of heat recovery not only establishes a steadily available heat source but also ensures that DH prices remain rather stable and unaffected by electricity prices. As spikes in electricity and heat demand have historically occurred simultaneously, sufficing peak heat demand with district heating instead of electricity-based heating promotes the stability of the electricity market and the reliability of electricity production [4]. Although DH production has traditionally relied on fossil fuels, several approaches can be used to heat water, facilitating a transition to sustainable energy sources.

3.1 District Heating Demand

From 2013 to 2022, annual district heating consumption in Finland has amounted to an average of 32 TWh [26]. Typically, dwelling houses account for slightly above

fifty percent of total demand. The remainder is consumed by other building varieties and industrial end-users. Heating is delivered by over 100 companies, of which a majority operate at a local level and supply only small quantities of heat, that is, less than 200 GWh yearly. However, some companies notably in the Finnish capital region deliver heat at a wider scale, at times in multiple municipalities and to several networks. [21]

Although networks exist as far north as Lapland, the consumption of district heating is by far greater in Southern Finland due to the higher population density of the region. Table 1 lists the populations and DH consumptions of important cities across Finland as of 2022. The consumption volumes experience relatively little yearly variation. Per resident, the DH consumption in cities mentioned in Table 1 range roughly from 7,7 to 10,5 MWh, with an average of 8,8 MWh per resident. Overall, the coverage of district heating in residential buildings is above 70 % in all cities with more than 100 000 habitants.

Table 1: Populations and district heating consumptions of Finnish cities, 2022 [26]

City	Total number of residents	Total DH Consumption (GWh)*	Share of residents connected to DH (%)
Helsinki	664 028	6 895,2	72,3
Espoo	305 274	2 344,4	80,8
Tampere	249 009	2 208,5	97,1
Vantaa	242 819	1 968,5	93,5
Oulu	211 848	1 906,4	74,0
Turku	197 900	1 746,9	93,1
Jyväskylä	145 887	1 203,2	73,5
Kuopio	122 594	1 088,6	91,7
Lahti	120 175	1 265,6	82,8
Pori	83 205	717,7	46,0
Rovaniemi	64 535	555,10	57,9

**Includes residential, industrial, and other district heating consumption with losses taken into consideration.*

The demand for heat fluctuates vastly during the year by cause of varying outdoor temperatures. The effect is presented for the case of Helsinki, 2022, in Figure 4. Temperatures are lowest and heat demand is highest during the main heating season, which comprehends the months from September to April. The demand for space heating during summer months is virtually nonexistent, but a baseline of heating is still maintained mostly for warm tap water supply.

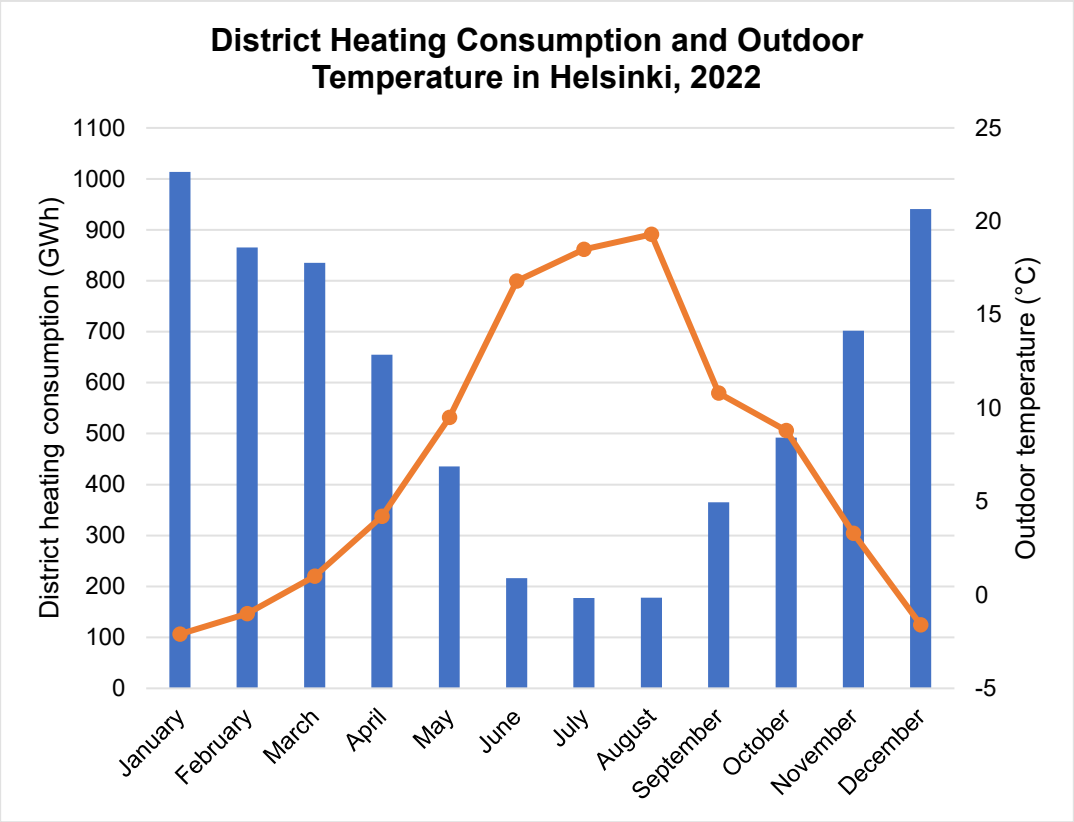

Figure 4: Monthly district heating consumption and outdoor temperature in Helsinki, 2022. [27], [28]

The highest hourly heat consumption during a year is described as the peak power demand. It is an important indicator of the maximum local heat demand and defines the dimensioning of district heating production facilities. Estimated average peak power demands of Finnish cities are listed in Table 2. The averages are based on Helsinki, where peak power demand is in the range of 2 000-2 500 MW [27]. Peak power estimates of other Finnish cities are formed by scaling Helsinki peak power with local DH consumption volumes.

Table 2: Estimates of average peak power demands formed by scaling Helsinki data from 2015-2022. [27]

City	Estimated average peak power (MW_{th})
Helsinki	2 300
Espoo	800
Tampere	700
Turku	700
Vantaa	600
Oulu	600
Jyväskylä	400
Lahti	400
Kuopio	400
Pori	200
Rovaniemi	200

3.2 District Heating Distribution

District heating is supplied through urethane-insulated steel pipes covered by a plastic protection pipe. The size of the DH pipes varies from DN20 in small residential service lines to DN1200 in pipes exiting major power plants. The design pressure for modern district heating networks is 16 bar, and pipes are dimensioned within pressure loss limits, which is 2 bar/km in main pipelines [29, pp. 1,7]. The district heating system is coupled indirectly with the end-user central heating system, implying that DH water is neither used as tap water nor circulated through radiators. The lengths of the main pipelines depend on the distance between a production facility and an urban center, and are calculated individually for each business case. For example in the Finnish metropolitan area, DH production facilities are in the radius of 10-30 km of city centers.

In general, district heating water is supplied at a temperature between 65 and 115 ºC. The temperature of the supply water is altered according to heating demand, which correlates with outdoor air temperature. The weather, time of day, and day of the week also influence demand and the temperature of the supply water. The correlation between outdoor temperature and DH supply water is shown in Figure 5. The supply temperature of DH water in existing networks is typically 90-115 °C during wintertime and 70-80 °C during summertime [30, p. 14].

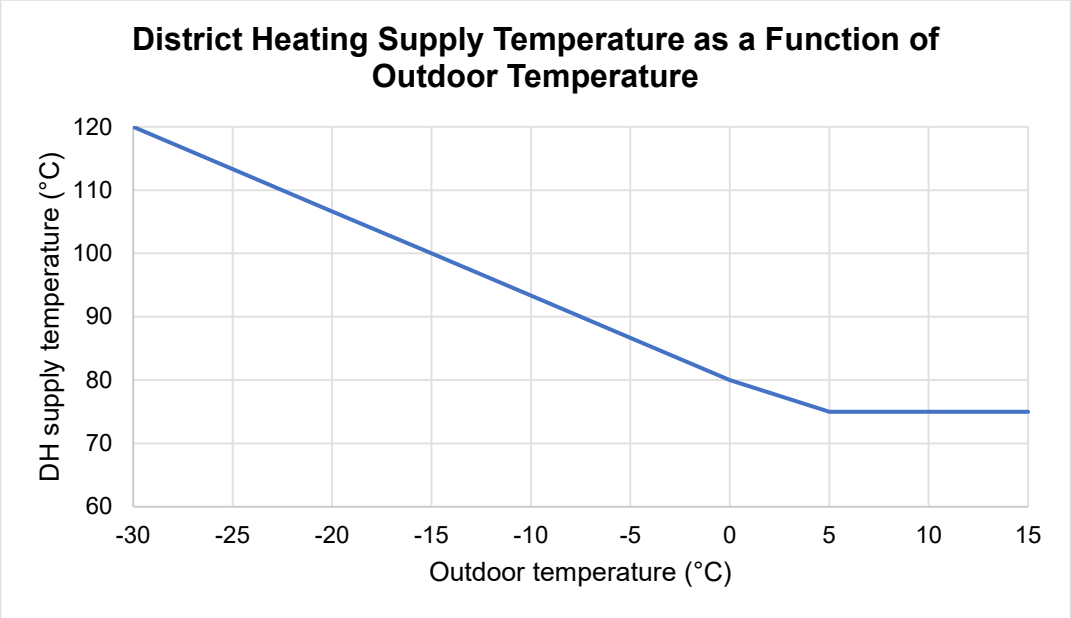

Figure 5: A DH supply temperature control curve as a function of outdoor temperature. [31]

Return water temperatures generally range between 40 and 60 °C. DH return water temperatures tend to rise in the summer, when the majority of the supplied district heating is used for domestic hot water, which must be heated to a high temperature. Similarly in the winter, overall high supply temperatures result in higher return temperatures. The temperature of the return water is largely affected by the designs of user-end heat distribution centers particularly during the winter. Furthermore, user behavior contributes to heat consumption and thus return temperatures. The heat demand between individual consumers may differ significantly as water consumption and heat exchanger performance vary. [31]

Finnish DH networks are currently transitioning to a low-temperature system. This implies that the previous supply water design temperature of 115 °C is being replaced by a lower design temperature of 90 °C. New DH networks with all-new equipment can be designed for supply temperatures as low as 80 °C. Distributing water at a lower temperature decreases heat losses and pumping costs. Moreover, it brings forth the possibility of heat production via unconventional methods, such as solar heat and heat pumps, that are not capable of providing the high temperatures required previously. The transition is made possible by, among other things, renewing customer-side heat exchangers and refurbishing DH distribution equipment to accommodate the required larger DH water flow. This is a gradual process, which will require several years to complete. [32]

3.3 District Heating Production

The yearly fluctuation in demand makes it sensible to utilize different production technologies for supplying base-, middle-, and peak load district heating. The merit order of production is defined by operational costs, which are lowest for baseload technologies that are operated continuously throughout the year. Contrarily, peak load technologies are high in operational costs but low in capital expenditures and capable of fast ramp up. Middle load technologies feature qualities from both extremes: they are capable of partial load operation and are moderately low in both operational and capital costs. The capacities of each technology are defined by utilizing a heat load duration curve, which describes the duration of the required capacity. An example is shown in Figure 6, which presents the estimated load duration curve for all of Finland in 2022.

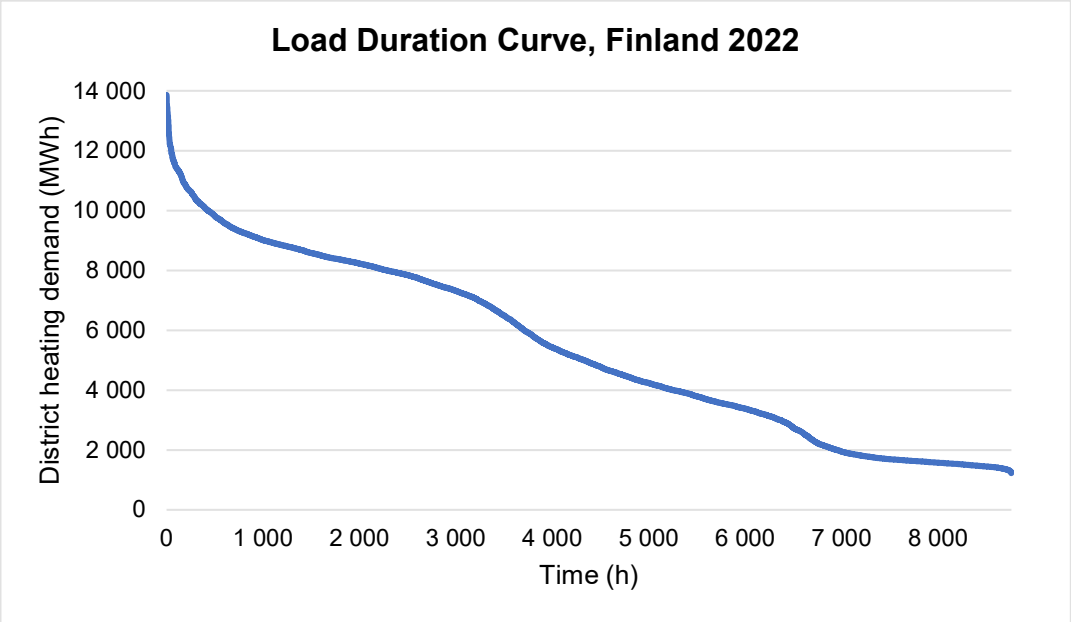

Figure 6: An approximate load duration curve for Finland formed by scaling Helsinki data. [27]

Total district heating production in Finland can be roughly divided between three primary technologies: CHP plants, heat-only boilers, and heat pumps. CHP plants and heat pumps serve to supply baseload capacity, whereas heat-only boilers suffice peak demand. In 2022, the total district heating capacity
of all production plants amounted to roughly 23 600 MW. The capacity of a production technology does not necessarily correlate with its total yearly production. For example, heat-only boilers have a higher production capacity than CHP plants because they are not operated regularly. This is evident from Figure 7 a) and b), showing the division of total DH capacity and production between the three primary technologies.

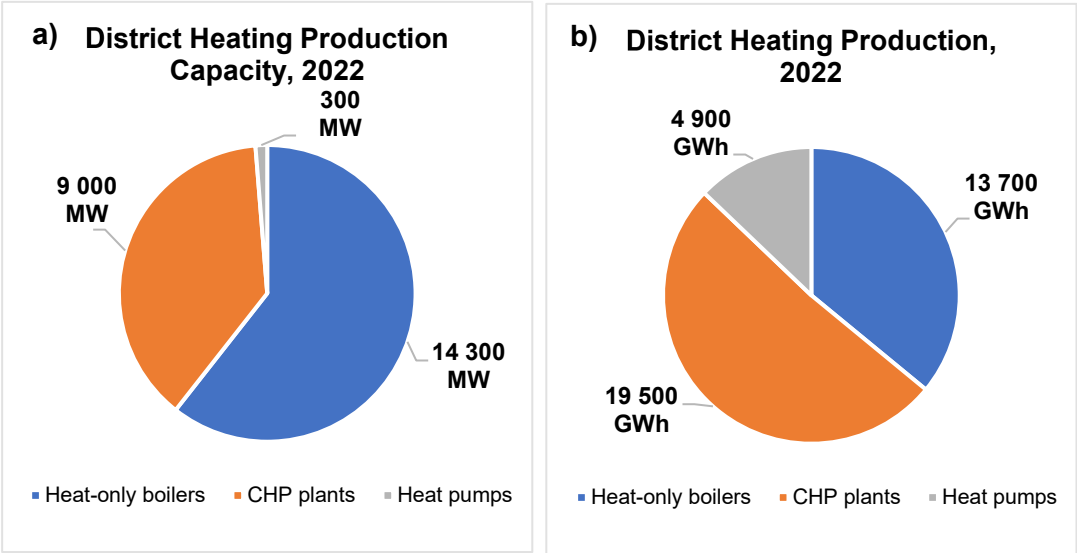

Figure 7: District heating a) capacity and b) production in 2022. [26]

3.3.1 Combined Heat and Power Production

Since the first networks, Finnish district heating has been based on combined heat and power (CHP) generation. Yearly production through CHP amounts to some 50 % of total district heating and some 10 % of total electricity supply. Today, a majority of CHP production is fueled by wood-based fuels as presented in Figure 8.

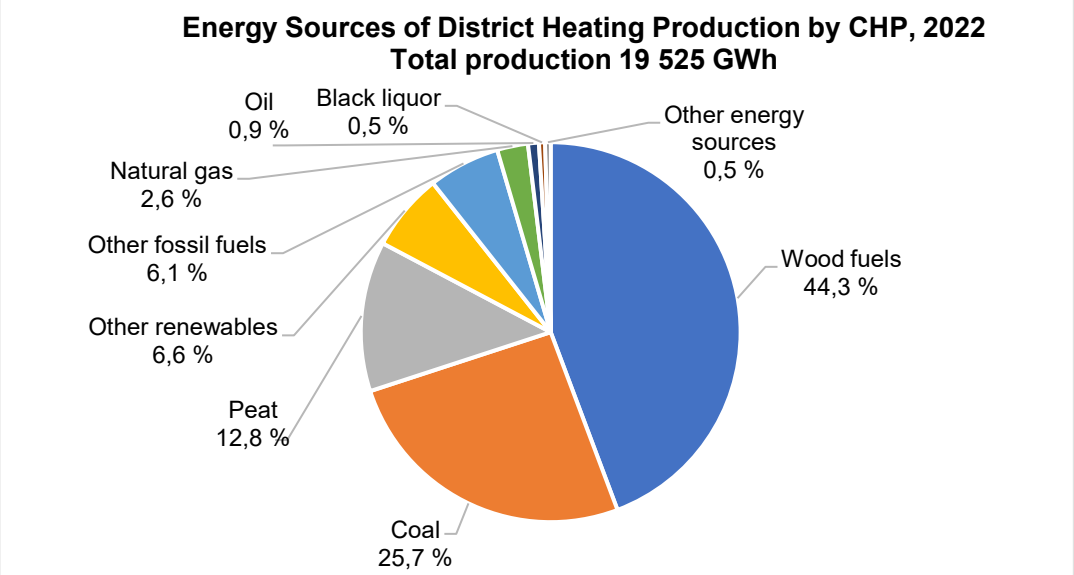

Figure 8: Energy sources[2] of CHP production in Finland. [33]

[2] Other fossil fuels include gas and coke, plastics fuels, fossil-based waste fuels, and fossil-parts of mixed fuels. Other renewable fuels comprise the bio-part of mixed fuels and biogas. Other energy sources include hydrogen, electricity, and the secondary heat of industrial processes. Renewable energy sources are peat, black liquor, wood fuels, and other renewables. [33]

Historically, the share of CHP in the district heating production mix has been noticeably higher than it is today: close to 75 % in the early 2000's [34, p. 10]. The decline of CHP technology is attributable to a multitude of factors, most of which are interconnected and reflect an wider transformation of the energy sector. A pivotal cause is the transition away from fossil fuels due to environmental, economic, and geopolitical concerns. This has led to a decrease in the usage of natural gas and a planned phase-out of coal by 2030 [3]. Consequently, large coal-fired CHP plants are shutting down, most recently the Helsinki Hanasaari B plant in 2023 with a thermal output of 420 MW. Concurrently, industrial heat pumps and electric production systems are now able produce higher output temperatures with greater energy efficiencies, which has facilitated their implementation into the heating scene and lessened the demand for CHP production [35].

Nevertheless, CHP production continues to serve a central function in the reliability of heat and electricity supply. Finland has slightly over 100 CHP plants with average DH and electric capacities of 170 MW_{th} and 100 MW_e [26]. CHP plants are traditionally backpressure plants with the primary purpose of sufficing heat supply. Thus, a general guideline for determining the capacity of a CHP plant is so as to cover half of the local DH peak demand [30, p. 12]. Peak power estimates of major Finnish cities were presented in Table 2. This ground rule is not necessarily applicable to metropolises or areas with complex energy mixes, as is evident from the case of Helsinki, where a plant supplying over 1 000 MW of heat would be impractical. The guideline does, however, provide an insight of the magnitude of the required heating capacity, particularly in the case of smaller cities.

The capacity of a CHP plant is defined by the overall state of the local DH network and electricity supply mix. Substitutive energy sources, the size of both the DH and the electricity networks, heat storages, and transmission distances, for instance, contribute to defining the actual capacity deficit. To gain an understanding of typical district heating outputs of CHP plants in Finland, CHP unit capacities are listed in Table 3.

Table 3: DH capacities of CHP units in Finnish cities as of 2022. [26]

City	Number of CHP units	DH capacity range of a CHP unit (MW_{th})**	Average DH capacity of a CHP unit (MW_{th})**
Helsinki*	4	160-430	330
Espoo	3	160-210	150
Tampere	3	50-260	160
Turku	2	170-260	300
Vantaa	4	90-150	120
Oulu	3	180-240	160
Jyväskylä	2	260	260
Lahti	5	90-200	110
Kuopio	2	300	300
Pori	3	140-160	150
Rovaniemi	1	140	140

**The data includes Hanasaari B (429 MW_{th}, 218 MW_e) shut down in April of 2023.*
***Capacities of conventional large-scale CHP plants. CHP plants with very small outputs are excluded.*

3.3.2 Separate Heat Production

District heating demand that cannot be fulfilled through baseload production is supplied through separate heat production, predominantly by heat-only boilers. Heat-only boilers are operated in times of high heating demand and during exceptional circumstances such as malfunctions. Like CHP production, separate heat production is mainly fueled by wood-based biofuels as shown in Figure 9. Electricity is increasingly utilized in boiler technology: district heating through electric boilers increased from 60 GWh to 710 GWh just between the years 2022 and 2023 [36].

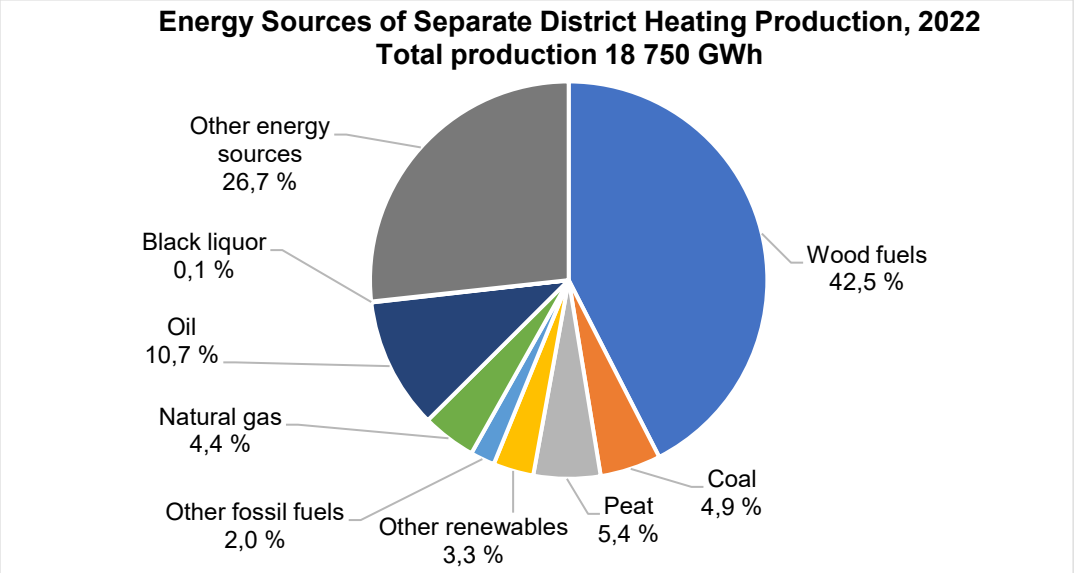

Figure 9: Energy sources of separate DH production in Finland, 2022. See Footnote 2 on page 17 for category definitions. [33]

Similarly, the utilization of heat pumps in district heating has increased by almost 50 % during 2017-2022 [36]. In 2022, heat pumps and waste heat recovery accounted for 4 900 GWh and 13,4 % of total district heating production. [34] Currently, over 30 heat pump facilities are operated across Finland. To produce heating, a heat pump uses external power to transfer heat from a low-temperature source to a high-temperature source. The low-temperature source is typically air or water. A key indicator describing how efficiently heat pumps operate is the Coefficient of Performance (COP), shown in Equation 1. The COP expresses how many units of heat a heat pump can produce by consuming one unit of external energy.

$$COP = \frac{Q_H}{W}, \quad (1)$$

where Q_H is the transferred heat and W is the work performed by the compressor of the pump. [37, p. 108]

The COP is increased if the heat pump is coupled with a waste heat source, which is usually the case with district heating pumps. The COP of most industrial-scale heat pumps tends to range between 3 and 4. Table 4 presents examples of district heating heat pump facilities and their COPs in Finland.

Table 4: Heat pump units used for district heating production in Finland. The COP is calculated in terms of maximum district heating power presented in the third column. [26]

Unit name	Heat source	District heating power (MW)	COP
Suomenoja 4, HP1 + HP2	Waste water	43	**3,31**
Suomenoja 4, HP3	Waste water	22	**3,14**
Katri Vala, Helsinki	Waste water, district cooling water	105	**3,50**
Esplanadi, Helsinki	District heating and cooling return water	22	**2,89**
Vuosaari heat pump	Power plant cooling circuit	12	**3,05**
Kakola heat pump	Waste water, district cooling water	2*21	**3,23**

3.3.3 Heat Storages

Thermal energy storages balance fluctuating district heating demand in a sustainable and cost-effective manner, as the emissions and operational costs of storages are essentially nonexistent. In CHP plants, heat storages enhance the coupling between heat and electricity production by enabling the optimization of plant loads based on electricity demand. Further, storages lessen frequent load changes of heat-only boilers, allowing for a more constant output and a better boiler efficiency. Overall, when operated during peak demand, heat storages reduce the need for installed peak capacity. [38, p. 627]

A DH storage is traditionally an insulated steel container placed above or underground. The storage is charged simply by directing hot water into the container and discharged by releasing water into the district heating network. The container may be pressurized or kept at atmospheric pressure, which defines the temperature limits and the coupling method of the storage with the DH network. The size of a heat storage can be defined to balance daily, weekly, or seasonal fluctuation in demand. In the case of intraday heat storages, it is generally most profitable to discharge the storage during the day when heat demand is high and charge the storage at night. Larger storages, such as weekly or seasonal storages, can account for a wider timespan and supply heating when overall periodic demand is low. As the size of the storage increases, the share of heat losses in total storage expenses increases. Thus, a large storage is not automatically profitable, although a larger heat storage is more cost-effective relative to its size. Table 5 lists examples of district heating storages either in operation or under construction in Finland.

Table 5: Examples of district heating storages in Finland. Compiled using sources [39], [40], [41, p. 23], [42], [43], [44], [45], and [46].

Operator and location	**Capacity (MWh)**	**Volume (m^3)**
Helen Oy, Mustikkamaa	11 600	260 000
Fortum Heat and Power Oy, Suomenoja	800	20 000
Tampereen sähkölaitos Oy	100	2 300
Turku Energia Oy AB	300	6 000
Vantaan Energia Oy, Kuusikonmäki*	90 000	1 100 000
Oulun Energia Oy, Laanila	8 000	190 000
Alva-yhtiöt Oy, Rauhalahti (Jyväskylä)**	800	1 500
Lahti Energia Oy	480	10 000
Kuopion Energia Oy, Haapaniemi	800	15 000

**Under construction, operation to begin in 2028.*
***Under construction, operation to begin in 2026.*

3.3.4 Nuclear District Heating

Although unseen in Finland, the concept of district heating production via nuclear energy is not novel. The plants of Beznau 1 & 2 in Switzerland [47, p. 32], Haiyang in China [48] and Bohunice 3 & 4 in Slovakia [49], for instance, supply district heating to nearby communities. Russia, Ukraine, Romania, Bulgaria, and Hungary are also known to have successful demonstrations of nuclear district heating [50, p. 16]

An effective Nordic showcase of nuclear district heating is the first power-producing nuclear reactor in Sweden, Ågesta, which produced both electricity and district heating from 1964 to 1974. The Ågesta reactor was a pressurized heavy-water reactor with a total capacity of 80 MW: 12 MW of electricity and 68 MW of district heating. Ågesta was a development project executed as a collaboration between Vattenfall and AB Atomenergi. Due to the experimental nature of the project, the developers encountered financial issues. Construction and material costs proved to be of concern already during the building phase, and eventually it became clear that prolonging the operation of the plant would require significant investments. The commissioning of Ringhals 1 in 1975 further supported the claim that Ågesta was to become outdated. Ågesta was shut down in June 1974, and the dismantling of the reactor began in 2020. [51]

In Finland, the possibility of nuclear district heating has been researched notably during the Loviisa 3 newbuild project in 2007-2010. The purpose of the Loviisa 3 project was to assess the possibility of a third reactor unit in connection to Fortum's two existing units, Loviisa 1 and 2. The three-year study included technical, economical, and environmental assessments as well as discussions with vendor candidates. A significant component of the study involved evaluating the feasibility of a large-scale CHP turbine providing district heating for the Helsinki metropolitan area. Ultimately, the Finnish Government did not grant a Decision in Principle for the new power plant, and the project was terminated. The gathered information has since been utilized for later nuclear newbuild projects in Finland. [52]

4 Fundamentals of Steam Power

Steam power plants are the most prevalent type of power generators in the world, accounting for over 60 % of total global energy supply [53, p. 6]. Steam power plants use steam as a medium to transfer heat and convert it into electrical energy. Table 6 presents examples of steam power plant types. Most steam power plants rely on the combustion of coal, oil, or biomass for thermal energy production, whereas in nuclear power plants this is achieved via nuclear fission.

Table 6: Capacities and efficiencies of steam power plants [54, p. 82]

Steam power plant	Electric capacity (MW)	Thermal efficiency (%)
Subcritical (lignite, coal)	300-1 200	42-45
Subcritical (gas, oil)	200-1 000	44-47
Nuclear, PWR	500-1 500	33-34

Even the most intricate steam power plants can be considered simple heat engines with the purpose of converting thermal energy into mechanical energy and further into electricity. In essence, a heat engine produces work by consuming heat from a high-temperature source and rejecting it to a low-temperature source. The acquired useful work from the cycle can thus be expressed as the difference between the heat added into and the heat rejected from the system. By repeating the processes of heat addition and heat rejection, a thermodynamic cycle is formed. [55, p. 87]

The fundamental operation of a heat engine can be studied using the Carnot cycle. The Carnot cycle is the ideal thermodynamic cycle for a heat engine with a reversible thermodynamic process. It is comprised of two isentropic and two isothermal processes, as shown on a temperature-entropy (T-s) diagram in Figure 10. The area outlined by the process on a T-s diagram is equivalent to the work done during the thermodynamic cycle. For any thermodynamic cycle, the thermal efficiency can be expressed as the ratio of obtained work (q_{net}) to supplied heat (q_{in}). For ideal, reversible cycles, the Carnot efficiency further simplifies the computation of the efficiency to be dependent of only the temperatures of heat addition (T_h) and rejection (T_c). Equation 2 presents the derivation of the Carnot efficiency using points in Figure 10. [56, pp. 35-37]

$$\eta_{Carnot} = \frac{q_{net}}{q_{in}} = \frac{(T_h - T_c)(s_3 - s_2)}{T_h(s_3 - s_2)} = \frac{T_h - T_c}{T_h} = 1 - \frac{T_c}{T_h} \qquad (2)$$

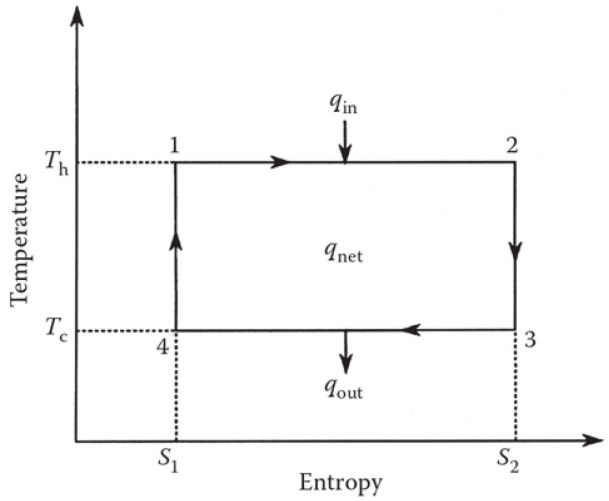

Figure 10: The Carnot thermodynamic cycle on a T-s diagram. [54, p. 76]

It thus follows that under ideal conditions, the Carnot cycle is completely reversible. In practice, the Carnot efficiency is never achieved as all thermodynamic cycles entail irreversibility, that is entropy generation. The Carnot efficiency is independent of the working fluid and merely sets a maximum for the efficiency of a heat engine operating between two fixed temperature levels. Despite being theoretical, the value aids in designing thermodynamic processes and provides a basis for comparison between heat engines. [56, pp. 37-38] The Carnot cycle also demonstrates that the efficiency of a power cycle can be improved by minimizing entropy generation [37, p. 352].

4.1 Rankine Cycle

The ideal cycle used for condensing steam power plants is instead the Rankine cycle. A simple Rankine cycle features four main components: a steam generator (or a boiler), a steam turbine, a condenser, and a pump. The four main components pictured in Figure 11 are the locations for the four main processes of the cycle. Between points 1 and 2, the fluid undergoes isobaric heat addition in the steam generator, during which saturated water is heated into saturated steam. From point 2 to point 3, the steam expands isentropically and releases energy in the turbine. In the next isothermal, isobaric process between points 3 and 4, most steam is condensed back into saturated water and some heat is rejected into the environment. Finally, between points 4 and 1, the water is compressed isentropically by a pump back to its original state. The resulting temperature-entropy diagram is shown in Figure 12 a).

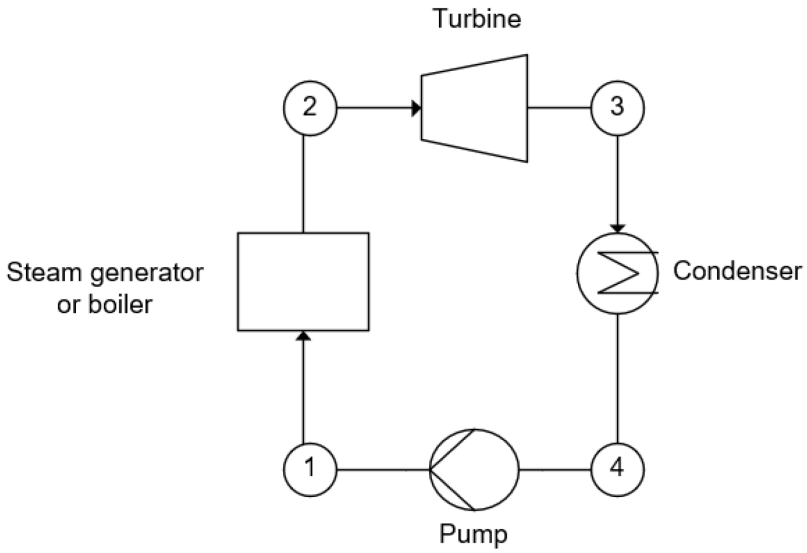

Figure 11: Components of a simple Rankine cycle.

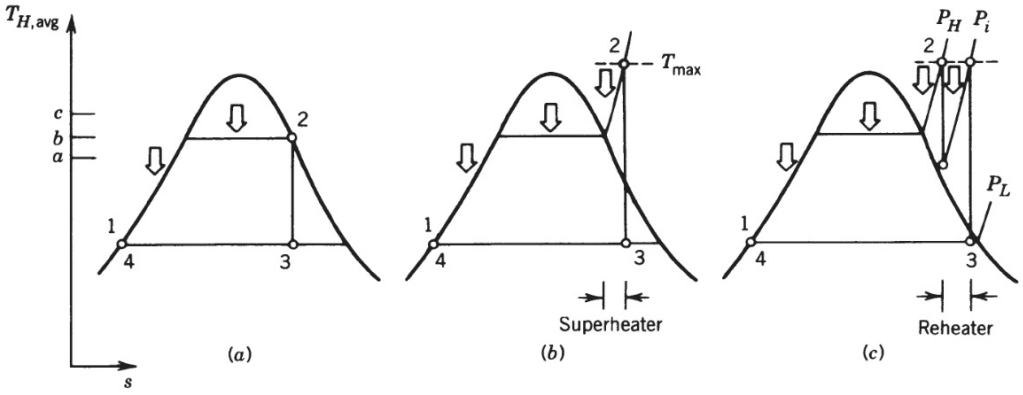

Figure 12: The T-s diagram of a) a simple Rankine cycle b) with one superheater and c) with both a superheater and a reheater. [37, p. 353]

The Carnot efficiency in Equation 2 demonstrated that the efficiency of a thermodynamic cycle can be improved by minimizing entropy generation, that is by a) increasing the temperature of heat addition or b) decreasing the temperature of heat rejection. To address the former, most Rankine cycles include the additional process of superheating. Shown in Figure 12 b), superheating involves heating the live steam above the saturation curve without boiling. Superheated steam is dry steam with a zero moisture content. The process is usually achieved by installing a superheater component before the steam turbine. Figure 12 c) demonstrates the effect of reheating, where the steam is reheated (or re-superheated) once more in between high- and low-pressure turbine stages. The process of reheating does not result in efficiency gains – in fact, re-superheating lowers cycle efficiency due to the lower

saturation pressure and boiling temperature of superheated steam. The advantages of reheating lie namely in an improved steam quality as steam wetness and the droplet erosion in the turbine are minimized. [37, p. 353]

In addition to superheating live steam, a common practice to increase the temperature of heat addition involves heating the water returning to the boiler. This process is referred to as feedwater preheating or regenerative feed heating. By heating the feedwater before it reaches the boiler, less fuel energy is needed to heat the water to the temperature of the live steam. Feedwater preheating is executed with additional contact heaters in which the feedwater is heated by steam bled from turbine stages. Figure 13 shows the T-s diagram of a preheating Rankine cycle, where the optimal number of feedwater preheaters (i) is such that the enthalpy change of the heated water is constant in each heater. [37, pp. 355-359] Conventional steam cycles usually incorporate between 6 to 8 preheater components [30, p. 64].

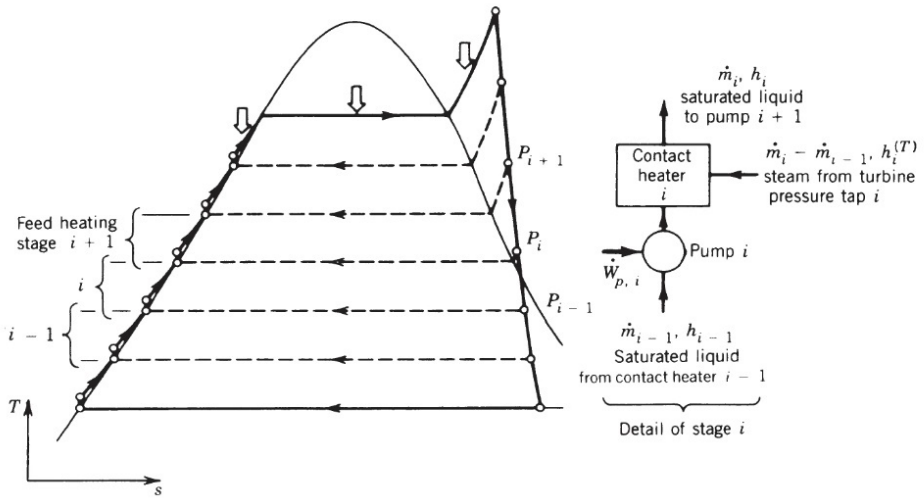

Figure 13: A Rankine cycle with a superheater and a train of feedwater preheaters. [37, p. 357]

Finally, a third approach to improving cycle efficiency is through lowering condenser pressure, which reduces condenser-ambient heat transfer. The condenser pressure is dependent on the temperature of the cooling source – the colder the medium, the lower the pressure. Water-cooled condenser pressures are typically close to 0,04 bar and may reach values lower than 0,03 bar with cooling water temperatures below 20 °C [54, p. 84]. Figure 14 demonstrates how a lower condenser pressure reduces exergy loss and increases the net work of the Rankine cycle.

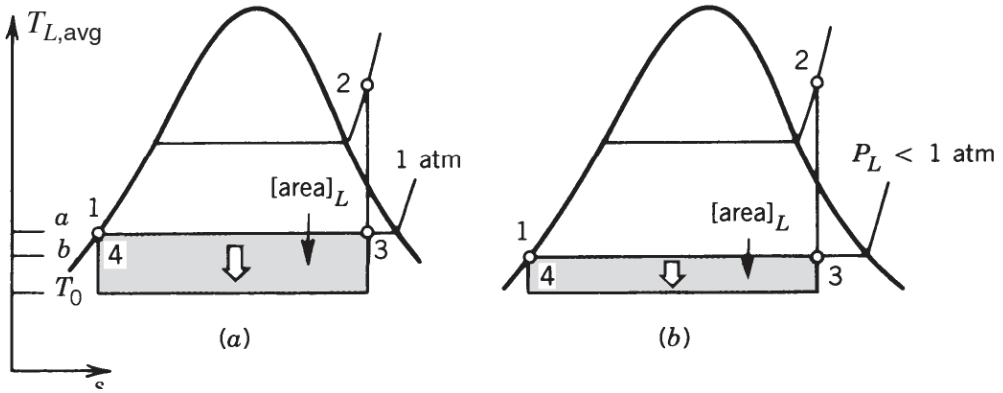

Figure 14: A Rankine cycle with one superheater and a) a condenser pressure of 1 atm and b) a condenser pressure below 1 atm. The shaded area $[a]_L$ represents the exergy lost due to heat transfer between the ambient environment and the condenser. [37, p. 354]

The net specific useful work of the Rankine cycle w_{net} is defined as the difference between the heat added into the boiler q_{in} and the heat rejected into the ambient q_{out}. Because pump work w_p is ideally isentropic, it can often be disregarded, and the net specific useful work is roughly equal to the specific work of the turbine w_t:

$$w_{net} = q_{in} - q_{out} = w_t - w_p \approx w_t = h_1 - h_2 \ \frac{kJ}{kg}, \tag{3}$$

where h_1 and h_2 are the enthalpies of the live steam and the turbine exhaust steam respectively.

Heat addition per mass unit of the working fluid is defined as the difference between the enthalpies of the live steam h_1 and the returning feedwater h_4. When $w_p \approx 0$, the enthalpy of the feedwater h_4 is equivalent to that of the condensate h_3:

$$q_{in} = h_1 - h_4 \approx h_1 - h_3 \ \frac{kJ}{kg}. \tag{4}$$

The efficiency of a Rankine cycle is defined as the ratio of the obtained net specific useful work to the heat added to the cycle. It follows that the efficiency can be determined according to the enthalpy of the working fluid after the steam generator (h_1), the turbine (h_2), and the condenser (h_3) [54, pp. 79-80]. The equation becomes

$$\eta_{th} = \frac{w_{net}}{q_{in}} = \frac{w_t}{q_{in}} = \frac{h_1 - h_2}{h_1 - h_3}. \tag{5}$$

4.1.1 Secondary Cycle of a Pressurized Water Reactor

In PWRs, the Rankine cycle takes place in a separate coolant circuit referred to as the secondary cycle. The cycle is completely isolated from the radioactive primary side, and heat transfer from the core occurs via a steam generator. While the fundamental thermodynamic cycle remains the same, some differences in process parameters and components occur compared steam power plants relying on combustion. Table 7 lists typical operating parameters of PWRs according to unit size.

Table 7: Technical parameters of conventional PWR plants. [7, p. 52]

		500 MW_e class	**800 MW_e class**	**1 100 MW_e class**
Primary circuit	Reactor thermal power (MW_{th})	1 645	2 652	3 411
	Primary side pressure (bar)	155	155	155
Secondary circuit	Live steam flow rate (t/h)	3 240	5 220	6 760
	Main steam pressure (bar)	57,9	54,5	61,3
	Feedwater temperature (°C)	221,1	221,0	223,3

The steam entering the secondary cycle from the steam generator is typically at a pressure of 55-70 bar and a temperature of 269-285 °C [57, p. 37]. The steam is in a saturated state and at a relatively low pressure compared to combustion-based steam plants, where live steam is superheated and at a high pressure. The state of the steam depends on the steam generator, which in most conventional PWRs is a vertical U-tube heat exchanger [57, p. 35]. U-tube heat exchangers are essentially parallel-flow heat exchangers, where the outlet temperature of the cold fluid cannot exceed that of the hot fluid. This implies that the generated steam can never be hotter than the exiting reactor coolant. In some cases however, a counterflow heat exchanger may be used, allowing for a superheated state. This is discussed in Chapter 5.1. Even then, the steam is not as superheated as in combustion-based steam plants due to operating conditions limited by the nuclear reactor. The choice of steam generator and the state of the steam are ultimately influenced by safety, material, and design considerations. [58, p. 679]

In terms of components, nuclear steam cycles utilize wet-steam turbines designed to accommodate the lower pressure and higher moisture content of steam. A lower main steam pressure results in a larger volume flow, which can be five-fold compared to combustion-based steam power plants [7, p. 54]. Consequently, wet-steam turbine components are larger in size. Wet-steam turbines incorporate internal moisture separation features within the steam path and are also commonly equipped with external moisture separators and reheaters. As stated, reheating lowers cycle efficiency, but the process is necessary to protect the turbine structures from water

droplet erosion. [59, pp. 40-43] Ordinarily, nuclear power plants utilize regenerative cycles with six or more feedwater preheaters [7, p. 54].

4.2 Combined Heat and Power Production

Combined heat and power (CHP) generation, also referred to as cogeneration, maximizes the potential of the primary energy supplied to a system. Cogeneration refers to simultaneously producing both electric power and useful heat from a single fuel source during the same steam cycle. The useful heat is produced in the form of steam or hot water and utilized for industrial processes or district heating. Whereas the average global efficiencies of condensing steam power plants is close to 35 % [53, p. 82], the overall thermal efficiencies of CHP plants can reach values between 80-90 %. [53, p. 206]

In Finland, cogeneration technology has existed since the early 1900s when the wood processing industry began combining electricity production with process heat generation. As district heating networks developed during the 1950s, cogeneration technology was shown to have applications in residential heating as well, which further fueled the construction of CHP plants. [24, p. 11] Today, CHP production is at the core of the Finnish energy supply. Generally, CHP covers a fourth of electricity, half of district heat, and three-fourths of industrial heat production [33].

The concept of CHP production involves harnessing useful heat from a steam cycle. The application of the heat determines the method and the temperature at which the useful heat is produced. For instance, the water lead into district heating networks ranges from 60 to 115 °C, while hot steam required for industrial processes can attain temperatures of 300 °C [60, p. 12]. Normally, the exhaust water from the condensers of condensing steam power plants is too cold to be utilized for useful heat supply as is. Therefore, cogeneration requires some changes in the components and the configuration of a condensing steam power plant cycle.

Most conventional CHP plants are backpressure plants, the concept of which is depicted in Figure 15. These plants utilize backpressure turbines, which are noncondensing steam turbines with an exhaust pressure in the range of 1 to 8 bar [54, p. 211]. The turbine is connected to a district heat exchanger, which defines the pressure level of the last turbine stage or the backpressure. Increasing backpressure reduces the enthalpy drop of the expanding steam, decreasing the net work and electric output of the cycle. Backpressure turbines also lack a condenser component. Consequently, the electric power production capabilities of backpressure plants are limited and without additional components, they are not capable of power-only production. For heat production however, the energy efficiency potential of backpressure plants is high, as theoretically no heat is lost through condensing. [54, p. 212]

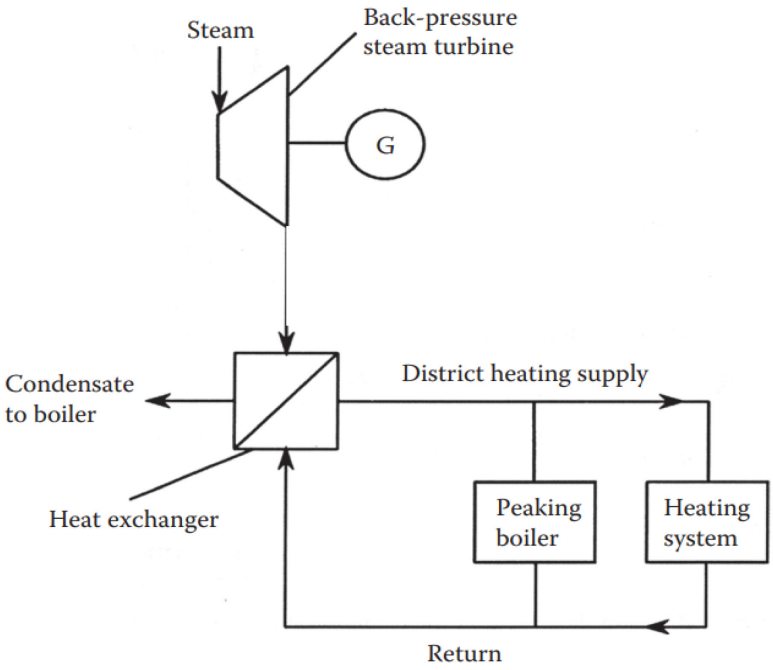

Figure 15: A schematic of a backpressure steam turbine paired with a district heating network. [54, p. 211]

Another feasible method of extracting useful heat is by bleeding steam from the midst of a turbine, commonly the low-pressure section. The configuration is depicted in Figure 16. An extraction turbine exhausts steam into a condenser at a pressure below 1 bar, usually in the range of 0,03-0,05 bar [54, p. 210]. The pressure of the extracted steam from the turbine corresponds to the DH supply water temperature. This cogeneration method offers improved operational flexibility compared to a backpressure turbine, as extraction-condensing turbines are capable of operating in condensing mode and during times of low heat demand. Due to the limited power adjustability of nuclear plants, this heat production method is likely more applicable for nuclear heat production.

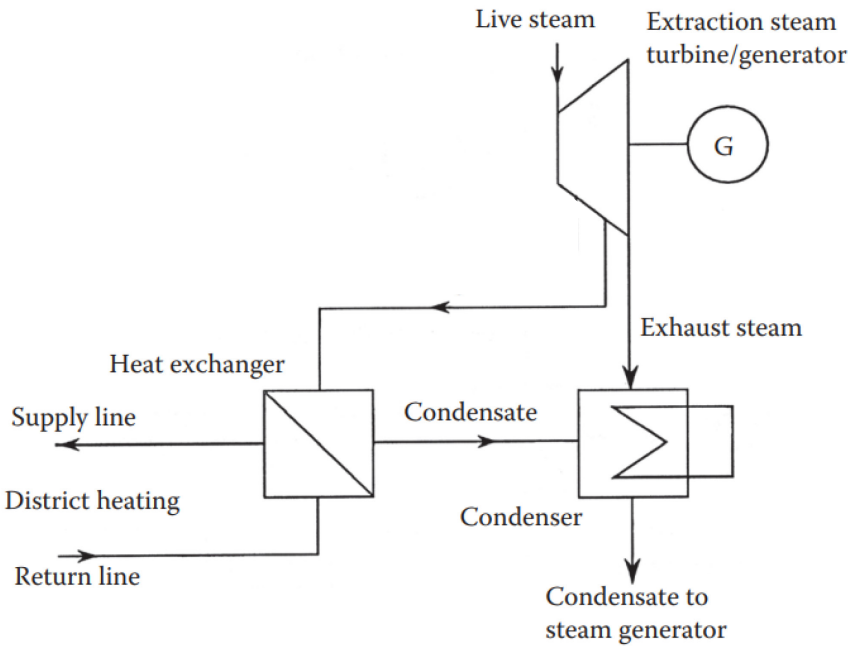

Figure 16: A schematic of an extraction-condensing steam turbine coupled with a district heating network. [54, p. 214]

4.2.1 Coefficient of Performance of Heating

Regardless of the method, the production of useful heat will inevitably lead to loss in electric power. A fundamental issue in CHP generation is the extent at which electricity production is lowered in order to produce useful heat. A key figure to describe this change is the coefficient of performance (COP) of heating. Comparable to the COP of a heat pump, the COP of a CHP plant describes how many units of heat power are produced with the cost of one unit of electric power. This ratio, shown in Equation 6, should be maximized:

$$COP_{CHP} = \frac{Q_H}{\Delta P_{el}}, \tag{6}$$

where Q_H is the obtained heating power and ΔP_{el} is the corresponding change in electric power.

There is no definite value for the COP of heating for existing CHP plants. Nevertheless, estimates of COPs for can be formed by comparing CHP plants to condensing steam power plants. In this case, the value of the COP depends heavily on the efficiency of the compared condensing power plant. If the boiler thermal power Q_{th}, the district heating output Q_{DH}, and the electric output $P_{el,2}$ of a CHP plant are known, the COP of heating for a CHP plant becomes

$$COP_{CHP} = \frac{Q_{DH}}{P_{el,1} - P_{el,2}} = \frac{Q_{DH}}{\eta_{th,c} * Q_{th} - P_{el,2}}, \quad (7)$$

where Pel,1 is the electric output of the condensing power plant calculated using its thermal efficiency $\eta_{th,c}$.

Table 8 provides some examples of coal-fired CHP plants in Finland and their COPs when compared to condensing power plants. The thermal powers are estimated by assuming all CHP plant efficiencies to be 90 %. The COPs are calculated in terms of maximum DH power, which implies that the COPs are accurate during times of high heat demand. The COPs may vary with lower DH outputs.

Table 8: Estimated COPs of coal-fired CHP plants in Finland.

CHP Plant	DH (MW)	Electricity (MW)	Thermal (MW)	COP1*	COP2**
Salmisaari B	300	160	511	**4,29**	**6,75**
Suomenoja 1	162	75	263	**3,72**	**5,34**
Martinlaakso 2	145	75	244	**4,14**	**6,37**

**COP1: Compared to condensing plant with efficiency of 45 %*
***COP2: Compared to condensing plant with efficiency of 40 %*

5 Dimensioning the SMR0 Secondary Cycle

The CHP steam cycle models presented later in this thesis are iterations of an SMR condensing secondary cycle referred to as SMR0. SMR0 is a small modular reactor unit entailing two pressurized water reactors and two corresponding secondary cycles. SMR0 produces electric power only. One secondary cycle of SMR0 is depicted in Figure 17.

The secondary cycle comprises a steam turbine with low- and high-pressure sections, a moisture separator, two reheaters, a generator, a condenser, four preheaters, and several pumps. The primary circuit and the steam generator are excluded from the model. In order to later simulate the cycle using Solvo software, key parameters of each steam cycle component must be defined. The following subchapters describe the dimensioning process.

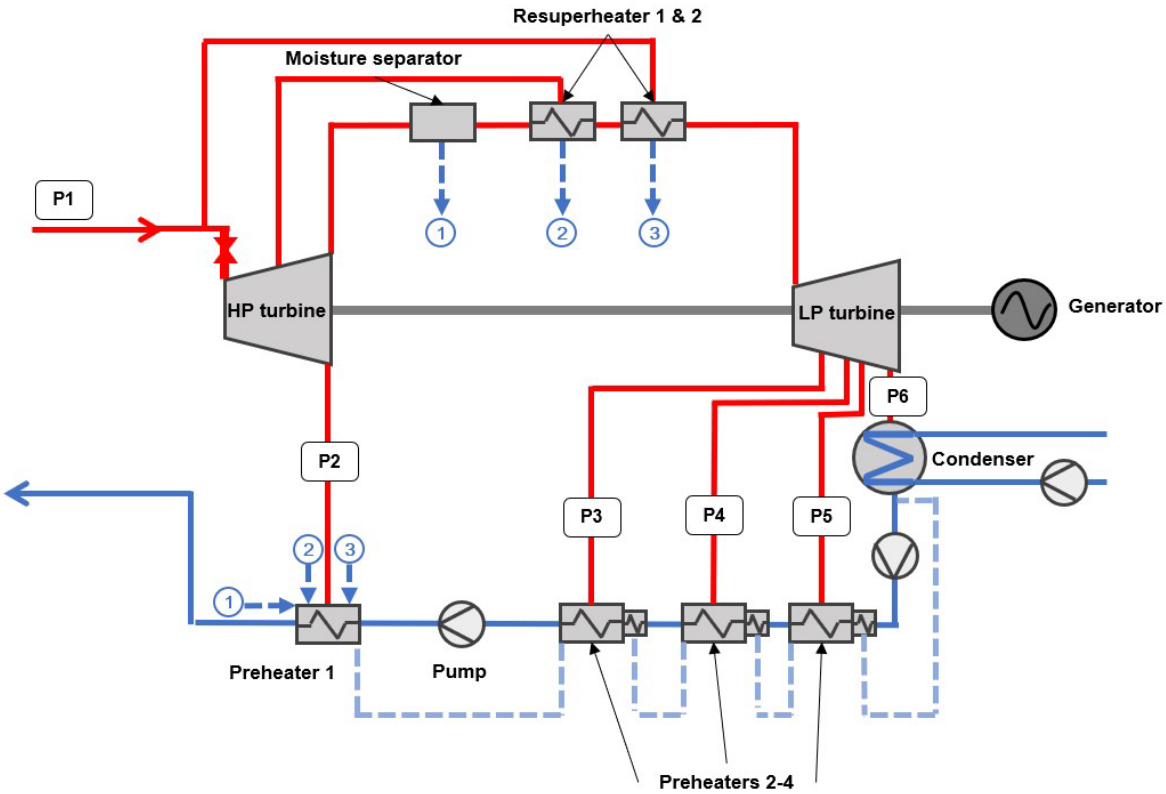

Figure 17: A schematic of the SMR0 steam cycle. One SMR0 unit contains two steam cycles.

5.1 Initial Data and Process Parameters

The conditions of the working fluid throughout the cycle are primarily established utilizing the process parameters presented in Table 9. The values are based on a small modular dual-reactor concept (NUWARD, private communication, Febr. 2024[3]). Any unknown values were estimated using thermodynamic theory, steam calculations, and Solvo software. Figure 18 depicts the outline of the SMR0 steam cycle, as determined by the dimensioning process, on a temperature-entropy (T-s) diagram.

Table 9: Initial process parameters used to dimension the SMR0 steam cycle

Parameter	Value	Unit
Reactor thermal power	540	MW
Approximate electric output of one cycle	185	MW
Live steam pressure (P1)	46	bar
Live steam temperature	300	°C
HP turbine outlet pressure (P2)	7,3	bar
Condenser pressure	0,05	bar
Cold sink temperature	17,5	°C
Feedwater outlet pressure	52	bar
Feedwater outlet temperature	150	°C
Number of feedwater preheaters	4	-
Number of reheaters	2	-

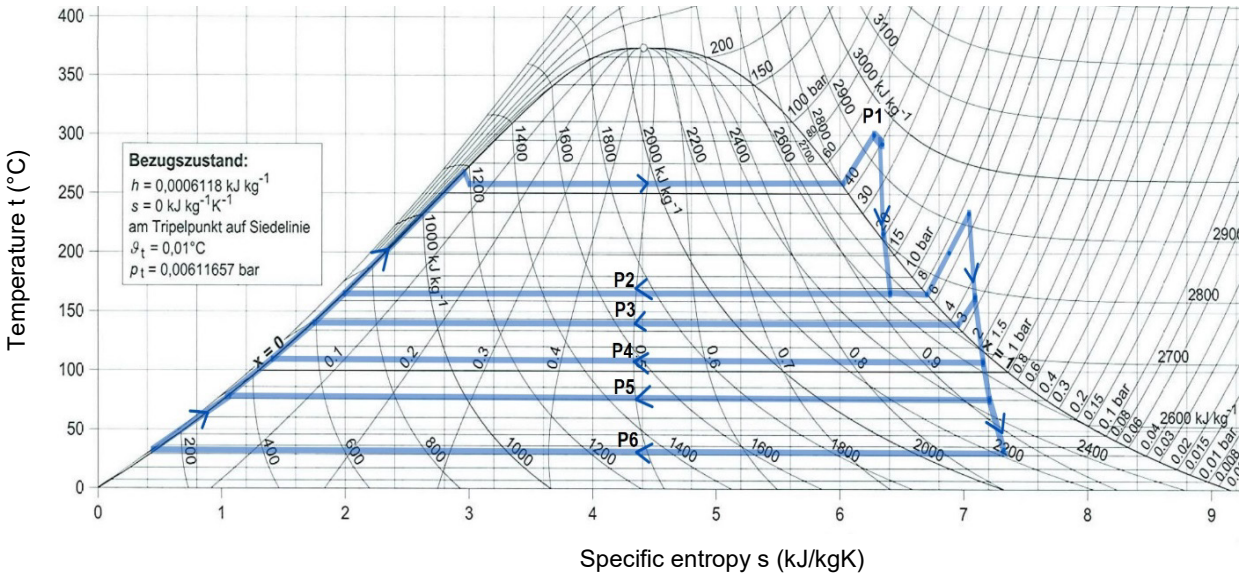

Figure 18: The steam cycle of SMR0 on a T-s diagram.

[3] This model does not take into consideration any potential design evolutions of NUWARD SMR after February 2024.

5.2 Steam Generator

In a nuclear steam generator, heat from the primary circuit vaporizes water in the secondary circuit. The steam generator is not modeled, but some definitions are made to justify steam conditions. The conditions of the steam exiting the steam generator and the entering feedwater were determined according to the initial data in Table 9. It is considered that a total pressure loss of 6 bar occurs during the steam generation process. Half of this is assumed to occur in a valve and the other half during the heating process itself.

Although nuclear power plants typically employ saturated steam, it is noteworthy that the live steam in this cycle is superheated. The superheated state is caused by the steam generator, which is assumed to be a once-through counterflow heat exchanger. As discussed in Chapter 4.1.1, traditional nuclear steam generators tend to be of parallel-flow type. For the same inlet and outlet temperatures, the log mean temperature difference of counterflow heat exchangers is greater than for parallel-flow heat exchangers, indicating a higher heat transfer rate. Unlike in parallel-flow heat exchangers, the steam exiting a counterflow heat exchanger may be at a higher temperature than the exiting reactor coolant, enabling a superheated state. [58, p. 679]

5.3 Steam Turbine and Generator

The steam turbine converts the thermal energy of live steam into mechanical energy and rotates the rotor of the generator, thus generating electricity. The steam turbine is divided into high-pressure (HP) and low-pressure (LP) turbine sections. Each section contains several pressure stages, inducing a phased expansion process of the steam.

The SMR0 steam turbine is a theoretical extraction-condensing steam turbine without a specified manufacturer. To simplify modeling, both the LP and the HP turbines are modeled as a single-flow turbines, where steam enters at one end, travels in one direction, and exits at the other end. In reality, at least the low-pressure section is likely to be of the double-flow type, where steam enters in the middle and travels in two directions. Compared to single-flow turbines, double-flow turbines are more complex in design and can operate with higher volumes of steam due to additional flow paths. This translates to a higher turbine efficiency. In practice, converting a double-flow turbine into a single-flow version would primarily require lengthening the turbine blades, but the fundamental steam expansion process would remain unchanged. [61, p. 140] Thus, the turbine flow configuration has no significant effect on the simulation outcome.

A key parameter describing the performance of the turbine is the turbine isentropic efficiency. The isentropic efficiency describes the ability of the turbine to perform expansion work isentropically. It is the ratio of the enthalpy change of the actual expansion process to the enthalpy change of the isentropic, ideal process. Mathematically, it is expressed as

$$\eta_{is} = \frac{\Delta h}{\Delta h_{is}} = \frac{h_1 - h_2}{h_1 - h_{2,is}}, \tag{8}$$

where h_1 is the enthalpy of the steam entering the turbine, h_2 is the enthalpy of the steam exiting the turbine, and $h_{2,is}$ is the enthalpy of the exiting steam in an ideal scenario.

The isentropic efficiency of conventional nuclear power plant steam turbines is found to be in the range of 84-92 % [7, p. 22]. Consequently, the isentropic efficiency of both the high- and low-pressure turbines is assumed to be 90 %. The isentropic efficiency is maintained at a constant value throughout the analysis, although in reality the efficiency might vary when turbine pressure levels are adjusted.

Steam for intermediate feedwater heating processes is extracted from both the HP and LP turbine sections. The HP turbine features one and the LP turbine three extraction outlets. Extraction pressures are determined by optimizing the feedwater heating process. In an optimal scenario, the enthalpy rise of the heated feedwater is divided evenly by the number of feedwater preheaters. This implies that the enthalpy change in each preheater is constant. [62, p. 74] The pressure of the extracted steam can then be solved by establishing the terminal temperature differences of the heat exchangers. This is discussed in the following subchapter.

The steam turbine is mounted on the same shaft with a generator. The generator converts the mechanical energy of the rotating turbine into electricity on the basis of electromagnetic induction. The generator is parameterized by establishing a known generator efficiency, which describes the ratio of the electrical power output to the mechanical power input. A generator efficiency of 98 % is assumed [7, p. 22].

5.4 Superheaters and Feedwater Preheaters

In total, the secondary cycle features six heat exchangers. Two steam-steam heat exchangers are located between the high- and low-pressure turbine sections. They serve the purpose of reheating the partially expanded steam after it has been dried through the moisture separator (see Chapter 5.4). Four steam-water heat exchangers are located after the condenser and preheat the water returning to the steam generator. Further specifications in terms of heat exchanger types are not made.

In the heat exchangers, steam or water is heated either by live steam or steam extracted from the turbine. Heat exchange occurs primarily due to the condensation of steam. However, at some points in the cycle, the steam is superheated and must first be desuperheated to be condensed. Therefore, the two reheaters and the first high-pressure preheater in some partial-load operating modes include a desuperheating component, which reduces the temperature of the extracted superheated steam back to its saturation point. The three low-pressure feedwater preheaters also include a subcooling component, which further cools the condensed steam below its saturation temperature. The process of subcooling prevents the condensate from later flashing back into steam, increases heat recovery in the heat exchanger, and ultimately improves cycle performance. [63, p. 882] The processes of desuperheating and subcooling are visualized in Figure 19.

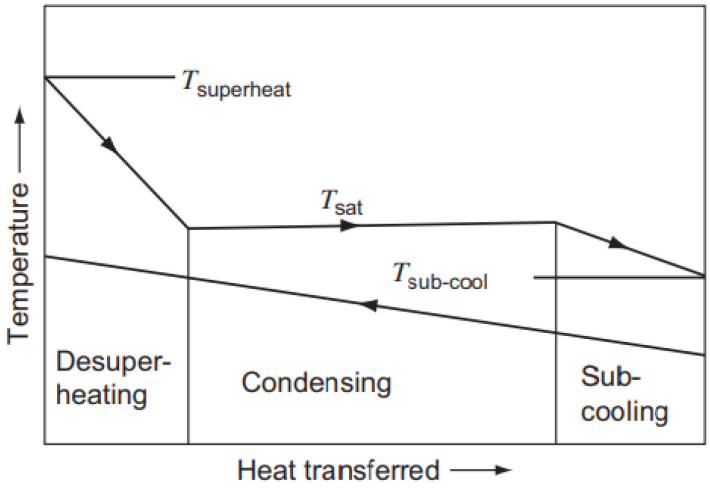

Figure 19: The temperature profile of condensing steam with the processes of desuperheating and subcooling. [63, p. 882]

In an ideal scenario, the condensed steam and the heated main flow exit the heat exchanger at the same temperature. In reality, there is always a temperature difference between the two streams. This difference between the saturation temperature of the extracted steam and the outlet temperature of the heated flow is referred to as the terminal temperature difference (TTD). [64, p. 156] Although a smaller TTD increases heat exchanger performance, it also increases the required heat transfer area and the size of the heat exchanger. The initial data determines the TTDs of the last reheater and the high-pressure preheater to be 23 K and 17 K respectively. The TTD of the first reheater and the rest of the preheaters is set to 15 K. This value is chosen to align with the known TTDs while slightly reducing it to enhance cycle performance.

The condensate streams of the heat exchangers are connected in a cascade formation, in which the condensates from each feedwater preheater are directed to the one

immediately preceding it. The condensates from the superheaters are led to the HP feedwater preheater, from where they enter the preceding preheaters. Finally, the total flow of the condensates is led to the condenser and back to the main water flow. If each individual heat exchanger were drained directly to the condenser, the enthalpy of the condensates would be lost. The cascade configuration improves cycle performance and reduces entropy generation by utilizing the hot heat exchanger drains in the feedwater preheating process. [65, p. 5]

5.5 Moisture Separator and Pumps

Before the steam is lead into the superheaters and then into the LP turbine, the water fraction in the steam flow is removed by a moisture separator. This is done to dry the steam to prevent water droplet erosion in the turbine. The separation efficiency is defined as the ratio of the amount of removed water to the total water content of the steam entering the separator [59, p. 195]. The moisture separation efficiency is assumed to be 99,5 %, resulting in the near-saturated state of the steam exiting the moisture separator.

The pumps used in nuclear power plant secondary cycles are most often centrifugal pumps. In an ideal case, the compression process in pumps is isentropic and isothermal. In reality, the process is not completely such: a value for isentropic efficiency is needed to describe the change in the flow's state during the pumping process. The isentropic efficiency of a pump relates the pump power in an ideal scenario to the actual power. This efficiency of centrifugal pumps may vary between 20-90 % [66]. In this simulation, an isentropic efficiency of 80 % is assumed for all pumps. The electric efficiency of the pump motor is set to 95 %.

5.6 Condenser and Cooling Solution

From the second law of thermodynamics, it follows that the thermal energy of the steam cannot be converted entirely into useful work and some heat is rejected into the environment or a heat sink. In nuclear power plants, this heat is removed from the system in the condenser by cooling water. [54, p. 78] The condenser is connected to the cooling option of choice so that two mediums flow through the condenser: a water-steam mixture from the turbine on one side and the cooling water on the other. The heat sink configuration determines the temperature of the cooling water, that is, the average temperature of heat rejection.

The cycle is parameterized using a 17,5-°C cooling water temperature at the condenser inlet. The cooling water could be supplied by once-through water cooling or by a cooling tower. As the cooling process per se is not the focal point of this simulation, the heat sink configuration is not specified. It is considered that the pumping head required for the cooling system equates to 1 bar, which would suffice

for a height difference of roughly 10 meters or for a 50-meter-long pipe with an inner diameter of 1 meter. The cycle is assumed to consume approximately 0,04 m^3/s of cooling water per MW of rated capacity, which is in line with the typical consumption of LNPPs [67].

The heat sink configuration ultimately depends on the geographical location of the plant. Near abundant bodies of cold water, freshwater cooling is often the most profitable alternative. Fresh water from a river or a sea, for example, is pumped through the power plant cooling system and discharged back into the original body of water. In locations where fresh water is not available or sufficient, a cooling tower which removes heat into atmospheric air can be utilized. Water from the condenser is sprayed inside the cooling tower, where it releases heat into the air mainly through evaporation and partly by convection. The air is both humidified and heated, and the cooled water falls to the bottom of the tower from where it is pumped back to the condenser.

The performance of a cooling tower is determined by atmospheric conditions as heat transfer occurs predominantly through evaporation. The combination of the relative humidity and the dry bulb temperature of air defines the air wet bulb temperature, which sets the limit for the lowest possible temperature of the water exiting the tower. The wet bulb temperature of air is defined as the temperature to which a thermometer covered by a moistened cloth sets to as it encounters an air flow. In reality, the wet bulb temperature is never reached, as this would require an infinite heat exchange surface. [67, p. 25] It follows that efficiency of a cooling tower is defined by the tower inlet (t_i) and outlet (t_o) water temperatures as well as the wet bulb temperature of air (t_{wb}):

$$\eta_{tower} = \frac{t_i - t_o}{t_i - t_{wb}}. \tag{9}$$

Cooling tower efficiency is generally found to be in the range of 70-75 % [68, p. 185]. For an efficiency of 70 % and a tower outlet temperature of 17,5 °C, the wet bulb temperature of the entering air in SMR0 would have to equal 13 °C. This is attainable with, for example, an air temperature of 19 °C and a relative humidity of 50 %, or an air temperature of 14 °C and a relative humidity of 90 %.

6 SMR0 Solvo Model

The design parameters established and described in Chapter 5 served as the basis for the construction of the SMR0 Solvo model. The following subchapters describe the modeling software used to simulate the cycle as well as individual configurations of each component. The simulations results including electric output of the plant are presented in Chapter 6.3.

6.1 Solvo® Simulation Software

Solvo® is a process simulator software developed by Fortum utilized to design and optimize power plants processes. The Solvo product line used in this thesis is the Solvo® DesignPlus, which is a power plant modeling tool with a focus on boiler design. In Fortum, the software has been used in the pre-design phase of power plants.

The Solvo tool functions based on steady-state mass and energy equations to simulate equipment operation. An iterative sequential modular approach is used to calculate the output value of each component based on incoming values. The output values of the components are recalculated until the difference between the on-going calculation cycle and the previous one does not exceed a given iteration criterion. The iteration criterion used for simulations in this thesis is the default value of 0,2 %. The sequence of calculation is determined by the program.

The construction of the model occurs in two stages: first, drawing the process diagram of the steam cycle in the drawing state, and then parameterizing the model using process values in the calculation state. In the calculation state, each component of the cycle is first parameterized using certain qualitative values, such as pressure levels and efficiencies. This parameterized state is referred to as the reference state, which is a state where all component data can be determined using mass and energy balance equations. Once the reference state has been established, the model can be set to a changed state. The attributes that have been determined in the reference state are recalculated to correspond to this new changed state. The solutions are based on mass and energy balance equations, heat transfer equations, and component-specific equations, such as the ellipse law for the steam turbine.

All components are validated when they are integrated to Solvo. The process values and parameters of the components are compared to correct, known values, which are derived from acceptance tests and operating measurements. [69]

6.2 Model Components

The Solvo model of one SMR0 steam cycle is presented in Figure 20. A comprehensive heat balance diagram of the SMR0 steam cycle constructed using Solvo software is attached as Appendix A.

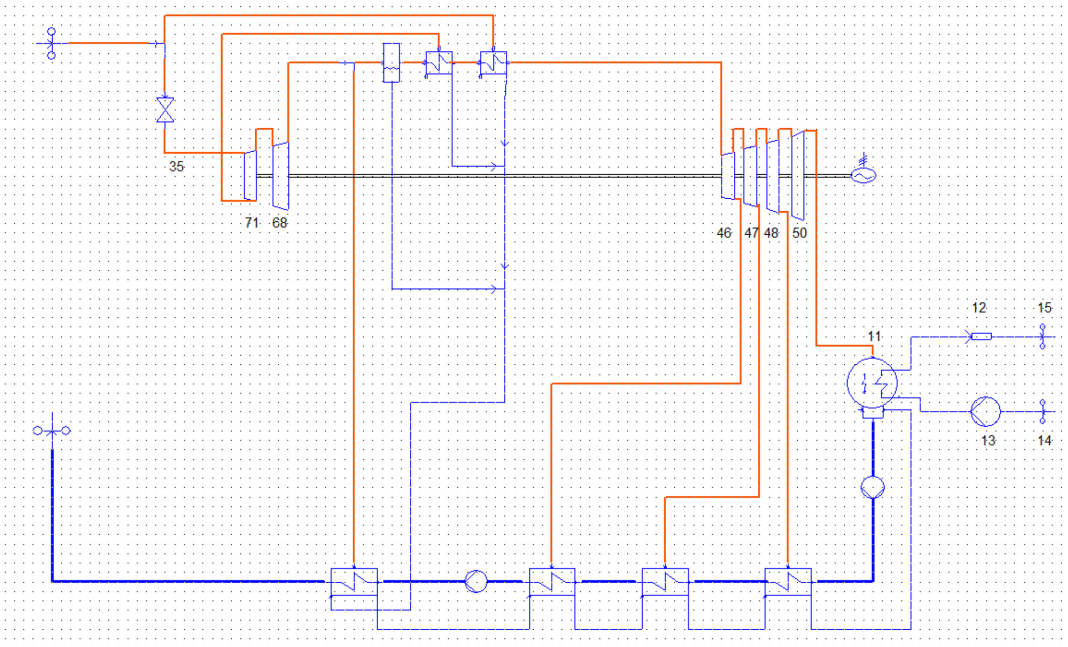

Figure 20: The secondary cycle of SMR0 in Solvo software. One SMR0 unit includes two steam cycles.

The primary cycle and the steam generator are excluded from the Solvo model. All simulations are executed at a full reactor thermal power of 540 MW. In each calculation, the mass flow rate of the live steam is adjusted to meet the reactor thermal power. The working fluid enters and exits the secondary cycle through a Limit component pictured in Figure 21.

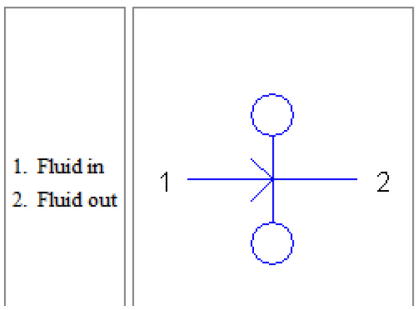

Figure 21: A Limit component used to simulate incoming and exiting working fluid.

6.2.1 Steam Turbine and Generator

In Solvo, a single steam turbine stage is represented by the SteamTurbine component, shown in Figure 22. Individual turbine stages are connected as in Figure 23 to form a section. Each stage is dimensioned using the "1 eff given" mode, which parameterizes the turbine based on the given isentropic efficiency of 90 %.

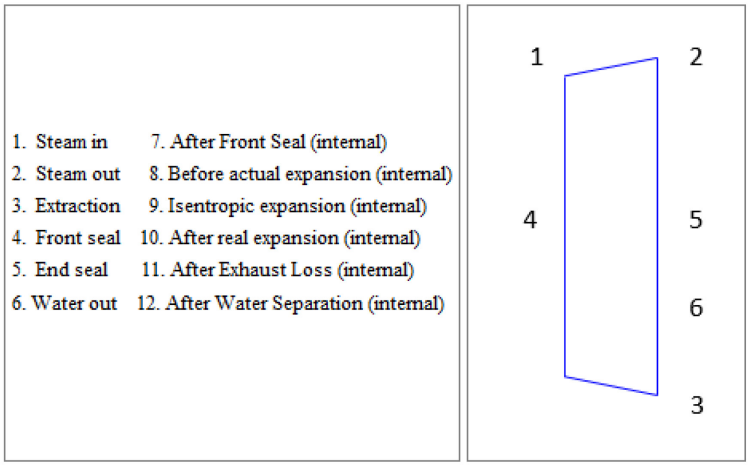

Figure 22: A SteamTurbine component in Solvo.

The generator is represented by the Generator component shown in Figure 23. The Generator component calculates the total shaft power of all turbine stages on the same shaft based on the given generator efficiency of 98 %.

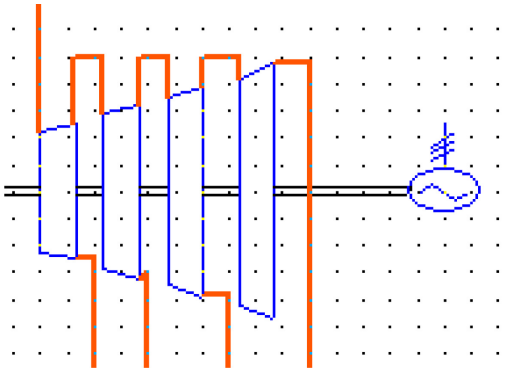

Figure 23: Several SteamTurbine components joined on the same shaft with a Generator component.

6.2.2 Reheaters and Feedwater Preheaters

The two resuperheaters are modeled using the HeatExchangerSS component in Figure 24 a), which superheats steam with live steam or steam extracted from the HP turbine. The feedwater preheaters are modeled using the HeatExchanger component in Figure 24 b), which heats water with steam from the HP and LP turbines.

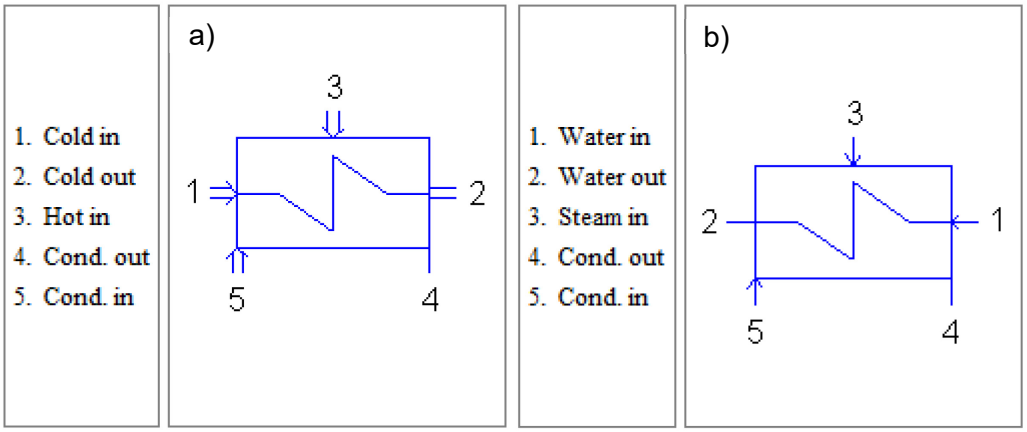

Figure 24: The heat exchanger components used in Solvo are a) the HeatExchangerSS for resuperheaters and b) the HeatExchanger for feedwater preheaters.

All heat exchangers are dimensioned using the mode “2 TTD, DCA and k: given”. This mode parameterizes the heat exchanger based on the given values for the terminal temperature difference, the drain cooler approach (DCA) and the overall heat transfer coefficient (k). The TTDs were discussed in Chapter 5.3. The drain cooler approach values and overall heat transfer coefficients were determined by Solvo.

6.2.3 Moisture Separator and Pumps

In Solvo, the moisture separator is modeled using the WaterSeparator component in Figure 25 and parameterized with an efficiency of 99,5 %.

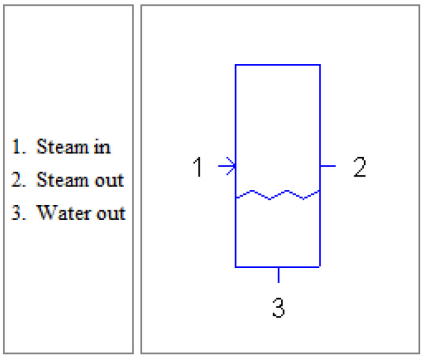

Figure 25: A WaterSeparator component in Solvo.

The Pump component shown in Figure 26 is used to portray all pumps in the Solvo model. All pumps are parameterized using an isentropic efficiency 85 %. The electric efficiency of the pump motor is set to 95 %.

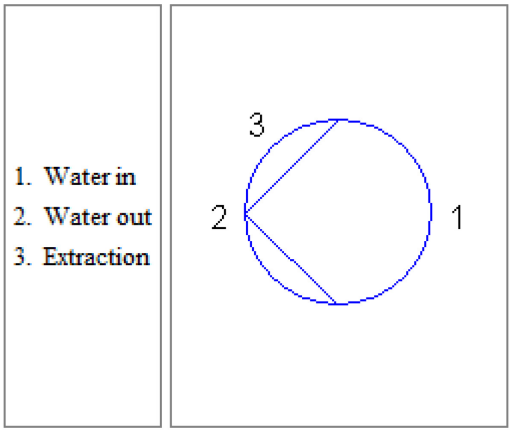

Figure 26: A Pump component in Solvo.

6.2.4 Condenser and Cooling Solution

As the cooling option of the model is unspecified, the Solvo model simply features a Limit component from which cooling water enters and is pumped through the condenser. The condenser pressure and the cooling water temperature are known to be 0,05 bar and 17,5 °C respectively. The Condenser component is shown in Figure 27.

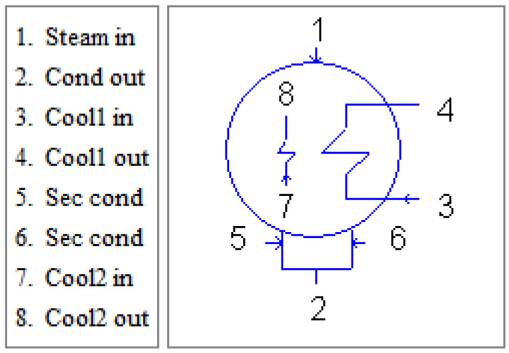

Figure 27: The Condenser component in Solvo.

The entire cooling arrangement is pictured in Figure 28. The cooling arrangement features the following components:

- 14 a Limit component for simulating entering cooling water,
- 13 a pump,
- 11 a condenser,
- 12 a pipe component to represent pressure loss during cooling, and
- 15 a Limit component for simulating exiting cooling water.

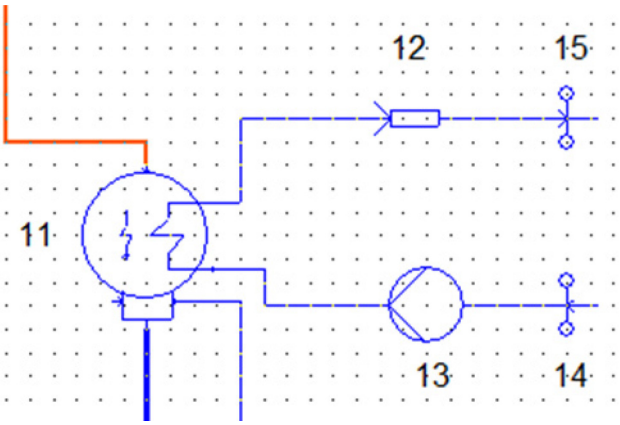

Figure 28: The cooling arrangement in Solvo.

6.3 Simulation Results

The performance parameters obtained by simulating the SMR0 are tabulated in Table 10.

It is to be noted that the electric outputs calculated in Solvo do not account for plant internal consumption. Their purpose is to enable comparison between different models rather than to serve as absolute values.

Table 10: Technical parameters of one SMR0 unit with two steam cycles

	Power (MW)
Electric output	2 x 187,7
Condenser power	2 x 350,1
Required pump power*	2 x 1,7

**Pump power of the secondary circuit only; excludes pump power required by cooling arrangement and primary circuit.*

7 Combined Heat and Power Steam Cycle Models

The extraction of useful heat requires altering the technical configuration of SMR0 presented in Chapter 6. This chapter discusses three combined heat and power steam cycle alternatives, hereafter referred to as SMR1, SMR2, and SMR3. SMR1 is constructed directly upon SMR0. Two iterations of this cycle, SMR2 and SMR3, aim to increase the coefficient of performance (COP) of heat production of SMR1 while also attaining higher district heating outputs. Each SMR is considered to contain two steam cycles, indicating that the total unit capacities are double those of a single steam cycle.

7.1 Calculation of the Coefficient of Performance of Heating

The coefficient of performance is investigated by simulating the steam cycle models in Solvo software. First, the COP at maximum DH power is established by comparing the electric outputs in condensing and full DH modes. The calculation is executed as follows:

$$COP_{max,DH} = \frac{Q_{DH}}{P_{condensing} - P_{DH}}. \quad (10)$$

where $P_{condensing}$ is the electric output of the cycle in full condensing mode, Q_{DH} is the maximum district heating power of the cycle, and P_{DH} is the corresponding electric power in full DH mode.

After demonstrating the COP at maximum DH power, the effect of modifying the DH load is investigated by calculating the COP at 10-MW_{th} intervals. This computation yields a correlation between the district heating load and the COP and describes how the efficiency of heat production may vary according to heat demand.

7.2 District Heating Components

In the CHP arrangements, no components are removed from the original condensing cycle described in Chapter 6. As the district heating components are added, the remaining steam cycle components remain in a changed state. This way, components are optimized for electricity production, and it is ensured that the plant can operate in full condensing mode.

In the Solvo models of all three SMRs, the extraction of heat requires adding a Branch component to the steam line parting from high- and/or the low-pressure turbine. The steam used for heating DH water passes through this Branch to the one or two steam-water HeatExchanger components. These heat exchangers with relatively large terminal temperature differences are used to represent several district

heat exchangers. Each configuration also features two Limit components for incoming and exiting DH water, one Branch component, and one Junction component. The Branch and Junction components connect a bypass line with the main DH water stream. The purpose of this bypass line is to control the district heating power output by directing a portion of the district heating water past the heat exchanger. When the plant is operated at the full district heating power, no water passes through the bypass line. The condensate draining configuration varies for each SMR. The district heating arrangement for one district heat exchanger is depicted in Figure 29.

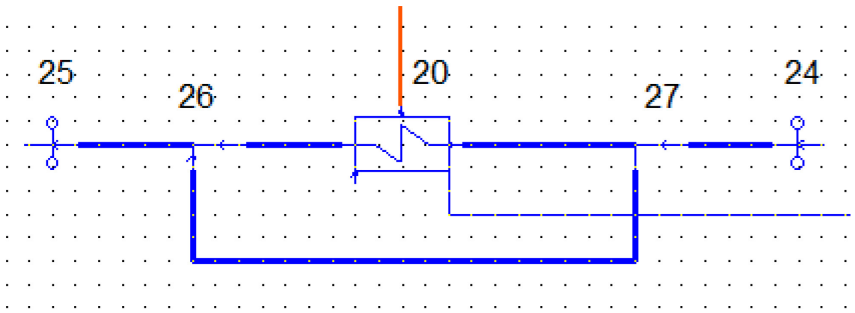

Figure 29: The district heating arrangement in the case of a single district heat exchanger (20). District heating water enters through Limit 24 and exits through Limit 25. The district heating power is altered by diverting water through Branch 27 into a bypass line. Junction 26 joins the two lines back together.

The district heating arrangement is dimensioned based on water temperatures commonly used in existing systems and the high heat demand. The district heating water is heated from 60 °C to 115 °C while the mass flow rate of the water is defined according to the maximum DH power. Future DH systems are likely to incorporate lower water temperatures, which enable utilizing more lower-pressure steam for the heating process. The calculations aim to account for the effects of this transition by calculating the COP of heating as a function of a varying DH load.

7.3 SMR1

The CHP configuration of SMR1 is built directly upon the condensing steam cycle of SMR0 presented in Chapter 5. SMR1 has a maximum electric power output of 187,7 MW in condensing mode, and it is designed to supply a DH power output equivalent to 10 % reactor thermal power, or 54 MW, by extracting steam from the HP turbine. The condensed steam from the district heat exchanger is reintegrated with the main working fluid flow at the condenser. The configuration is presented in Figure 30, and a comprehensive heat balance diagram is attached as Appendix B.

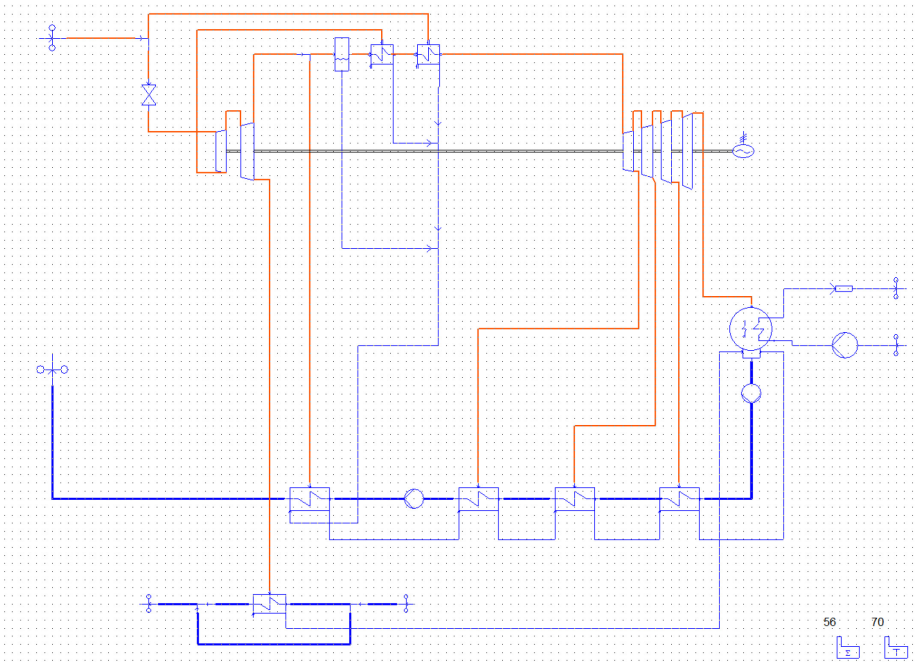

Figure 30: The SMR1 steam cycle in Solvo software.

With SMR1, producing 54 MW of district heating yields an electric power of 172,4 MW and a corresponding COP of 3,54. Figure 31 presents how the COP is directly proportional to district heating power, although the rate of growth is rather insignificant as the COP is an average of 3,5 at all loads.

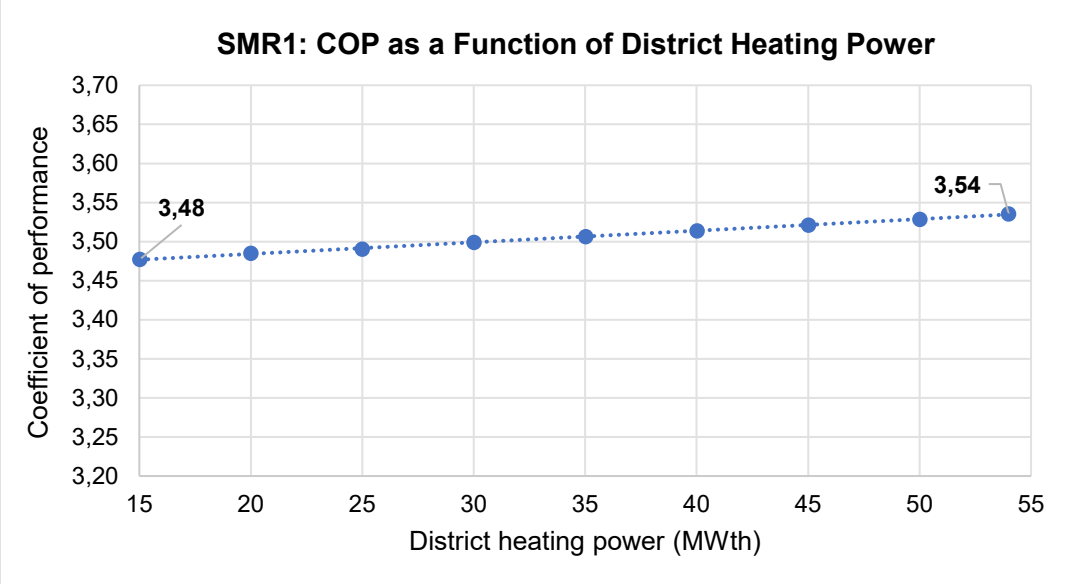

Figure 31: The COP of SMR1 as a function of DH output.

A source of inefficiency in SMR1 is the condensate stream configuration from the district heat exchanger to the condenser. In the district heat exchanger, steam from the HP turbine is condensed into saturated water. This occurs at a temperature corresponding to the turbine outlet saturation pressure. At full DH power, the extracted steam is at a temperature of roughly 160 °C, which is noticeably higher in comparison to the main fluid flow at the location of the condenser. Therefore, when directed backwards to the condenser, the enthalpy of the hot condensate stream is wasted. To minimize the lost enthalpy of the condensate stream, two options are imaginable:

1. Lowering the temperature of the saturated water in the heat exchanger through subcooling, or
2. directing the condensate to a point in the main cycle where the temperature of the main stream is as close as possible to the temperature of the condensate stream.

The first option of subcooling is achieved in the heat exchanger by cooling the condensed steam below its boiling point. The process was described in Chapter 5.4. Consequently, the condensate temperature is lowered closer to the temperature of the main fluid flow at the location of the condenser, reducing entropy generation. Simulation results indicate that subcooling the saturated water to 80 °C could increase the COP by 20 %, that is to 4,2 at full DH power. However, for this to be an advantageous solution, the heat released by the condensate should be applied towards a useful purpose, or else it is wasted. Without an apparent application for the heat, it is more sensible to utilize it in the feedwater preheating process by directing the condensate to a different point in the main cycle.

Simulations show that district heating production inflicts a decrease in the HP turbine outlet pressure. The low- and high-pressure expansion curves are drawn on a enthalpy-entropy diagram in Figure 32. For instance, producing 54 MW of district heating causes a pressure loss of slightly above 1 bar compared to the HP turbine outlet pressure in condensing mode. The outlet pressure reduces as DH power grows, and the increased pressure difference induces a higher steam mass flow rate through the HP turbine. This may become problematic as a large steam flow can erode turbine structures. To limit the risk of erosion, the HP turbine outlet pressure should be controlled. However, raising the outlet pressure in DH mode would require re-dimensioning the HP turbine to operate at higher pressure levels also in condensing mode.

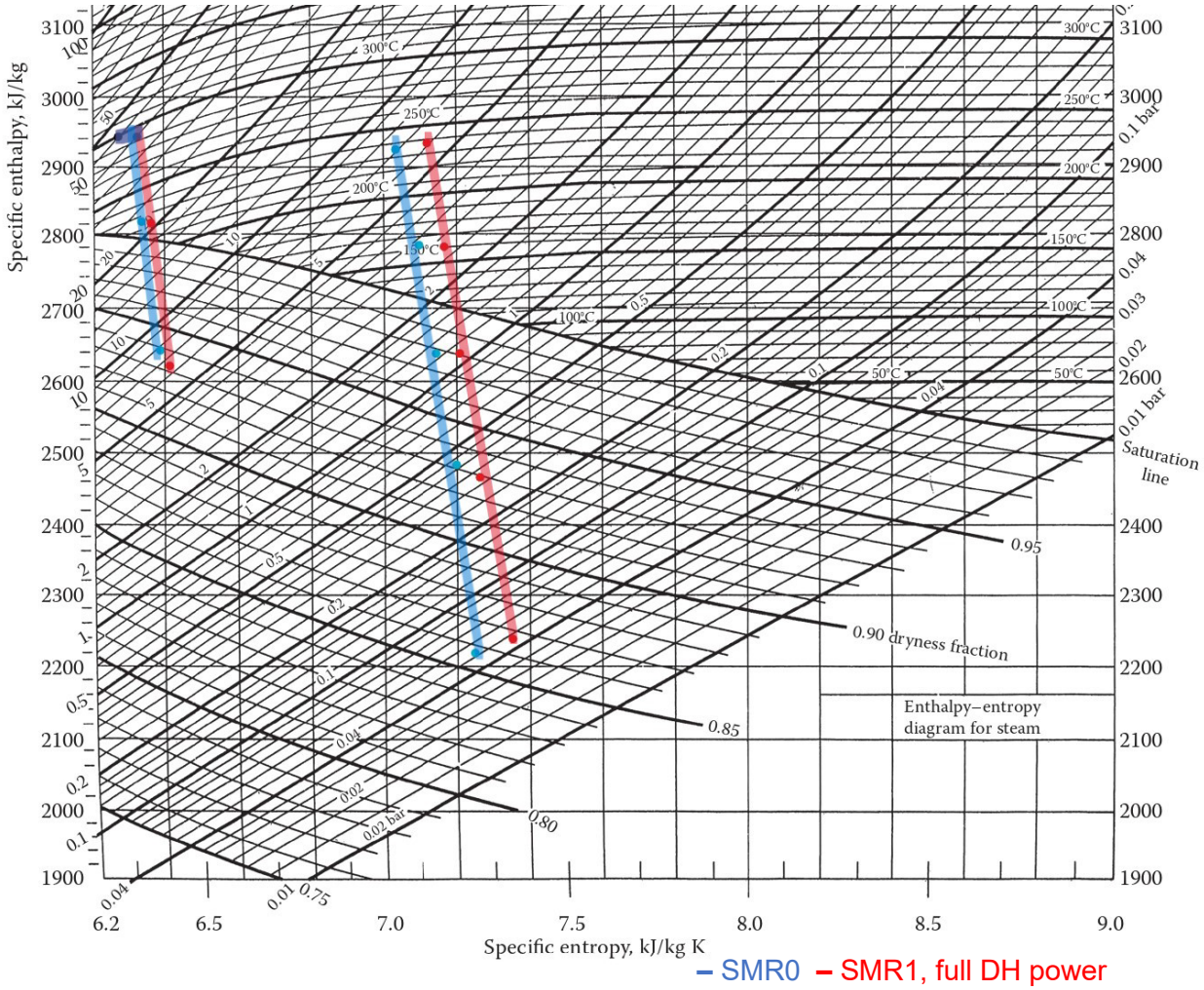

Figure 32: The low- (left) and high-pressure (right) turbine expansion curves of SMR0 (condensing mode) and SMR1 (full DH power) on an H-s diagram. Producing district heating leads to pressure loss.

Without re-dimensioning the entire turbine, the exhaust pressure of the HP turbine can be controlled by adding a valve. The valve is placed before the moisture separator, and its purpose is to restrict steam flow in such a manner that the exhaust pressure remains constantly at 7,3 bar as intended in the condensing configuration. The placement of the valve is shown in Figure 33.

By fixing the turbine exhaust pressure to a higher value, it is possible to raise the DH power by almost 7 MW, from 54,0 MW to 60,8 MW. However, this results in less steam entering the low-pressure turbine and a loss in expansion work. Consequently, electric power output at full DH power drops by some 3 %. Although an additional valve slightly increases district heating power, this is achieved with a lower COP than in the initial configuration. On the other hand, this is likely a favorable solution in terms of protecting the turbine structures. Because the HP turbine outlet pressure

remains constant, the COP of SMR1 with a valve is rather independent of the DH load. Results indicate a constant COP of 2,9 at all loads.

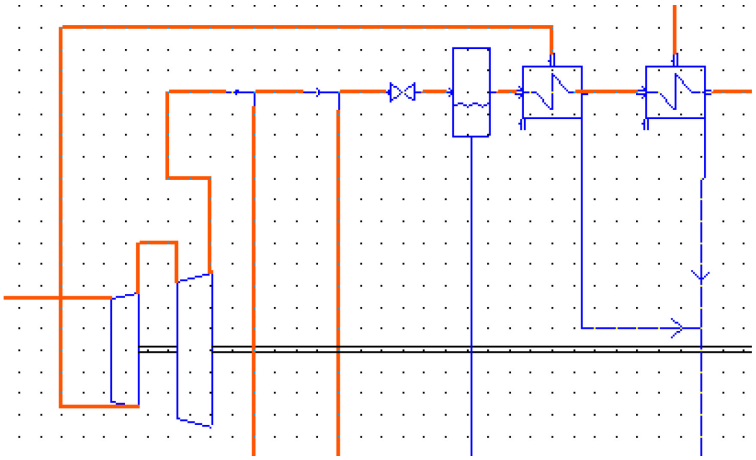

Figure 33: A valve to control the high-pressure turbine outlet pressure placed in SMR1.

From this first CHP steam cycle model of SMR1, it is evident that utilizing high-pressure steam limits both the extractable DH power and the attainable COP. Without a valve, increasing DH power results in low pressure levels that the HP turbine may not endure. With a valve, expansion work and electric power is lost. Furthermore, due to the condensate draining configuration, the enthalpy of the extracted high-temperature steam is wasted. Hence, increasing the DH power and the COP proves to be challenging without changing the concept of heat extraction.

7.4 SMR2

The first iteration of SMR1, SMR2, features moderate technical changes. Compared to SMR1, the HP turbine outlet pressure of SMR2 is lowered by some 10 % to increase expansion work during DH production. A valve maintains the outlet pressure at least at 6,7 bar. Consequently, the TTD of the HP preheater is lowered to ensure that the feedwater returns to the reactor at a temperature of 150 °C as intended in the design of SMR0. The remaining turbine extraction pressures, condenser pressure, and heat exchangers are unaltered. The resulting electric power of SMR2 in condensing mode is 187,6 MW. The SMR2 steam cycle is presented in Figure 34, and a comprehensive heat balance diagram is attached in Appendix C.

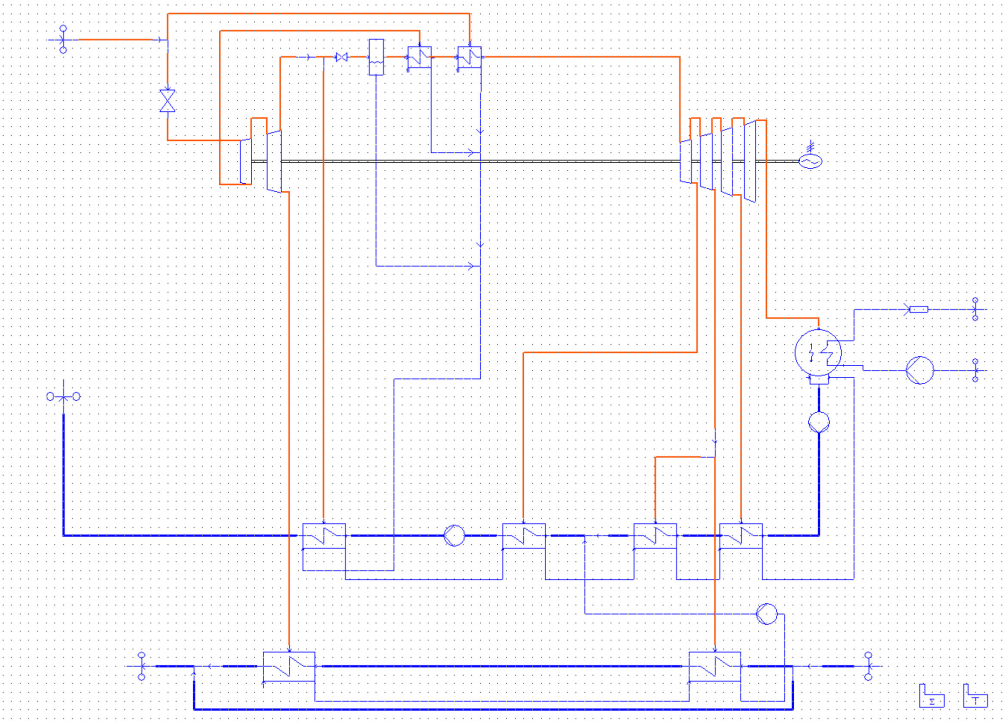

Figure 34: The Solvo model of the SMR2 CHP steam cycle.

The steam cycle of SMR2 heats the DH water flow in two phases by extracting steam partly from the low-pressure turbine. Bleeding some of the required steam later in the cycle allows a greater amount of steam to expand further than in SMR1. Consequently, the electric power of the turbine is increased. In Solvo, two-phased heating requires adding a second HeatExchanger component connected to an extraction flow from the LP turbine.

Next, the condensate drains of the two DH heat exchangers are altered. In SMR1, the condensate stream from the single DH heat exchanger is directed back to the main flow via the condenser. In SMR2, entropy generation is minimized by connecting the condensate streams to a point in the main cycle where the temperatures of the two flows are as close as possible. The condensate streams from the two heat exchangers are thus connected in a cascade configuration and joined with the main feedwater cycle in a later phase. An additional pump component is required to raise the pressure of the condensate to match the feedwater pressure.

In theory, to increase expansion work, it would be beneficial to heat a greater portion of the DH water with low- rather than high-pressure steam. However, extracting steam from the midst of a turbine stage is limited by the physical construction of the turbine. Steam is restrained by the size of the opening in the turbine casing, due to which the extracted mass flow is rather unimportant in comparison to the main steam flow. In general, some 5 to 10 % of steam entering a turbine stage can be extracted

through an opening in the turbine casing [70, p. 6]. Using this estimate, it follows that the extractable flow of steam from the second LP turbine extraction opening is in the range of 10-20 kg/s depending on the operation mode.

Establishing a maximum for the steam exiting the second LP turbine stage allows defining the individual power capacities of the two district heat exchangers. The TTD of the high-pressure heat exchanger is first set to achieve a DH supply water temperature of 115 °C. Next, the TTD of the LP heater is adjusted so as to attain the desired DH power while maintaining the turbine extraction flow at a value close to yet less than 10 % of the steam entering the turbine pressure stage. The TTD of the LP district heat exchanger is limited to a minimum of 10 K.

The cycle is first parameterized to supply a maximum DH power of 10-250 MW between intervals of 10 MW. This is done to investigate what the maximum DH power should be set as to achieve COP gains. In Solvo, the simulation is executed by adjusting the DH power with the DH water flow rate. In each case, the district heat exchangers are re-parameterized in design mode while other components remain in off-design mode. The DH water is always heated from 60 °C to 115 °C.

Figure 35 shows the graphed simulation results. With SMR2, a DH power of 250 MW could be achieved with a COP of 3,86. A DH power of 54 MW corresponds to a COP of 4,62, indicating an improvement of above one unit compared to SMR1. The COP is seen to grow as DH power decreases due to the growing ratio of low-pressure to high-pressure heating. The correlation is illustrated in Figure 36. The growth is somewhat linear between DH power outputs of 100 and 250 MW. Below 100 MW, the rate of growth of the COP becomes significant, although a majority of heating is still executed with high-pressure steam. This dynamic changes below DH power outputs of 50 MW, when the heating process is dominated by low-pressure steam. The highest COPs are thus attained at very low DH power outputs. The maximum COP would likely be greater if the TTD of the LP district heat exchanger were not restricted.

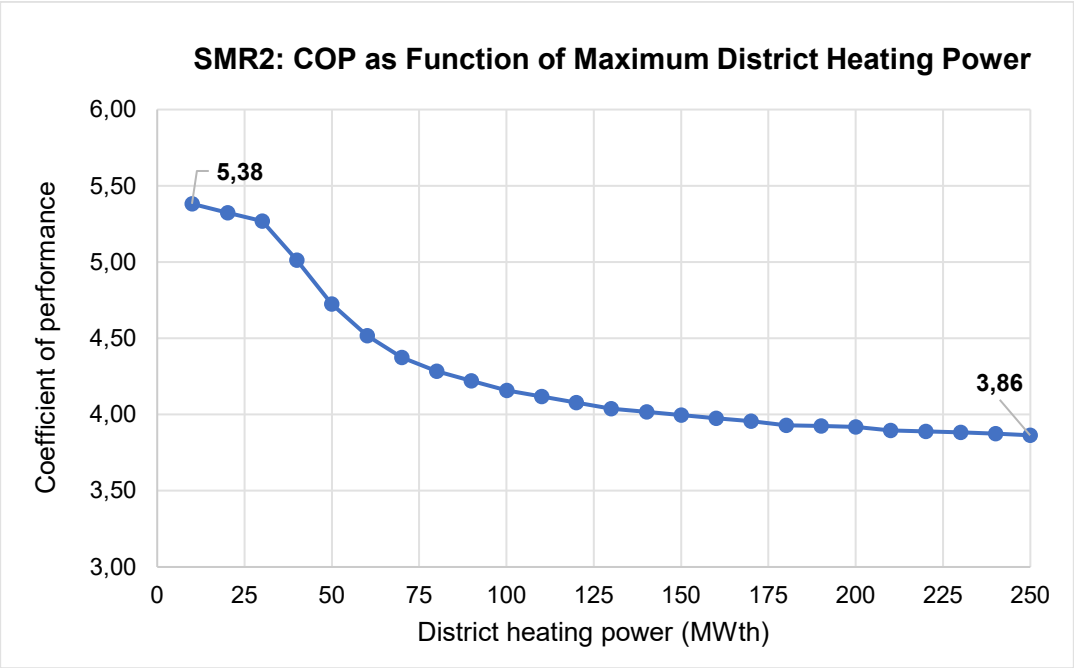

Figure 35: The COP of SMR2 when its maximum district heating power is varied.

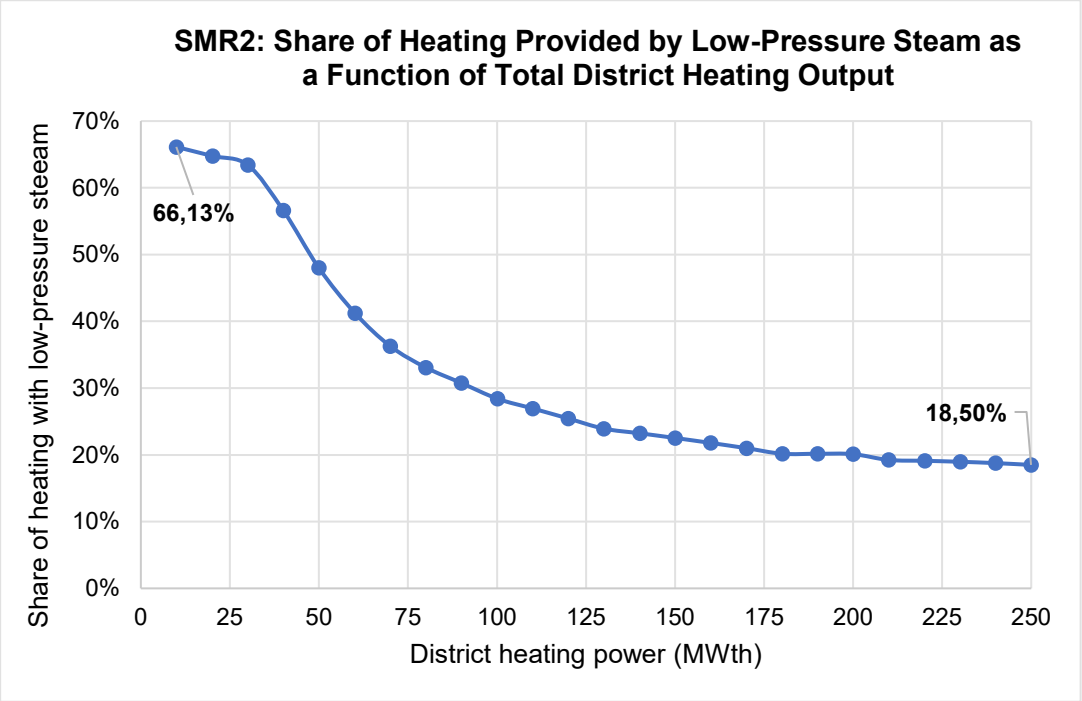

Figure 36: The share of low-pressure heating of SMR2 when its maximum district heating power is varied.

Figure 35 indicates that a COP of 4,0 is achieved when SMR2 is dimensioned for a maximum DH power of 150 MW. This represents a viable objective for the district heating output as it shows a 13 % improvement in the maximum COP and almost a three-fold increase in heating capacity compared to SMR1. Hence, this solution is examined individually in Figure 37. The COP varies between 4,0-4,3 with an average of 4,1. An increase in the COP at low heat loads is observed, which again proves to be a result of the increased utilization of low-pressure steam. Nevertheless, variation is minimal, and the share of low-pressure heating remains between 22-35 % at all loads.

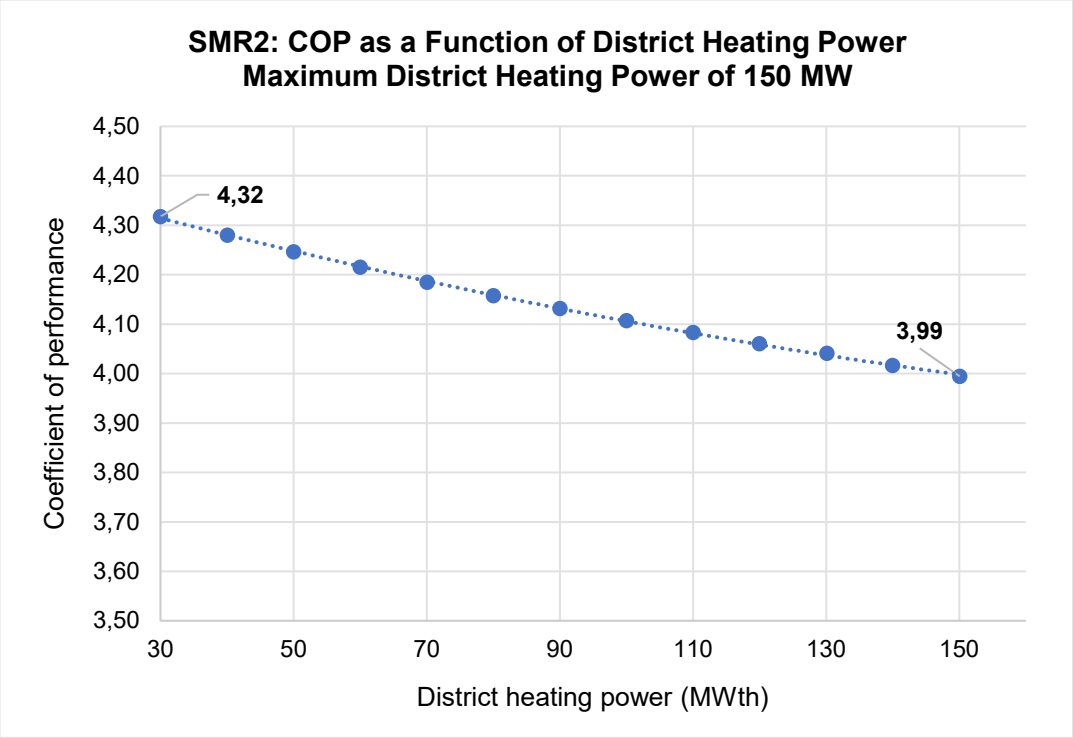

Figure 37: The COP of SMR2 when dimensioned for a maximum district heating power of 150 MW.

Overall, the method of steam extraction limits the performance of this CHP steam cycle. District heating outputs above 50 MW utilize high-pressure steam for the majority of the heating process, which compromises electric power output. Lowering the HP turbine exhaust pressure even further could increase the COP, but simulation results suggest that a greater reduction in HP turbine outlet pressure leads to extraction flows exceeding 10 % of the incoming flow. Therefore, it is unlikely that the technical configuration of the turbine as it is would be able to withstand lower pressures and higher extraction flows. If a higher DH output were to be achieved with a sensible COP, the method of heat extraction should be revised.

7.5 SMR3

The final CHP steam cycle of SMR3 demonstrates how the COP of heat production is affected if the steam cycle is modified significantly. Furthermore, subchapters 7.5.1 and 7.5.2 examine the effects of altering the cycle cooling water temperature and optimization point. The solution presented hereafter is technically feasible, but it has not been proven to function in practice. The discussed modifications will likely require redesigning the steam turbine. Moreover, the presented solution is not optimized, and it is possible that superior results could be achieved. A schematic of SMR3 is shown in Figure 38 and a comprehensive heat balance diagram is attached in Appendix D.

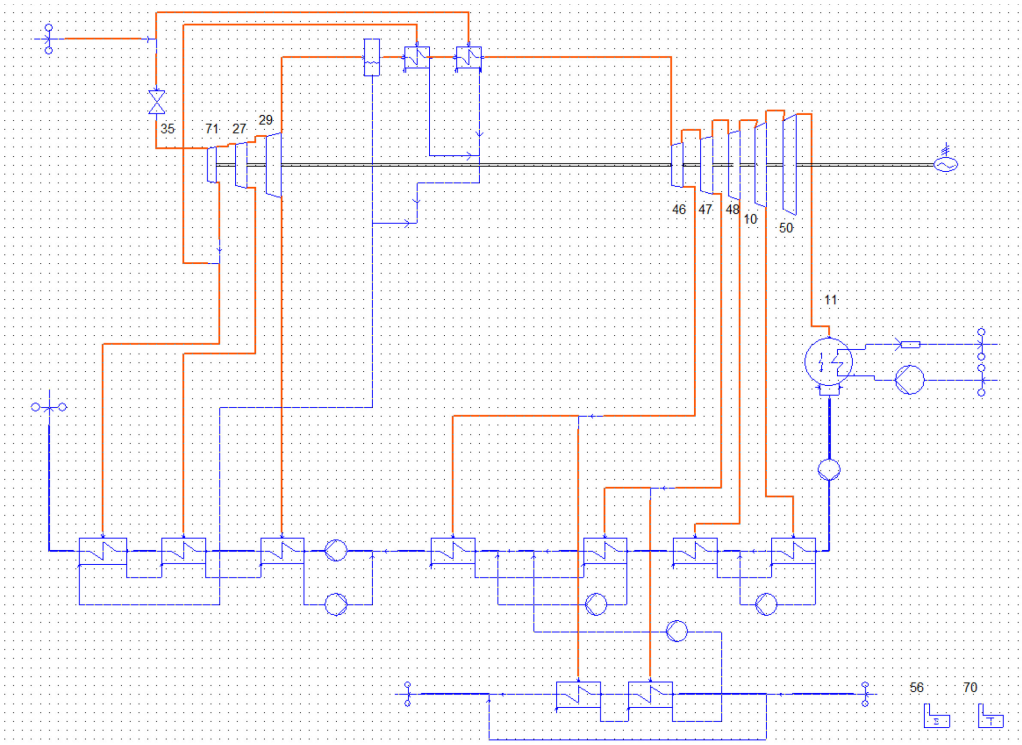

Figure 38: The SMR3 CHP steam cycle in Solvo Software.

7.5.1 Modifications to the Condensing Configuration

In SMR3, the baseline model of SMR0 is altered to achieve gains in cycle performance. Modifications are made in terms of the heat exchanger condensate arrangement, turbine pressure stages, and heat exchangers.

Firstly, the number of feedwater preheaters is increased from four to seven. The effect of feedwater preheating was discussed in Chapter 4.1. The addition of three preheaters requires constructing three new lines from the steam turbine: two from the high-pressure side and one from the low-pressure side. In condensing mode, the

feedwater of SMR3 returns to the steam generator at some 205 °C instead of the previous temperature of 150 °C. On the temperature-entropy diagram in Figure 39, the added preheaters are shown as new constant pressure lines.

To increase heat transfer, the TTDs of all heat exchangers are lowered to 10 K. The condensates streams from the heat exchangers are connected in three cascade configurations. The streams are returned to the main flow at three separate locations with temperatures as close to the condensate streams as possible. Correspondingly, three additional pump components are needed to execute this.

Previous models affirmed that using low-pressure steam for district heating results in an increased COP. Thus, instead of demanding a constant enthalpy change of the feedwater flow, extraction pressures of the LP steam turbine are defined to supply steam at a favorable temperature for district heating. Although this definition is likely to result in a loss of 1-2 MW in electric power, it is seen as a reasonable compromise to enhance the COP. The HP turbine inlet and outlet pressures as well as the condenser pressure remain unaltered.

The improvements made to the steam cycle raise the simulated electric power of SMR3 in full condensing mode to 193,7 MW, that is 6 MW more than SMR1. The steam cycle of SMR3 in condensing mode is pictured on a temperature-entropy diagram in Figure 39.

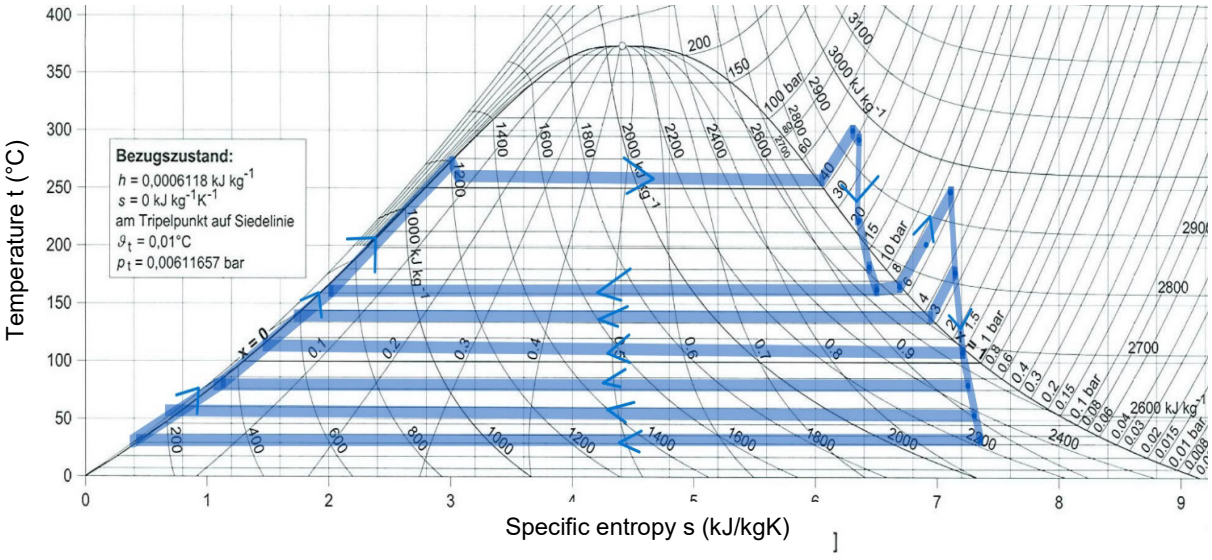

Figure 39: The steam cycle of SMR3 in condensing mode on a T-s diagram.

7.5.2 Combined Heat and Power Configuration

In SMR3, district heating water is heated entirely with low-pressure steam from the first two LP turbine extraction openings. The TTDs of the two district heat exchangers are set to 10 K, and the extraction steam flows from the turbine are not limited. District heat exchanger condensate streams are joined in a cascade configuration and used in the feedwater preheating process.

Given the described conditions, SMR3 is able to provide a maximum district heating power of 181 MW with a COP of 5,99. The rate of change of the COP is rather minimal: the COP ranges from 6,0-6,1, as demonstrated in Figure 40. Similarly to SMR2, the COP of SMR3 increases with reducing DH loads as the heating process is executed with lower-pressure steam. When operated at full DH power, the extraction flows from the first and second LP turbine openings amount to 30,5 % and 25,6 % of the steam flow entering the respective stage, indicating a three-fold increase compared SMR1 and SMR2. The low- and high-pressure turbine expansion curves are shown on an enthalpy-entropy diagram in Figure 41.

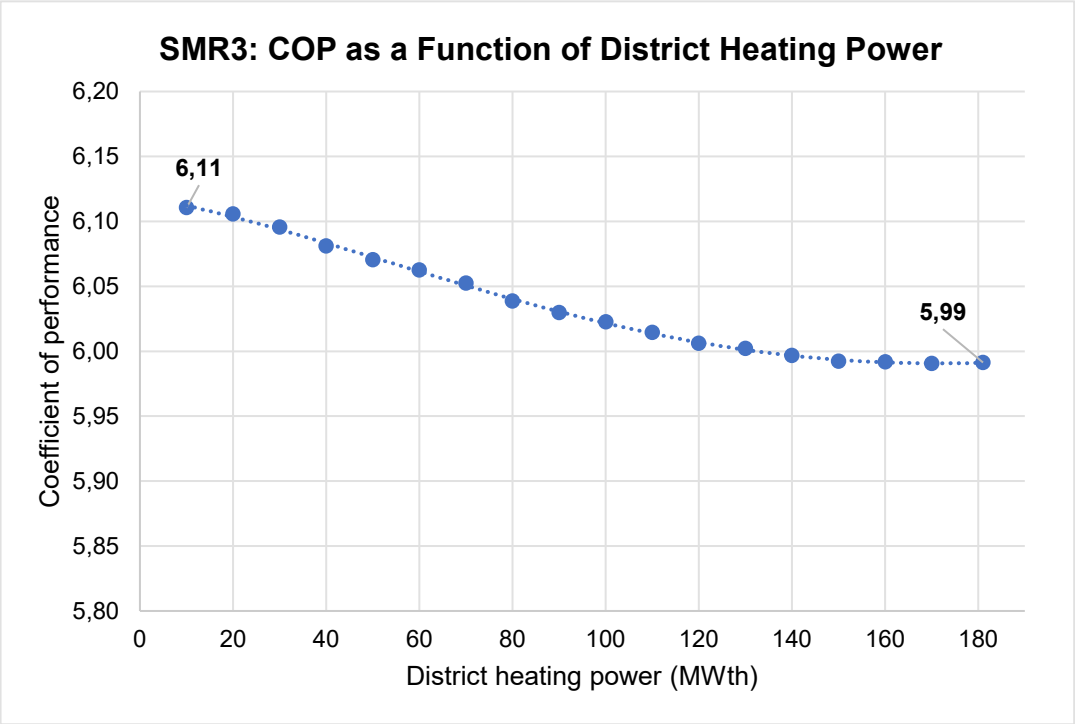

Figure 40: The COP of SMR3 as a function of DH power.

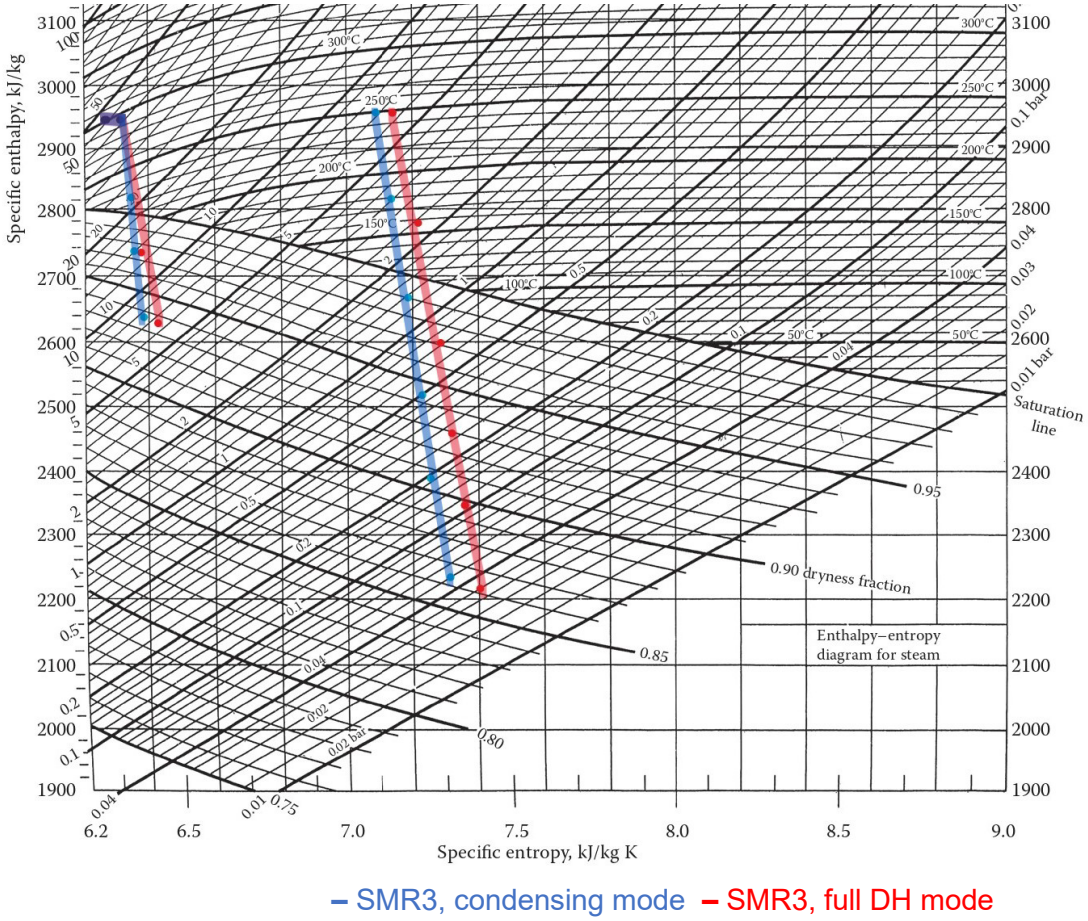

Figure 41: The low- (left) and high-pressure (right) turbine expansion curves of SMR3 in condensing and full DH modes.

7.5.3 Effect of Heat Sink Temperature

As stated in Chapter 4.1, a means to increase the performance of a steam cycle is to reduce the condenser pressure by lowering the temperature of the cold source medium. This is proven for the case of SMR3 by repeating the simulation procedure with a cooling water temperature of 10 °C instead of 17,5 °C. This temperature better represents the average climate conditions in Finland. At maximum DH power and with a cooling tower operating at an efficiency of 70 %, a tower outlet water of 10 °C could be achieved with, for example, an air temperature of 10 °C and a relative humidity of 75 %.

In Solvo, the simulation is repeated by re-parameterizing all SMR3 steam cycle components using cooling water at a temperature of 10 °C and setting this as the new reference state. No further changes to other components are made, although in actuality, a new point of dimensioning would presumably require redefining process parameters. The cooling water mass flow rate also remains unchanged despite the

fact the a colder cooling medium would require a smaller flow. Because no additional changes are made, the electric output of SMR3 in full condensing mode remains at 193,7 MW.

Lowering the cooling water temperature by 7,5 °C results in an 18-% reduction in condenser pressure at full district heating power. The pressure is reduced from 0,034 bar to 0,028 bar. A lower condenser pressure allows steam to expand further in the LP turbine, which in turn increases electric output. A district heating output of 181 MW is now achieved with a COP of 6,36, and the average COP of the cycle is increased by 8,5 %. As shown by Figure 42, the rate of change of the COP is also steeper than with warmer cooling water.

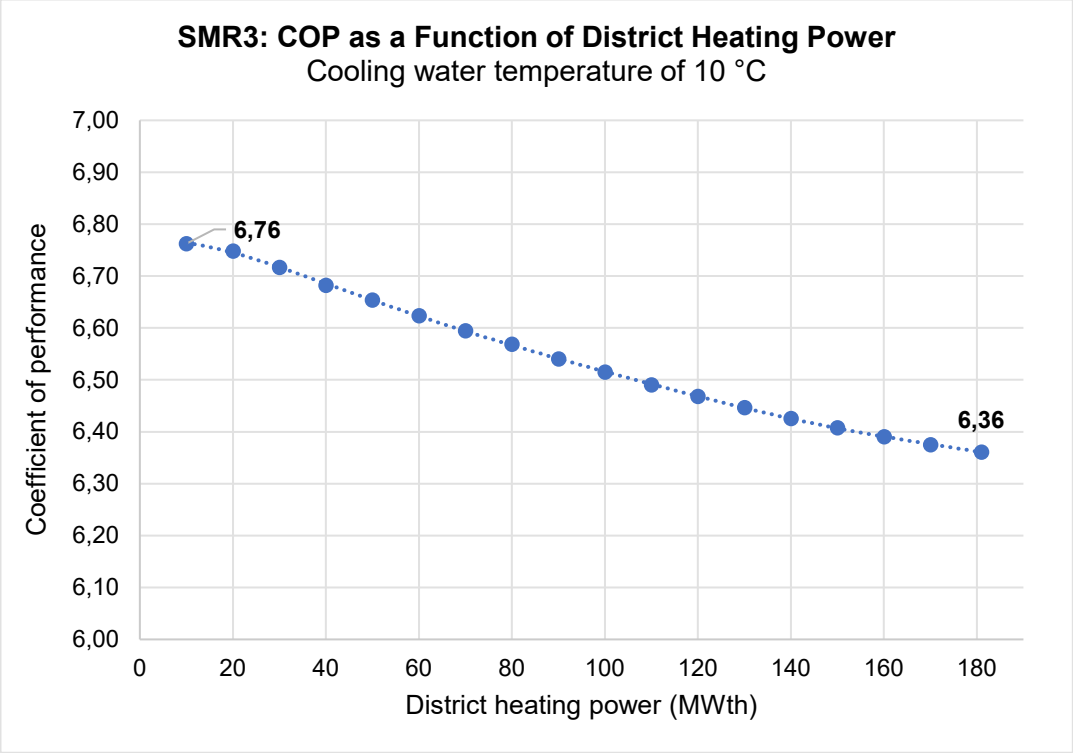

Figure 42: The COP of SMR3 when cooling water temperature is lowered.

7.5.4 Effect of Optimization for Heat Production

The steam cycles thus far have been optimized for electricity production to ensure operation at low heat demands. However, the ability of a CHP plant to operate in condensing mode in high heat demand areas may be unnecessary as a level of heating is required throughout the year. This is the case with conventional backpressure CHP plants, which are designed for heat production and often lack the ability to operate in condensing mode. Components dimensioned for high district heating outputs are likely to yield a higher COP of heating.

To study how the optimization point affects the performance of a CHP plant, SMR3 is re-parameterized once more. The simulation is now repeated with the purpose of giving the model a new reference state corresponding to the maximum district heating power load. In Solvo, the process starts by restoring the reference state and resetting all components to design mode. No individual component qualities or process parameters are changed. Then, all components are parameterized at a maximum district heating power of 181 MW. This implies that the steam turbine, for example, is now dimensioned for a steam mass flow rate corresponding to operation at maximum district heating power. To incorporate the results from the heat sink analysis, the cooling water is lowered to 10 °C.

The new reference state results in an output of 193,8 MW_e in condensing mode. A significant improvement in the COP is observed: a maximum district heating power of 181 MW is now achieved with a COP of 6,54. Figure 43 demonstrates the rate of change of the COP, which is also greater in comparison to the previous simulations.

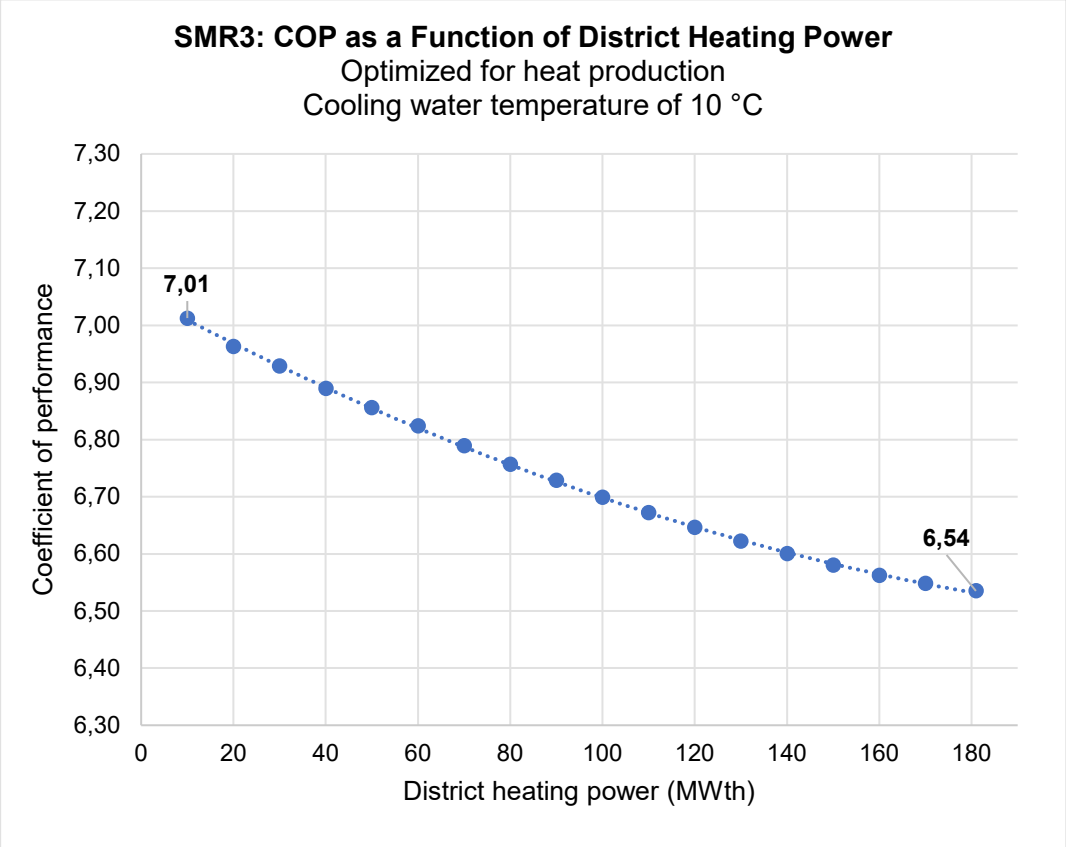

Figure 43: The COP of SMR3 with a lower cooling water temperature when it is optimized for heat production.

The simulation model of SMR3 does not yield an error when it is operated in condensing mode, suggesting that it may be able to operate at small heat loads. However, configurations designed for heat production are not expected to function

in full condensing mode. In the case of SMR3, optimizing the cycle for full DH power requires dimensioning the steam turbine for small steam flow rates through the low-pressure section. If the DH power is decreased, steam flow passing through the turbine increases, which the turbine will not be able to endure if the change is not accounted for in the design. Therefore, the drawback of favoring heat production in plant design is the risk of plant standby when heat demand is low. Furthermore, if a CHP SMR were designed to prioritize heat production, the presented model would most likely not be the optimal technical solution to doing so. Thus, this simulation serves merely as an example of how the optimization of a CHP plant can affect plant performance.

7.6 Summary of Models

Table 11 compiles the main technical parameters of each steam cycle discussed in this chapter. Electric outputs calculated in Solvo do not account for plant internal consumption, and their purpose is to enable comparison between different models rather than to serve as absolute values.

Table 11: Compilation of the CHP steam cycles and COPs.

Configuration	**Electric power in condensing mode (MW_e)**	**Maximum DH power (MW_{th})**	**Electric power in full DH mode (MW_e)**	**COP at maximum DH power**
SMR1	187,7	54,0	172,4	3,54
SMR1 with an additional valve	187,7	60,8	166,8	2,91
SMR2	187,6	150,0	150,0	4,00
SMR3	193,7	181,0	163,5	5,99
SMR3 with cooling water of 10 °C	193,7	181,0	165,3	6,36
SMR3 optimized for heat production with cooling water of 10 °C	193,8	181,0	166,1	6,54

8 Operational Analysis

In this chapter, the operation of the SMR configurations presented in Chapter 7 are applied to actuality. The SMRs are matched with Finnish cities based on the assumption that a CHP SMR should supply approximately 50 % of local peak DH demand. A summary of possible city matches is presented in Table 12.

Table 12: A summary of the CHP SMRs and possible city matches.

CHP SMR	Maximum DH power of two reactors (MW_{th})	Best city matches*	Other possible city matches**
SMR1	108, 122 (valve)	Pori	Rovaniemi
SMR2	300	Vantaa, Oulu, Turku	Jyväskylä, Lahti
SMR3	362	Tampere, Turku	Vantaa

**Cities where 50 % of peak power demand is as close as possible to the SMR maximum DH power*
***Cities where 50 % of peak power demand is slightly less than the SMR maximum DH power*

An SMR investment may involve constructing several SMR units. Determining the number of commissioned SMR units requires detailed financial and energy system analysis, which is outside the scope of this thesis. Therefore, this analysis assumes the construction of only one SMR unit in one city. SMR3 with the best overall COP and highest DH output is chosen as the subject of analysis. One plant containing two reactors has a total maximum DH power output of 360 MW. This implies that it could accommodate a city with a peak power demand of 700 MW and an average yearly DH demand of 2 000 GWh. Out of the 11 cities considered and listed in Table 2, Tampere and Turku show to correspond best with these criteria. Tampere as the closest match is chosen as the location for the operational analysis.

The yearly operation of SMR3 is investigated by running it against hourly heat demand in Tampere. An approximate heat load curve for Tampere, shown in Figure 44, is constructed using open Helsinki data from 2019. The year 2019 is chosen because it closely matches the 2015-2022 averages for peak power demand and annual DH consumption. A specific year instead of average values is analyzed as forming averages of hourly demands over a long period of time would distort shifts in peak power demand. Helsinki data is scaled for Tampere by utilizing the total district heating demand during the same year. Using this approach, the peak power demand of Tampere during this example year is estimated to be 730 MW.

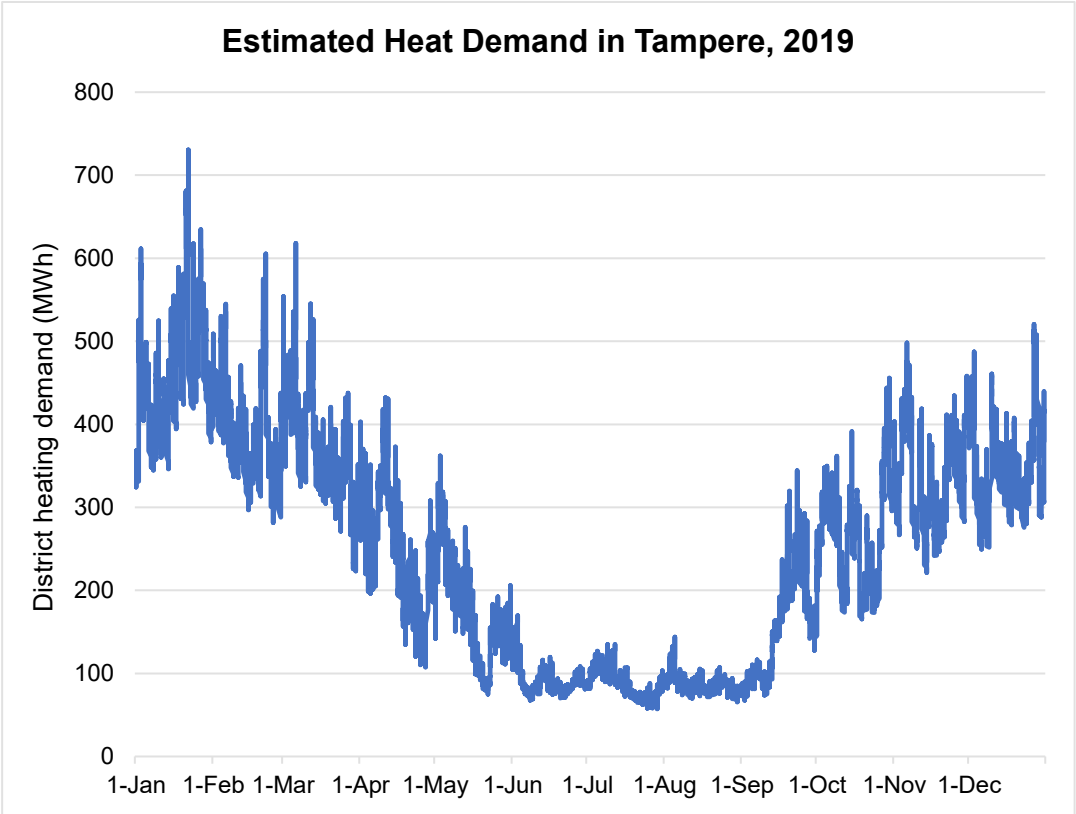

Figure 44: A heat load curve for Tampere, 2019. The curve is formed by scaling Helsinki data from the same year. [27]

The simulation scenario is defined as follows. First, the SMR is operated for 8 016 h during a year, implying that it is shut down for maintenance during the month of July. This month is often the hottest month with the lowest heat demand. In addition, the configuration of the steam cycle is optimized for electricity production to ensure that the plant is capable of operation in full condensing mode if necessary. Nevertheless, the plant load is defined purely according to DH demand. Electricity prices and all other optimization is disregarded. Finally, the cooling water flow is maintained at a constant temperature of 10 °C to increase electric output. It is also a temperature that could be achieved in Tampere, where the average air temperature and relative humidity in 2019 were 6 °C and 80 % respectively [71]. The cooling water mass flow rate is not altered, although in reality using colder water would entail a smaller mass flow rate. All simulations are executed at a full reactor thermal power of 540 MW.

It is first studied how SMR3 functions without supporting heat production capacity. In this simple scenario model, the hourly power output of SMR3 is defined only by the hourly heat demand. If the hourly heat demand exceeds the maximum DH power of SMR3, the plant is simply operated at full power. Electric output is defined by the heat output and the COP corresponding to the heat load.

Figures 45, 46 and 47 present the DH and electricity output as well as the COP of SMR3 during the sample year. Operating SMR3 in this manner yields a total DH output of 1 996,7 GWh and a total electricity output of 2 795,0 GWh with an average yearly COP of 6,48. SMR3 alone is able to suffice 89,6 % of total yearly district heating demand. The plant is always operated at 85-98 % of rated electric capacity and never in full condensing mode. Results show that SMR3 alone meets heat demand during 5 011 hours of the year, that is 62,5 % of its operational time and 57,2 % of the total year.

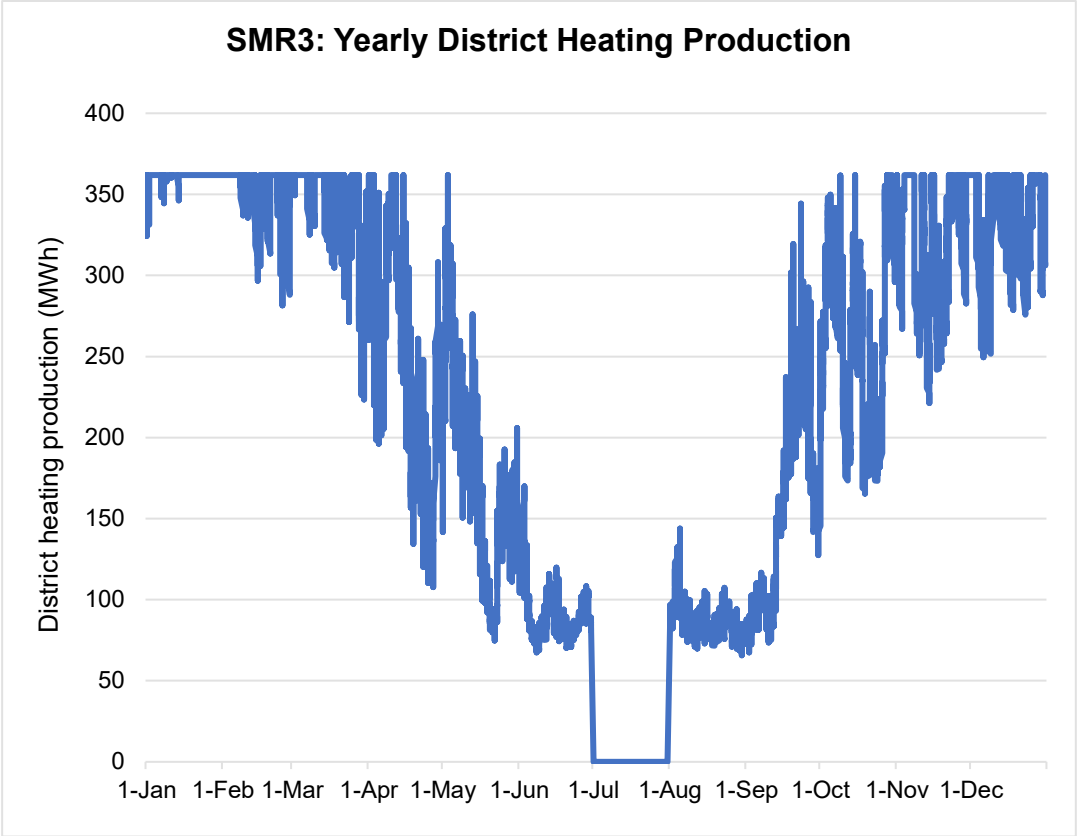

Figure 45: The yearly district heating production of SMR3. The plant is ramped down in July.

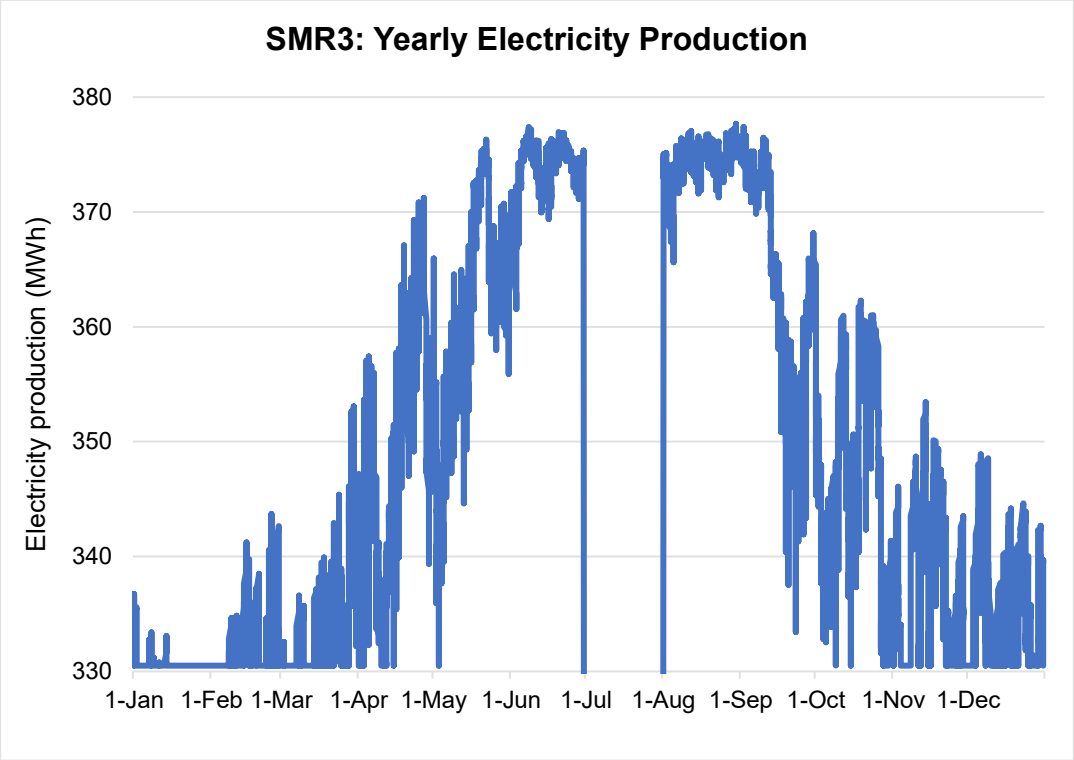

Figure 46: The yearly electricity production of SMR3 when it is operated without supporting capacity.

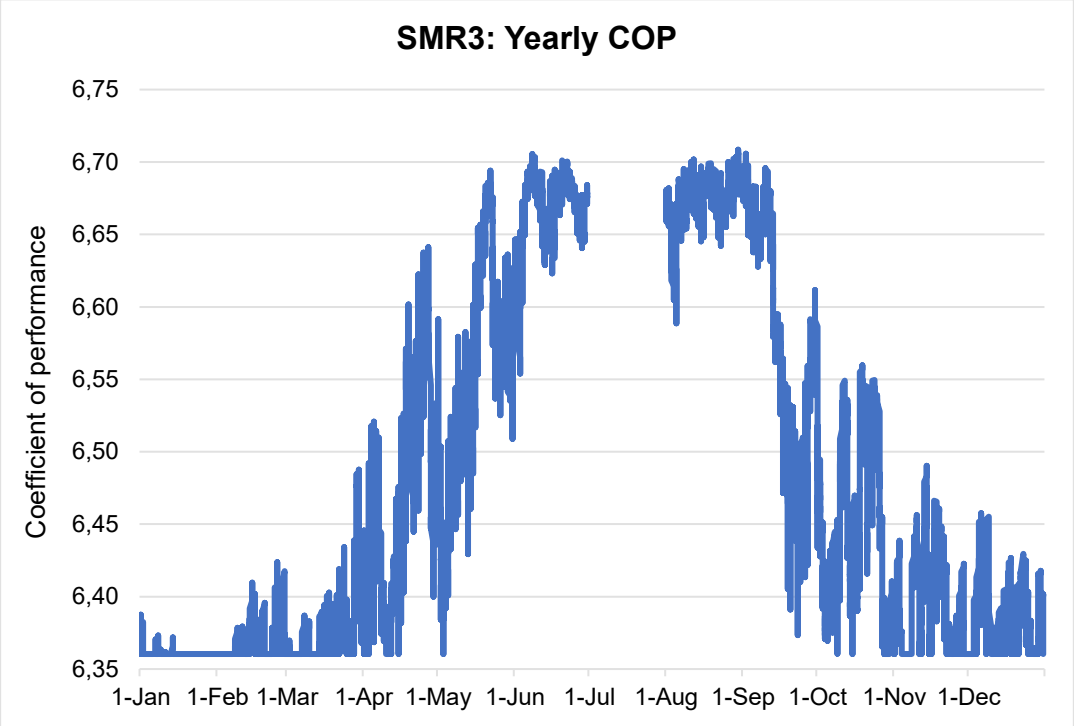

Figure 47: The yearly COP of SMR3 when it is operated without supporting capacity. The COP increases as DH load decreases.

8.1 Supporting Heat Production

It is established that a total of 233 GWh of additional production during 3 749 hours is required to suffice heat demand during the entire year. Therefore, to complete the operational analysis, SMR3 is assessed as a component of an energy mix. The most cost-effective approach to balancing demand and supply is through a district heating storage, which is used at the first hand in this scenario. Remaining demand is supplied through other production methods.

Tampere has one existing district heating storage of a 100-MWh vicinity and a total peak power production capacity of some 600 MW through heat-only boilers [26]. Currently, there are no heat pumps for district heating in the area. The existing heat storage holds a volume of 2 300 m^3 [72, p. 60], and a second storage of 15 000 m^3 is under construction in connection to a new electric boiler unit in Lielahti, where operation is expected to begin in 2025 [73]. The capacity of the new storage will reach 2 000 MWh. Both the existing and planned storage serve the purpose of regulating intraday demand. [41, pp. 23-24].

SMR3 is now run alongside one thermal energy storage with a capacity of 2 000 MWh and a maximum charge and discharge power of 200 MW. The heat storage is full at the beginning of the simulation, and it is discharged as often as possible without exceeding the maximum discharge power and storage capacity limits. The storage is charged whenever SMR3 has charging potential and the storage is not full. The utilization of the heat storage featured in this simulation scenario is not optimized, and it serves merely to demonstrate how a heat storage can decrease the need for peak production plants. Any leftover demand is supplied by other supporting production methods, the capacity of which is determined according to SMR3 and heat storage outputs. These supporting production methods are not explicitly defined.

Otherwise, the simulation scenario remains as defined in the previous chapter. SMR3 is operated during all months expect July for a total of 8 016 hours. The heat storage and other production units continue operation after SMR3 has been ramped down, although the heat storage is no longer charged. The period of analysis begins from the first of August after yearly maintenance, when the heat storage is fully charged.

The results of this simulation and the total district heating production distribution is presented in Figure 48. SMR3 produces the same amount of district heating as previously, but now it also charges the heat storage during 901 hours. Consequently, SMR3 produces a total of 2 024,7 GWh of heat, either directly for district heating or to charge the storage. A slightly higher heat output results in a corresponding decrease in electric production, generating a yearly total of 2 799,7 GWh. The

average COP of heating is minimally impacted: it is decreased only by 0,03 % and follows the same curve pattern presented in Figure 47.

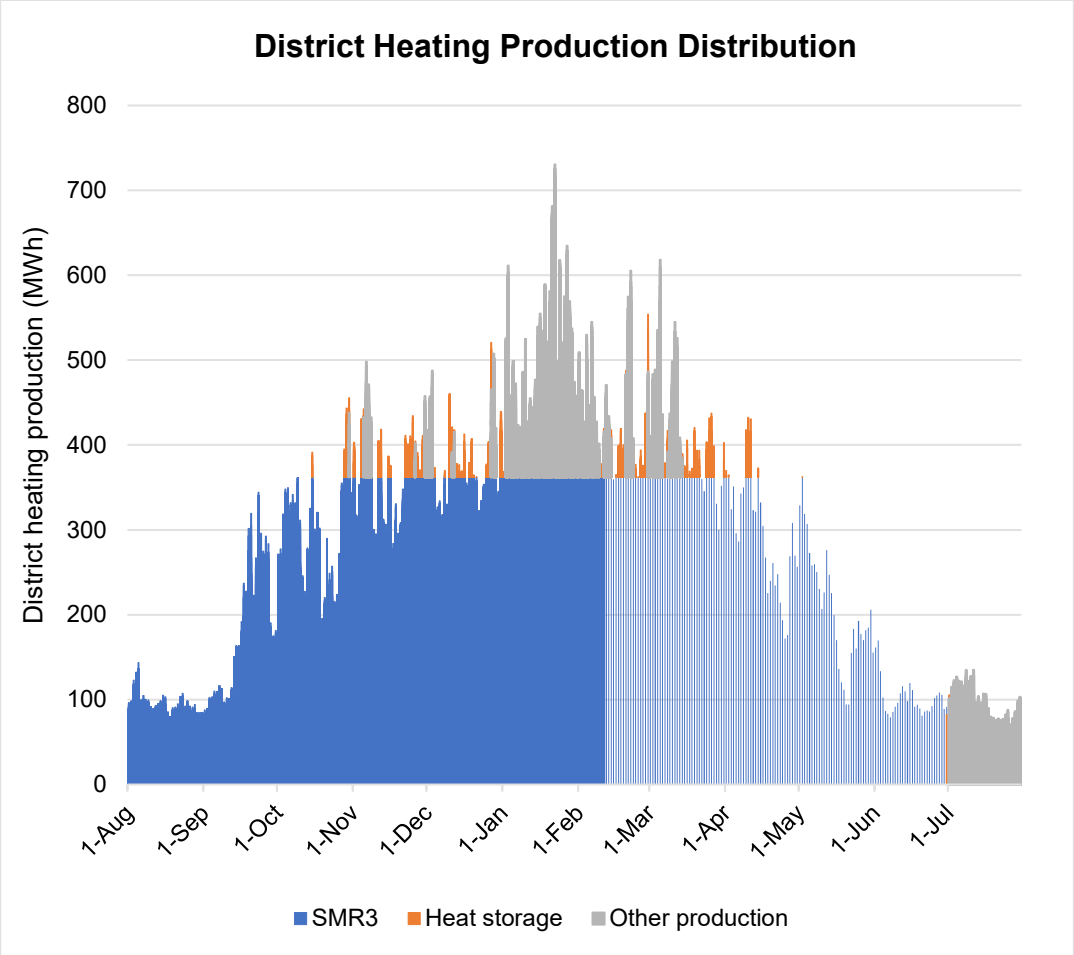

Figure 48: Yearly district heating production distribution between three different production categories. SMR3 is ramped down in July.

The heat storage is discharged during 809 hours at an average power of 32 MW. The heat storage produces 27,9 GWh of district heating during the year, that is 1,3 % of total annual demand. The storage is not required in the summertime, but during the highest demand peaks in January-February, the storage is discharged at almost full power and storage capacity is exhausted. The storage is most utilized during the late spring and early winter. The storage continues operation for a day or so after SMR3 is ramped down, but without additional charging power, it is unable to continue operation in July. Figure 49 shows the charging and discharging powers of the storage, and Figure 50 presents the storage level as a function of time.

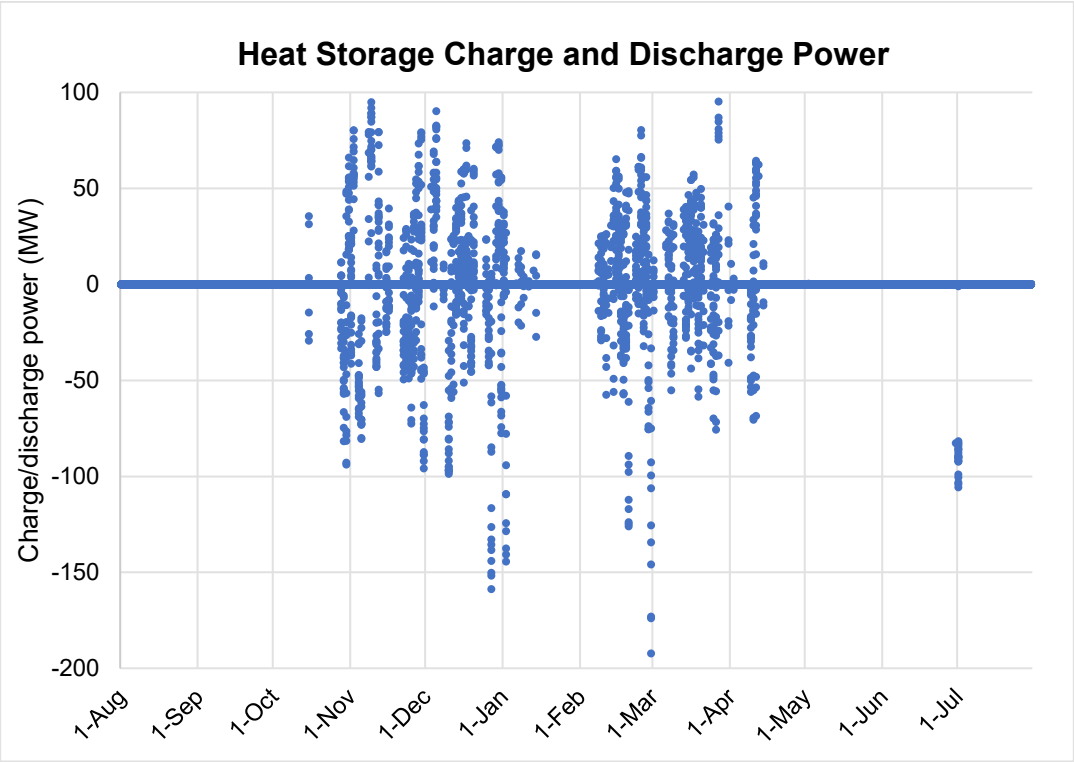

Figure 49: The discharging and charging powers of the heat storage.

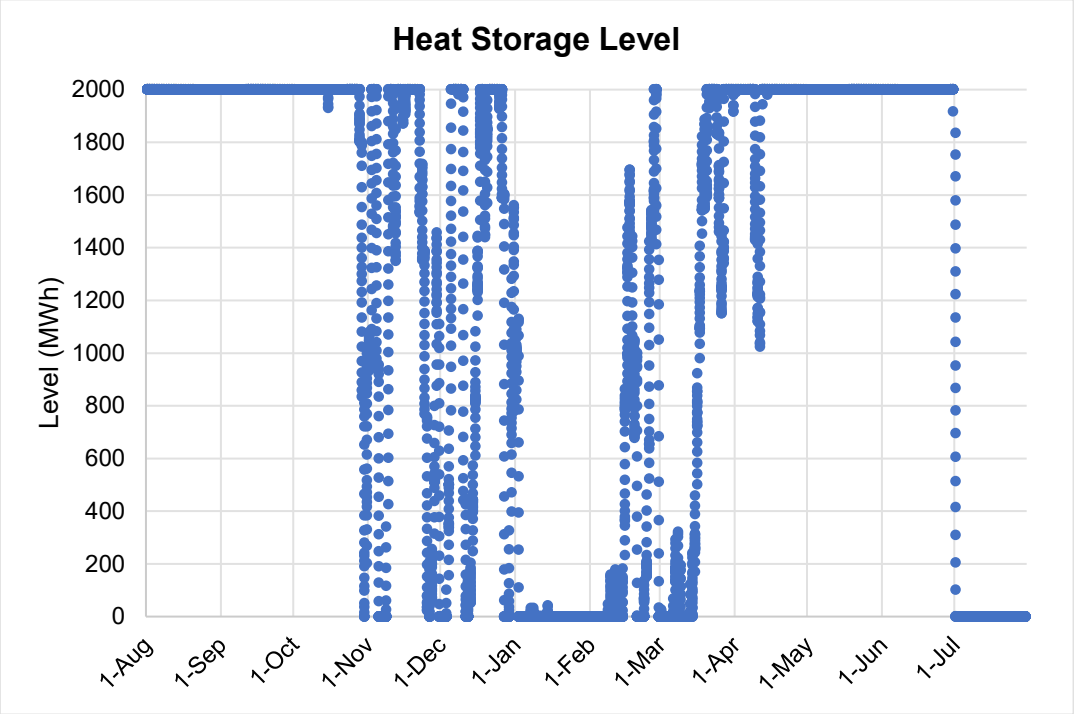

Figure 50: The thermal energy content of the heat storage. The storage would likely be utilized significantly more if electricity demand were considered in the simulation.

In total, some 205 GWh of additional production is needed to complement the operation of SMR3 and the heat storage. This corresponds to 9,2 % of total yearly demand. The considerable variation in the required additional capacity is depicted in Figure 51. From late spring until the autumn, SMR3 is able to supply all district heating demand. Other production methods are most utilized in the months of January and February, when a maximum of 370 MW of additional capacity is needed. On average, some 90 MW of additional capacity is required in July when SMR3 is ramped down. Overall, considering the boiler capacity of 600 MW in Tampere currently, results suggest that existing peak capacity could suffice this demand.

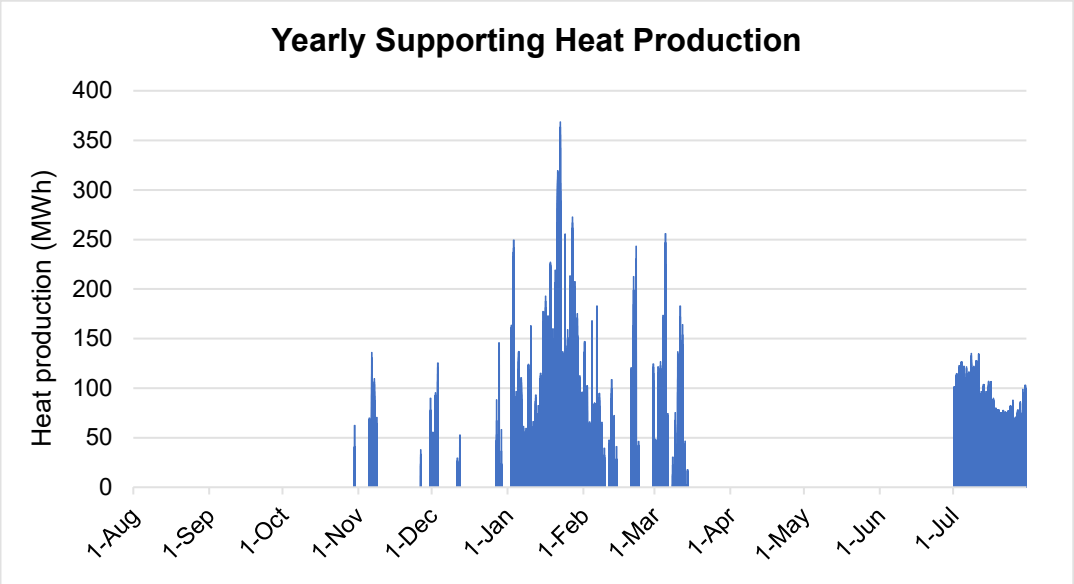

Figure 51: Required district heating capacity of other production methods.

8.2 Load Following Capability

The previous analysis did not account for plant startup time and assumed that the plant load could be adjusted sufficiently fast to meet fluctuation in heat demand. This is a tolerable assumption considering that the output of SMR3 was varied without altering reactor power and all simulations were executed at a full reactor thermal power. Electric power could be modified by utilizing excess reactor thermal power for district heating. This method of control is a less complicated process compared to adjusting electric output by modifying reactor power.

Although the simulation scenario assumed that the operation of SMR3 is defined according to heat demand, load following capabilities and ramp rates are generally discussed in terms of electric output. For reference, the load following capability of typical steam power plants is in the range of 3-5 % of rated electric capacity per minute [7, p. 202]. The IAEA states the generic ramp rate of a 900-1 300-MW_e

nuclear plant to be 30 MW/min [16, p. 17], that is some 2-3 %/min. The resulting rate of change of heat production is influenced by the steam cycle COP and the implemented DH control mechanisms. The SMR3 steam cycle model did not define the control mechanisms used to alter the DH output, although they are likely to affect the rate at which heat load changes can be executed.

Evaluating the ramp rate of a plant requires specifying steam turbine characteristics. SMR turbine manufacturers aim to provide operational flexibility corresponding to at least the requirements of the local electricity grid code. The Finnish grid code VJV2018 states that the rate of change of the power of CHP plants must be at least ±5 % of the rated electrical capacity per minute. This applies when the plant is operated in the range of 60-90 % of rated capacity, in which case the change of power taking place at a time shall not exceed 20 % of the rated capacity [74, p. 57]. In the simulation scenario, SMR3 is always operated at 85-98 % of rated electric capacity. Therefore, a minimum adjustability of ±5 % and a maximum adjustability of ±20 % are applicable. The lower and upper boundaries of the plant's load changes according to the grid code are presented in Table 12.

Table 13: Analysis of the load adjustability of SMR3 according to the Finnish grid code VJV2018. Thermal powers are calculated using an average yearly COP of 6,5.

Share of rated capacity	Rate of change of electric power	Rate of change of thermal power
5 %	19 MW_e/min per unit 10 MW_e/min per turbine	126 MW_{th}/min per unit 63 MW_{th}/min per turbine
20 %	77 MW_e/min per unit 39 MW_e/min per turbine	504 MW_{th}/min per unit 252 MW_{th}/min per turbine

Because heat demand is balanced by other production means, the operation of SMR3 in this analysis is very steady. Excluding ramp-down in July, the average hourly difference in the electric output of SMR3 is some ±1 MW/h. The largest power changes are in the range of ±10-15 MW_e/h, that is ±2,5-4,0 %/h or ±0,04-0,06 %/min. Thus, if the steam turbine is designed to comply with the grid code and the plant is operated according to heat demand, SMR3 would have no difficulty in adapting to load changes. The hourly load changes are well within the minimum requirements. It is also evident that a 20-% change in plant output is unlikely and unnecessary during normal operation. The case may be different if the plant operation is determined according to electricity, where fluctuation in demand is greater.

9 Discussion and Conclusions

This thesis presented the computational analysis of three combined heat and power steam cycles of a small modular reactor: SMR1, SMR2, and SMR3. The three CHP steam cycles were constructed by modifying a baseline model of a condensing secondary cycle referred to as SMR0. The objective was to study the coefficient of performance of heat production and factors affecting it. In the end, the implications of the COP on plant operation were analyzed by simulating the operation of one SMR design according to heat demand in Finland. This chapter discusses the results and conclusions of the work.

9.1 Summary of Results

Starting from SMR1, the average COP of heat production was raised from 3,5 to 4,1 in SMR2 and finally to 6,0 in SMR3. Maximum district heating outputs were increased from 2*54 MW to 2*150 MW to 2*181 MW. The COP of SMR1 particularly resembles existing DH heat pump facilities in Finland. The COP of SMR2 is similar to those of coal-fired CHP plants when compared to condensing power plants with a thermal efficiency of 40 %. SMR3 demonstrates a COP surpassing that of heat pumps and conventional coal-fired CHP plants.

SMR2 shows that with the initial steam cycle of SMR1, a) extracting over 150 MW of district heating with b) a COP above 4 while c) making no changes to the steam turbine appears unfeasible. This is validated by SMR3, where the configuration requires redesigning the steam turbine. The modifications made in terms of the condenser pressure and the feedwater preheating process in SMR3 affirm that minimizing entropy generation improves the efficiency of a thermodynamic cycle. Moreover, optimizing the steam cycle components of a CHP SMR for heat production further augments the COP of heat production. However, this may be achieved at the expense of limiting plant operation in condensing mode.

A key difference in the district heating configurations of the three SMR steam cycles is the method of steam extraction. Calculations confirm that using lower-pressure steam for district heating production is favorable for electric production and hence the COP of the unit. When steam from the low-pressure turbine is utilized for heat production, the COP decreases as DH output increases. The COP of producing heat with high-pressure steam could be increased by utilizing the enthalpy of the hot condensed steam either in an external process or towards feedwater preheating. If the pressure of the steam heating the DH water is maintained at a constant level, the COP also remains constant.

A CHP SMR with a district heating capacity of 362 MW could meet most yearly district heating demand in a city with a local peak power demand of 730 MW. This

is shown by SMR3, which satisfies 89,6 % of total yearly DH demand in a case representing Tampere when heat demand data is formed according to Helsinki. Coupling a 2 000-GWh heat storage with SMR3 saves 800 hours' worth of heat production that would otherwise be produced via other peak production forms. If SMR3 were to replace a conventional CHP plant in the Tampere region, the existing peak production capacity and planned heat storage capacities could complement its operation.

The operational analysis showed that if a CHP SMR is dimensioned to supply 50 % of local peak power demand and operated according to heat demand, hourly changes in the plant load are small. Comparison with the Finnish grid code implied that the load following capabilities of such a plant are well within minimum requirements. CHP production facilitates the operational flexibility of nuclear power plants, as electric power can be controlled without modifying reactor power by utilizing the excess reactor thermal power to produce district heating. Operating a heat storage alongside a CHP SMR further balances heat production and reduces the need for installed peak production capacity.

9.2 Discussion and Prospects for Future Research

SMR2 and SMR3 have a higher COP with smaller DH loads. The overall COP of these units is elevated during the summertime, which is somewhat impractical in the Nordics, where heat demand is significantly greater during the winter. On the other hand, this inverse correlation makes the transition to low-heat DH networks beneficial as the COP of heating will be improved if DH is supplied at lower temperatures. The steam cycles in this thesis were designed to supply DH water at 115 °C to account for existing systems. This is a high temperature, as the common target today is to supply DH water below 100 °C. Supply temperatures as low as 80 °C are imaginable in the future as heat distribution equipment and the energy efficiency of buildings improve. Therefore, in practice, the COPs may be greater than claimed.

The cases of SMR2 and SMR3 indicate that higher heat production efficiencies can be attained by making additional investments to the steam cycle. The reasonableness or the nature of the required investments were not specified, and a compromise between a high COP and a profitable CHP plant may have to be made. This should be determined separately by evaluating the business case of a CHP SMR. As piping and pumping costs comprise a significant portion of the initial investment of a DH production plant, the distance between a CHP SMR and a population center should be defined. This in turn is closely related to safety and legislative matters. Furthermore, efficient nuclear CHP production may require efforts and eagerness from industrial stakeholders and component manufacturers. For instance, it is

unlikely that a conventional steam turbine would be re-modeled in the interest of only one new power plant design. The case requires strong economic justification.

The operation principle of the heat storage in this simulation results in the storage being idle for a great majority of the year. Although the storage is empty and ineffective during peak consumption, this does not necessarily indicate that its capacity is insufficient. It is possible that the heat storage capacity would suffice if the operation of the CHP SMR were optimized. The optimization could be approached via an optimization model, which in the context of CHP production is typically a linear programming model, where a linear objective function is minimized or maximized while accounting for linear equality or inequality constraints. The objective function is usually to minimize operating costs and to maximize revenues. Neither objective automatically results in maximized energy efficiency, as this requires minimizing fuel consumption. [75, p. 731]

The cost-optimal operation of CHP plants in an energy system has been discussed in several studies over the years. An example of heat storage optimization is described in a paper by Fang and Lahdelma [76], where a sliding time window method is used to optimize CHP plant operation with a heat storage. The optimization results demonstrate that a heat storage can improve the cost-efficiency of a backpressure CHP plant considerably. Furthermore, a demonstration of evaluating the techno-economic aspects of CHP generation with peak production units is discussed by Wang et al. [77]. The research indicates that there is an optimal design heat load for CHP plants that minimizes net heating costs. Ultimately, achieving a realistic and cost-efficient simulation model of a CHP SMR involves optimizing the operation of both the SMR and components coupled with it.

The optimization of a CHP SMR is strongly linked to the electricity market. The variability in electricity demand and price is a critical element that extends beyond the scope of this work yet could significantly impact the results. Compared to a conventional CHP plant, a CHP SMR could be impacted by market conditions to a greater extent assuming the utilization of an extraction-condensing turbine. This allows for more flexible electricity generation in comparison to a backpressure turbine. A complete operational analysis of a CHP SMR should thus involve considering electricity demand. Furthermore, the operation of the CHP SMR is affected also by costs, which define the merit order of power plants. Thus, a logical progression for research is to examine the marginal costs of a CHP SMR and alternative heat production methods. This would also give insight into the profitability of a CHP SMR.

This thesis explicitly mentions heat pumps as an alternative heat production method due to the similar concept of the heat pump COP. Calculations indicate that the COP of a CHP SMR may surpass that of a heat pump. Although the two technologies are

compared to one another, they could be complementary rather than competitive. Heat pumps contribute to the issue of electricity supply-demand imbalance, whereas a CHP SMR could contribute to the solution by offering heat production independent of electricity. The choice between a DH heat pump and CHP SMR will depend on aspects beyond the COP of the unit – factors such as public acceptability, capital and operational expenditures, and licensing, to name some, are expected to influence the decision. In the long run, integrating various available technologies could provide a flexible and secure method of sustainable heating. Therefore, alternative solutions beyond CHP SMRs and heat pumps should be researched.

To comprehensively evaluate the efficiency of nuclear heat production, further technical solutions should be assessed. Such analysis could include examining the feasibility of a backpressure turbine, which in addition to extraction-condensing turbines, is the second primary technical approach to CHP production. Backpressure turbines have been shown to have great heat production efficiencies in conventional CHP plants, yet they remain a rather unexplored subject in the context of nuclear reactors. A further approach to nuclear heat production is through heat-only reactors, which could be seen as competing or complementing substitutes for CHP SMRs. In this case, calculating a COP is unfeasible, and the efficiency of a heat-only solution should be evaluated using alternative methods.

Finally, this thesis focused exclusively on technical factors, intentionally excluding other aspects. The topic of nuclear CHP entails at least social, political, environmental, legislative, and safety-related elements. These dimensions are crucial to the overall context of a CHP SMR and should be explored in future research.

9.3 Limitations and Sources of Error

The results of these simulations cannot be entirely expanded to other SMR designs. Apart from the initial data, steam cycle process parameters were calculated independently, and some simplifications were made. Live steam was assumed to be superheated, when often in nuclear power plants it is in a saturated state. The estimated process parameters were not verified by SMR manufacturers, and the calculations may involve errors. Moreover, the CHP SMRs contain two steam turbines, which is not the case in all SMR designs. The operation of two turbines is not fully comparable to one. For example, energy losses and equipment costs may be doubled.

Some simplifications were made in terms of district heating capacities and demand. Firstly, estimates of possible CHP SMR capacities were based on current heat demands and existing heat production units. This thesis did not evaluate the potential capacity of a future CHP SMR. It is possible that the CHP SMRs would not conform with the DH networks in the claimed cities. Conversely, the SMRs could suit many other cities not covered in this work. Secondly, open data regarding hourly district heating demand was available only for the case of Helsinki. This data was scaled for other cities including Tampere. The Finnish capital city of Helsinki features a large population density and a diverse energy mix compared to smaller Finnish cities. Scaling Helsinki data for other cities is likely to result in at least some level of error.

The results of the operational analysis could be swayed by a different simulation scenario. The annual maintenance of the CHP plant was planned for the month of July when heat demand is low. However, due to staff-related reasons or the simultaneous maintenance of other nuclear plants, the maintenance could take place during another time. It is also not unusual that maintenances are prolonged due to unforeseen circumstances. Should the outage of a CHP unit occur during the main heating season, it would lead to a considerable deficit in baseload heat production capacity. Moreover, heat demand data was derived from the year 2019, which took place before COVID-19 and the energy crisis. The conditions of the energy market then are not entirely comparable to the present day. Furthermore, the analysis is based on the case of one individual year rather than long-term trends. Because demand data was formed by scaling, the results of the operational analysis could be applied to essentially any city with a yearly DH consumption of 2 000 GWh and a peak power demand of 700 MW.

9.4 Conclusion

Targeting a high COP of heat production is motivated by several factors. Readily apparent reasons are related to energy efficiency and cost savings, as a higher COP enables greater heat production with the same equipment and fuel resources. The COP also influences the load following capability of a CHP unit: with a high COP, a greater amount of heat power is produced for the same amount of electric power, improving the plant's capability to meet varying demand. These findings imply that a CHP SMR with a high COP has the potential to produce heat and power flexibly and cost-effectively.

While a high COP serves as an incentive to deploy a CHP SMR, actual implementation will depend on factors outside of the COP. Integrating a CHP SMR into a DH production mix would transform the operating principle of the DH network in question. The undertaking represents a major financial commitment. For the project to be feasible, licensing, environmental and safety-related considerations would have to align with the business case. On a global scale, the state of the energy system and advancements in other technologies will significantly impact the deployment of SMR technology. Growth in renewable energy sources and the electrification of heat production, for example, are directly linked to the viability of CHP SMRs. Ultimately, the applicability of a CHP SMR into a Finnish DH network depends on multiple aspects that cannot possibly be examined carefully within the scope of one thesis.

To conclude, the findings of this thesis underscore the importance of the design of nuclear steam cycles. Steam cycles contribute to overall plant efficiency and optimizing them can lead to considerable cost savings and increased competitiveness. While new SMR designs may present sophisticated technology and complex design features, the fundamental power production of most commercial nuclear power plants relies on the same Rankine cycle. Continued focus on refining nuclear steam cycle design remains essential to advance nuclear technology and reinforce its role in a clean, efficient energy future.

Bibliography

[1] Finnish Government, A Strong and Committed Finland, Helsinki: Prime Minister's Office, 2023.

[2] Finnish Energy, “Puhdistuva kaukolämpö,” 2024. [Online]. Available: https://energia.fi/energiapolitiikka/vahahiilisyyden-tiekartta/puhdistuva-energia/puhdistuva-kaukolampo/. [Accessed 15 February 2024].

[3] Finnish Government, “Act of Banning the Use of Coal for Energy Generation, 416/2019,” 2019. [Online]. Available: https://www.finlex.fi/fi/laki/alkup/2019/20190416.

[4] Finnish Energy, “Kaukolämmön vuositilastot: päästöt romahtivat, kaukolämpö tasoittaa sähkön hintavaihteluita, uusissa kerrostaloissa kaukolämmön suosio kääntynyt kasvuun,” 25 January 2024. [Online]. Available: https://energia.fi/tiedotteet/kaukolammon-vuositilastot-paastot-romahtivat-kaukolampo-tasoittaa-sahkon-hintavaihteluita-uusissa-kerrostaloissa-kaukolammon-suosio-kaantynyt-kasvuun/. [Accessed 15 February 2024].

[5] NEA, “Meeting Climate Change Targets: The Role of Nuclear Energy,” The OECD Nuclear Energy Agency, 2022.

[6] Uppsala University, “ANItA,” 25 April 2024. [Online]. Available: https://www.uu.se/forskning/anita/om-oss. [Accessed 1 June 2024].

[7] T. Tanuma, Advances in Steam Turbines for Modern Power Plants, 2nd ed., Cambridge, Massachusetts: Woodhead Publishing, 2022.

[8] IEA, “Nuclear Power,” 2024. [Online]. Available: https://www.iea.org/energy-system/electricity/nuclear-power. [Accessed 2 February 2024].

[9] IAEA, “Country Statistics,” 2024. [Online]. Available: https://pris.iaea.org/PRIS/CountryStatistics/CountryStatisticsLandingPage.aspx. [Accessed 4 April 2024].

[10] IAEA, “Energy, Electricity and Nuclear Power Estimates for the Period up to 2050,” International Atomic Energy Agency, Vienna, 2023.

[11] Fortum, “Voimalaitoksen toiminta,” [Online]. Available: https://www.fortum.fi/tietoa-meista/energiantuotanto/voimalaitoksemme/loviisan-voimalaitos/voimalaitoksen-toiminta. [Accessed 1 June 2024].

[12] TVO, “OL1 ja OL2,” [Online]. Available: https://www.tvo.fi/tuotanto/laitosyksikot/ol1jaol2.html. [Accessed 1 June 2024].

[13] Finnish Energy, “Energy Year 2023,” Finnish Energy, Helsinki, 2024.

[14] Kantar Public, “Opinions on Nuclear Power,” Finnish Energy, Helsinki, 2023.

[15] R. L. Murray and K. E. Holbert, Nuclear Energy - An Introduction to the Concepts, Systems, and Applications of Nuclear Processes, 7th ed., Waltham, MA: Elsevier, 2015.

[16] IAEA, “Non-baseload Operation in Nuclear Power Plants: Load Following and Frequency Control Modes of Flexible Operation,” International Atomic Energy Agency, Vienna, 2018.

[17] IAEA, “Small modular reactors,” [Online]. Available: https://www.iaea.org/topics/small-modular-reactors. [Accessed 5 May 2024].

[18] IAEA, “Small and Medium Power Reactors: Project Initiation Study Phase 1,” International Atomic Energy Agency, Vienna, 1985.

[19] Z. Csereklyei, P. W. Thurner, A. Bauer and H. Küchenhoff, “The effect of economic growth, oil prices, and the benefits of reactor standardization: Duration of nuclear power plant construction revisited,” *Energy Policy,* vol. 91, pp. 49-59, 2016.

[20] NEA, “The NEA Small Modular Reactor Dashboard: Second Edition,” OECD Publishing, Paris, 2024.

[21] J. Patronen, E. Kaura and C. Torvestad, “Nordic Heating and Cooling - Nordic Approach to EU's Heating and Cooling Strategy,” Nordic Council of Ministers, 2017.

[22] DEA, “Danish Experiences on District Heating,” 2024. [Online]. Available: https://ens.dk/en/our-responsibilities/global-cooperation/experiences-district-heating. [Accessed 25 March 2024].

[23] IEA, “District Heating,” 2024. [Online]. Available: https://www.iea.org/energy-system/buildings/district-heating. [Accessed 25 March 2024].

[24] P. Hieta, “Energiatoimialan kehitys Suomessa,” Elinkeinoelämän Tutkimuslaitos, The Research Insititue of the Finnish Economy, Helsinki, 1993.

[25] Helen, Hyvää energiaa helsinkiläisille - Kaukolämmön ja kaukojäähdytyksen menestystarina jatkuu, Helsinki: Edita Prima Oy, 2012.

[26] Finnish Energy, “District Heating in Finland 2022, tables,” Finnish Energy, Helsinki, 2023.

[27] Helen, “Helen Open Data,” 2024. [Online]. Available: https://www.helen.fi/en/about-us/helen-ltd/about-us/open-data. [Accessed 2 2 2024].

[28] FMI, “Monthly Statistics / Kuukausitilastot,” 2024. [Online]. Available: https://www.ilmatieteenlaitos.fi/kuukausitilastot. [Accessed 1 June 2024].

[29] Finnish Energy, “Kaukolämpöjohtojen suunnittelu- ja rakentamisohjeet,” Finnish Energy, Helsinki, 2013.

[30] M. Huhtinen, R. Korhonen, T. Pimiä and S. Urpalainen, Voimalaitostekniikka, Kotka: Opetushallitus, 2008.

[31] Finnish Energy, “Kaukolämmön menolämpötilan optimointi,” Energiateollisuus ry, Helsinki, 2021.

[32] Finnish Energy, “Rakennusten kaukolämmitys - Määräykset ja ohjeet,” Energiateollisuus, Helsinki, 2021.

[33] Statistics Finland, “Production of heat and electricity, 1960-2022,” 2022. [Online]. Available: https://pxdata.stat.fi/PxWeb/pxweb/fi/StatFin/StatFin__salatuo/. [Accessed 19 February 2024].

[34] Finnish Energy, “District Heating in Finland 2022 in graphs,” Helsinki, 2023.

[35] Motiva, “Suomen teollisuuden sähköistyminen ja sen vaikutus energiatehokkuuteen ja hukkalämpöjen hyödyntämiseen,” Motiva Oy, Helsinki, 2021.

[36] Finnish Energy, “Energy Year 2023 - District Heating,” Helsinki, 2024.

[37] A. Bejan, Advanced Engineering Thermodynamics, 4th ed., Newark: Wiley, 2016.

[38] L. F. Cabeza, Advances in Thermal Energy Storage Systems - Methods and Applications, 2nd ed., Amsterdam: Elsevier, 2021.

[39] Helen, “Jättimäinen luolalämpövarasto toteutetaan Helsingin Mustikkamaalle,” [Online]. Available: https://www.helen.fi/uutiset/2018/mustikkamaa_toteutus. [Accessed 1 June 2024].

[40] Fortum, “Fortum rakentaa Suomen suurimman kaukolämpöakun Espoon Suomenojalle,” [Online]. Available: https://www.fortum.fi/media/2015/03/fortum-rakentaa-suomen-suurimman-kaukolampoakun-espoon-suomenojalle. [Accessed 15 May 2024].

[41] Tampereen Energia, “Selvitys polttoon perustumattomaan ja hiilinegatiiviseen kaukolämpöön siirtymisestä,” Tampereen Energia, Tampere, 2023.

[42] Turku Energia, “Komea kaasukello varastoi lämpöä,” 21 February 2022. [Online]. Available: https://www.turkuenergia.fi/valopilkku/komea-kaasukello-varastoi-lampoa. [Accessed 26 May 2024].

[43] Vantaan Energia, “Varanto eli lämmön kausivarasto,” [Online]. Available: https://www.vantaanenergia.fi/energiantuotanto/hiilinegatiivinen/lammonkausivarasto/. [Accessed 16 May 2024].

[44] Oulun Energia, 25 January 2022. [Online]. Available: https://www.oulunenergia.fi/ajankohtaista/blogi/lampoakku-lammittaa-koteja-talvella/. [Accessed 1 June 2024].

[45] Alva, “Sähkökattiloilla puhtaampaa lämpöä ja hintavakautta,” 11 April 2024. [Online]. Available: https://www.alva.fi/blog/2024/04/11/sahkokattiloilla-puhtaampaa-lampoa-ja-hintavakautta-alvan-lammontuotantopaletti-monipuolistuu/. [Accessed 3 June 2024].

[46] Sähköviesti, “Kaukolämpöakku tuottanut miljoonan jo ensimmäisenä vuonna,” [Online]. Available: https://www.sahkoviesti.fi/paikalliset/kaukolampoakku-tuottanut-miljoonan-jo-ensimmaisena-vuonna.html. [Accessed 4 June 2024].

[47] Axpo, “Beznau nuclear power plant – reliable, environmentally compatible electicity production”.

[48] World Nuclear News, “Chinese long-distance nuclear heating project begins operation,” 27 11 2023. [Online]. Available: https://world-nuclear-news.org/Articles/Chinese-long-distance-nuclear-heating-project-begi. [Accessed 1 June 2024].

[49] I. Paley, “Heat Delivey from Bohunice NPP, Slovakia (IAEA-TECDOC--1056),” International Atomic Energy Agency (IAEA), Bohunice, 1998.

[50] IAEA, “Opportunities for Cogeneration with Nuclear Energy,” International Energy Agency, Vienna, 2017.

[51] Vattenfall, “Ågesta Power Plant,” 2024. [Online]. Available: https://history.vattenfall.com/stories/agesta-power-plant#:~:text=%C3%85gesta%20was%20the%20country's%20first,benefit%20when%20designing%20today's%20reactors.. [Accessed 13 February 2024].

[52] Fortum, “Newbuild Loviisa 3,” [Online]. Available: https://www.fortum.com/services/nuclear/our-references/newbuild-loviisa-3. [Accessed 1 June 2024].

[53] IEA, Key World Energy Statistics 2021, Paris: International Energy Agency, OECD Publishing, 2021.

[54] N. V. Khartchenko and V. M. Kharchenko, Advanced Energy Systems, 2nd ed., Boca Raton, USA: CRC Press, 2013.

[55] M. Kassim, D. Khudhur, H. Hussain and L. Habeeb, Engineering Thermodynamics - An Introduction, Dulles: Mercury Learning and Information, 2022.

[56] D. Winterbone and A. Turan, Advanced Thermodynamics for Engineers, 2nd ed., Oxford: Elsevier, 2015.

[57] J. Riznic, Steam Generators for Nuclear Power Plants, Woodhead Publishing, 2017.

[58] F. P. Incropera, D. P. DeWitt, T. L. Bergman and A. S. Lavine, Fundamentals of Heat and Mass Transfer, 6th ed., Hoboken, New Jersey: John Wiley & Sons, Inc., 2007.

[59] A. S. Leyzerovich, Wet-Steam Turbines for Nuclear Power Plants, 1st ed., Tulsa, Oklahoma: Pennwell Corporation, 2005.

[60] IAEA, "Opportunities for Cogeneration with Nuclear Energy," International Atomic Energy Agency, Vienna, 2017.

[61] C. Soares, Gas Turbines: A Handbook of Air, Land and Sea Applications, 2nd ed., Waltham: Elsevier, 2015.

[62] R. Wikstén, Lämpövoimaprosessit, 4th ed., Helsinki: Gaudeamus Helsinki University Press, 1995.

[63] G. Towler and R. Sinnott, Chemical Engineering Design - Principles, Practice and Economics of Plant and Process Design, Oxford: Elsevier, 2022.

[64] IAEA, "Thermal Performance Monitoring and Optimization in Nuclear Power Plants - Experience and Lessons Learned," International Atomic Energy Agency, Vienna, 2021.

[65] US NRC, "Section 7.2 Condensate and Feedwater System," in *Westinghouse Technology Systems Manual*, United States Nuclear Regulatory Commission.

[66] Motiva, "Energiatehokkaat pumput," Motiva Oy, Helsinki, 2011.

[67] IAEA, "Efficient Water Management in Water-Cooled Reactors," International Atomic Energy Agency, Vienna, 2012.

[68] S. Hall, Rules of Thumb for Chemical Engineers, 5th ed., Waltham: Elsevier, 2012.

[69] Fortum, "Solvo 5.2," 2024.

[70] J. S. Wright, "Steam Turbine Cycle Optimization, Evaluation, and Performance Testing Considerations," GE Power Systems, Schenectady, NY, 1996.

[71] FMI, "Havaintojen Lataus/Tampere Siilinkari Weather Station," 2019. [Online]. Available: https://www.ilmatieteenlaitos.fi/havaintojen-lataus. [Accessed 1 5 2024].

[72] Pöyry Management Consulting Oy, "Älykäs kaupunkienergia - Raportti Energiateollisuus ry:lle," Vantaa, 2018.

[73] Tampereen Energia, "Miljoonainvestointi vihreään siirtymään – Tampereelle tulee kaksi uutta kaukolämpöä tuottavaa sähkökattilaa," 19 12 2023. [Online]. Available: https://www.tampereenenergia.fi/uutiset/miljoonainvestointi-vihreaan-

siirtymaan-tampereelle-tulee-kaksi-uutta-kaukolampoa-tuottavaa-sahkokattilaa/. [Accessed 1 6 2024].

[74] Fingrid, “Grid Code Specifications for Power Generating Facilities VJV2018,” Fingrid, Helsinki, 2018.

[75] F. Tingting and R. Lahdelma, “Optimization of combined heat and power production with heat storage based on sliding time window method,” *Applied Energy,* vol. 162, pp. 723-732, 2016.

[76] T. Fang and R. Lahdelma, “Optimization of combined heat and power production with heat storage based on sliding time window method,” *Applied Energy,* no. 162, pp. 723-732, 2016.

[77] H.-C. Wang, W.-L. Jiao, R. Lahdelma and P.-H. Zou, “Techno-economic analysis of a coal-fired CHP based combined heating system with gas-fired boilers for peak load compensation,” *Energy Policy,* vol. 39, no. 12, pp. 7950-7962, 2011.

[78] H. Wang, P. Hua, X. Wu, R. Zhang, K. Granlund, J. Li, Y. Zhu, R. Lahdelma, E. Teppo and L. Yu, “Heat-power decoupling and energy saving of the CHP unit with heat pump based waste heat recovery system,” *Energy,* vol. 250, no. 123846, 2022.

List of Appendices

Appendix A	SMR0 heat balance diagram
Appendix B	SMR1 heat balance diagram
Appendix C	SMR2 heat balance diagram
Appendix D	SMR3 heat balance diagram

Appendix A: SMR0 Heat Balance Diagram

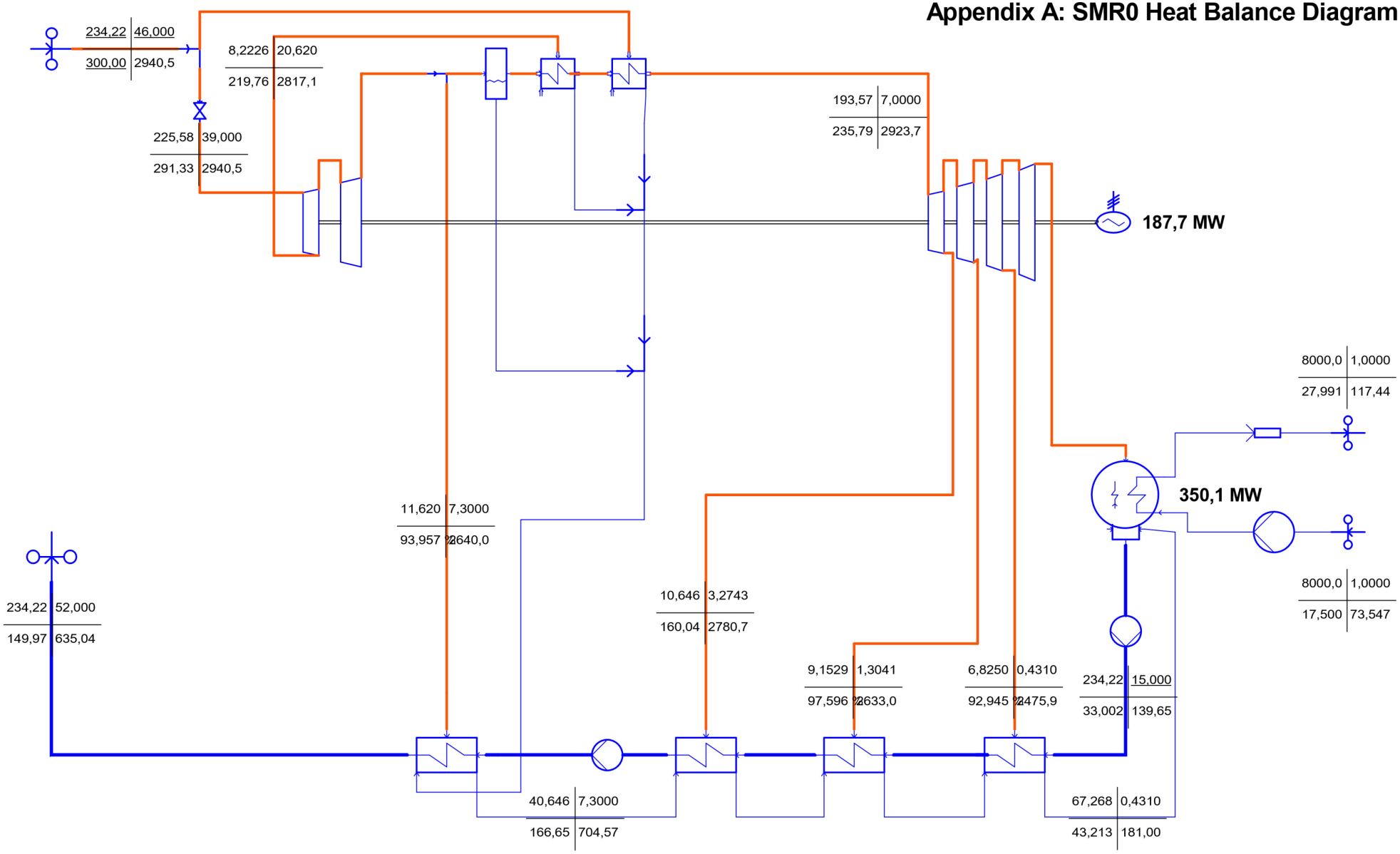

Appendix B: SMR1 Heat Balance Diagram

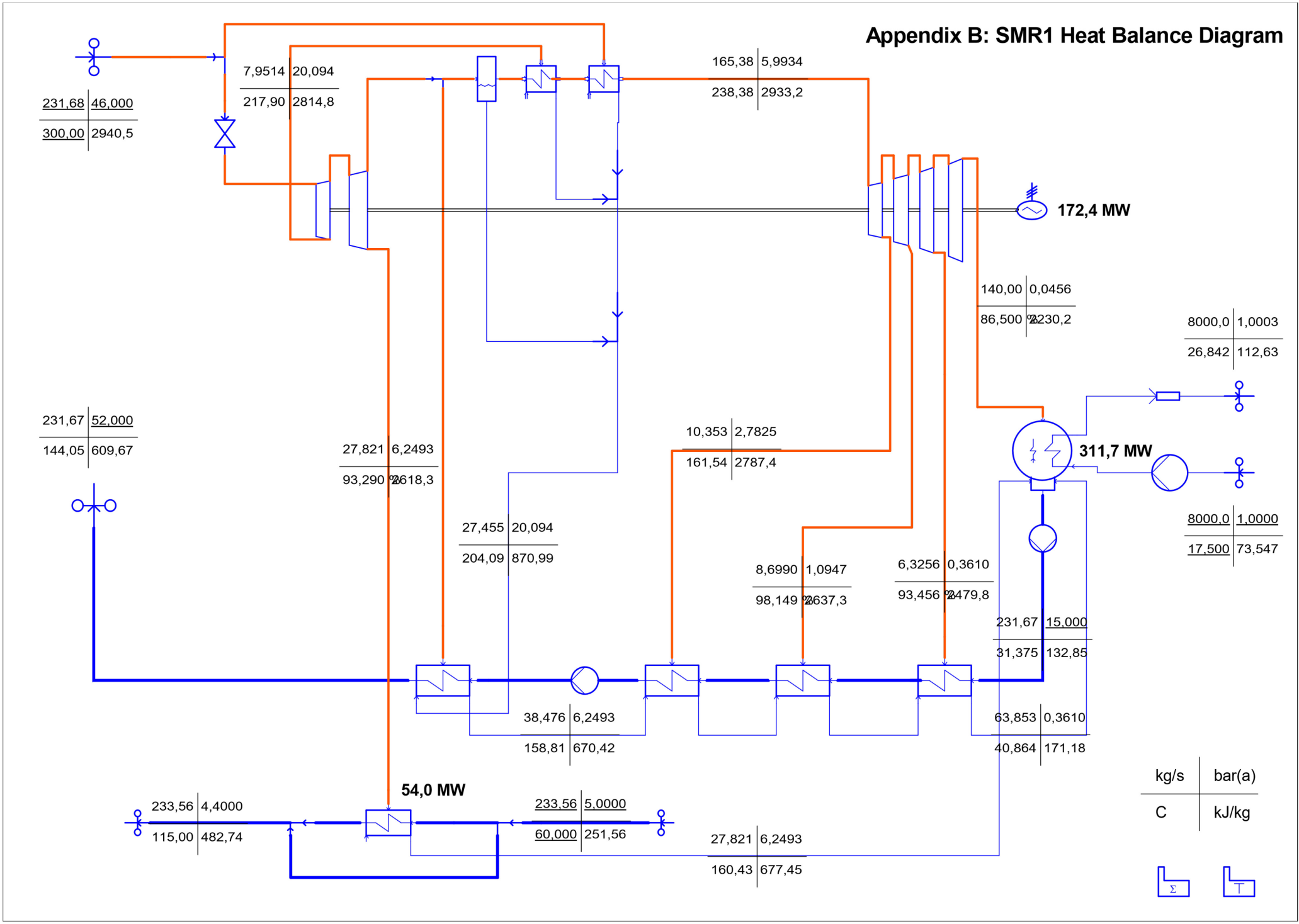

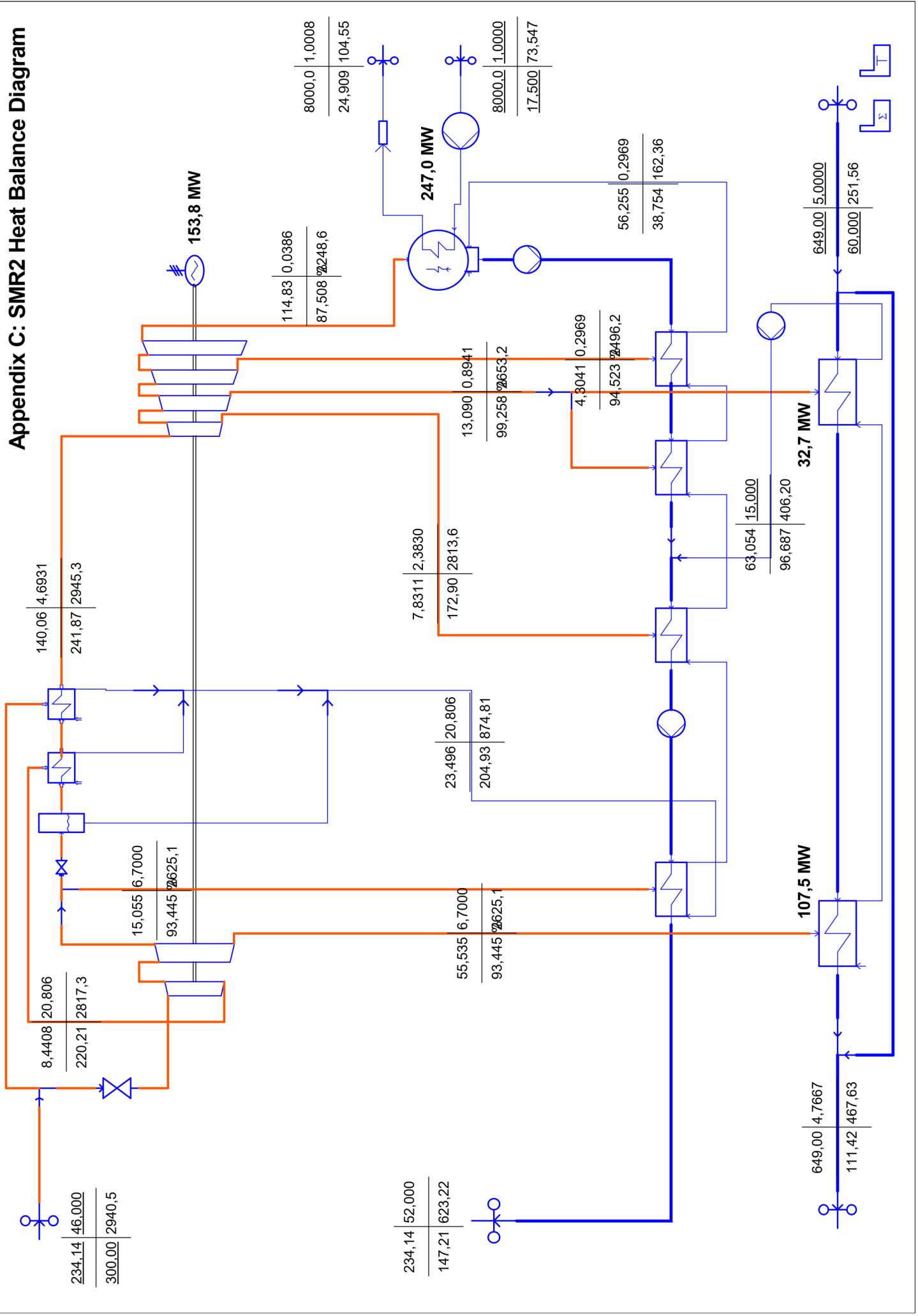
Appendix C: SMR2 Heat Balance Diagram
153,8 MW
247,0 MW
32,7 MW
107,5 MW
8000,0 | 1,0008
24,909 | 104,55
8000,0 | 1,0000
17,500 | 73,547
114,83 | 0,0386
87,508 | 2248,6
56,255 | 0,2969
38,754 | 162,36
649,00 | 5,0000
60,000 | 251,56
13,090 | 0,8941
99,258 | 2653,2
4,3041 | 0,2969
94,523 | 2496,2
140,06 | 4,6931
241,87 | 2945,3
7,8311 | 2,3830
172,90 | 2813,6
63,054 | 15,000
96,687 | 406,20
23,496 | 20,806
204,93 | 874,81
15,055 | 6,7000
93,445 | 2625,1
55,535 | 6,7000
93,445 | 2625,1
8,4408 | 20,806
220,21 | 2817,3
234,14 | 46,000
300,00 | 2940,5
234,14 | 52,000
147,21 | 623,22
649,00 | 4,7667
111,42 | 467,63

Appendix D: SMR3 Heat Balance Diagram

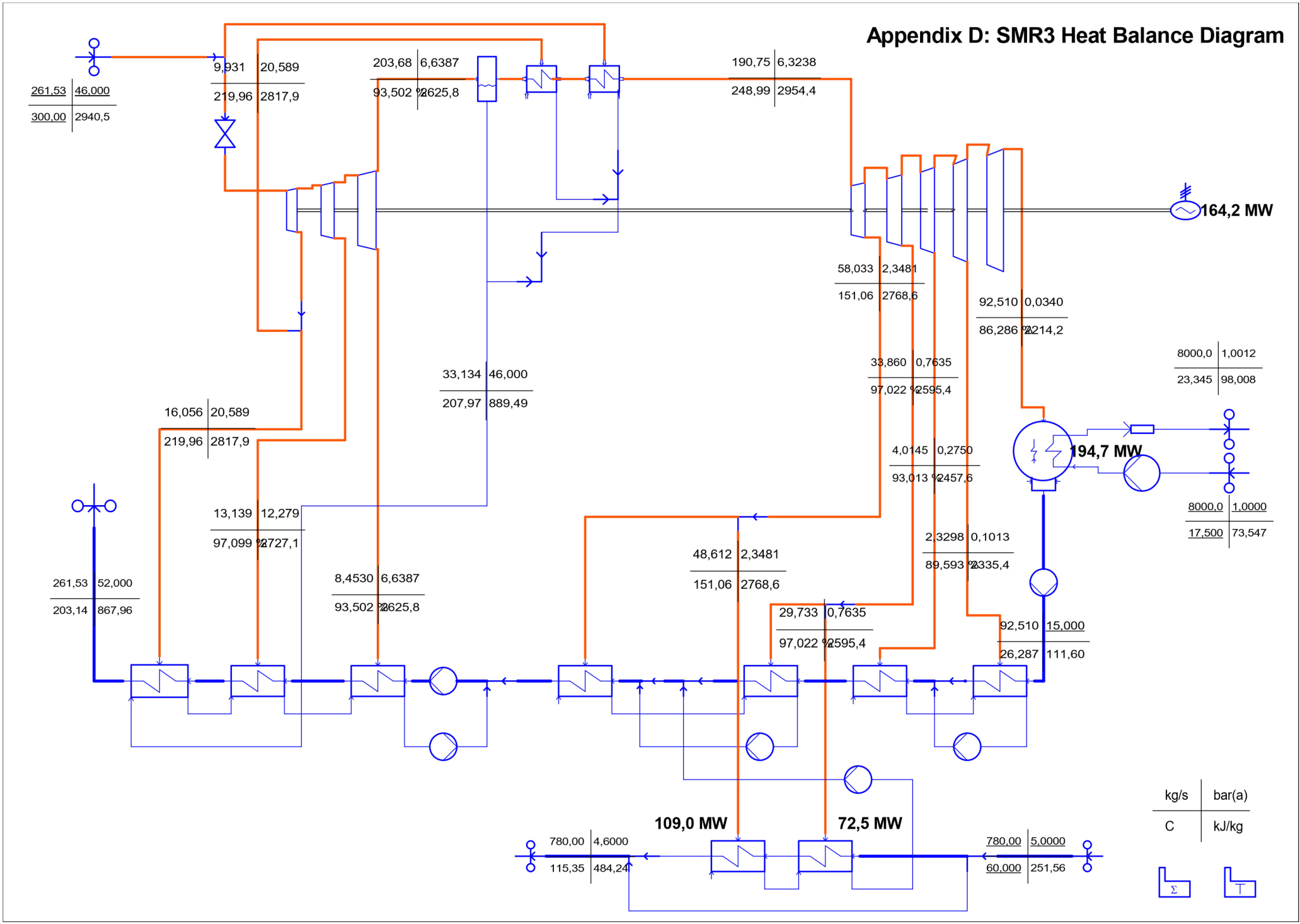

DEPARTMENT OF SPACE, EARTH AND ENVIRONMENT
CHALMERS UNIVERSITY OF TECHNOLOGY
Gothenburg, Sweden 2024
www.chalmers.se

CHALMERS
UNIVERSITY OF TECHNOLOGY